ΕΘΝΙΚΟ ΜΕΤΣΟΒΙΟ ΠΟΛΥΤΕΧΝΕΙΟ
ΣΧΟΛΗ ΜΗΧΑΝΟΛΟΓΩΝ ΜΗΧΑΝΙΚΩΝ
ΔΠΜΣ ΣΥΣΤΗΜΑΤΑ ΑΥΤΟΜΑΤΙΣΜΟΥ

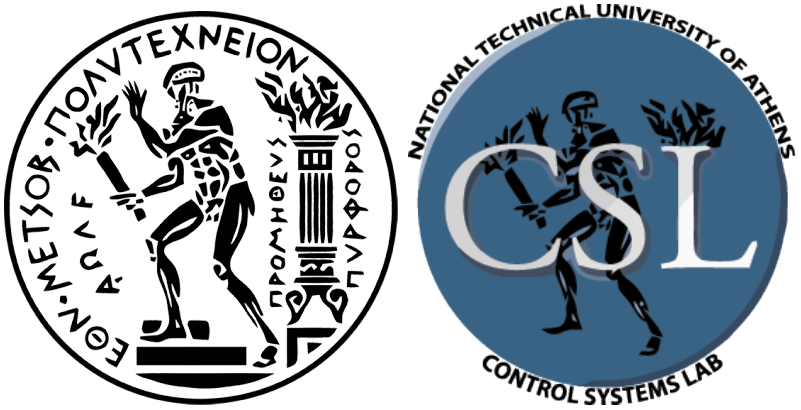

Μεταπτυχιακή Εργασία

Ανάλυση, Μοντελοποίηση και Μη Γραμμικός Έλεγχος Ενός Καινοτόμου Ιπτάμενου Ρομποτικού Χειριστή

Συγγραφέας: Αλέξανδρος Νίκου

Επιβλέπων: Κώστας Ι. Κυριακόπουλος

Κατατέθηκε για την μερική εκπλήρωση των υποχρεώσεων για την απόκτηση του Μεταπτυχιακού Διπλώματος Ειδίκευσης στον Αυτόματο Έλεγχο και στη Ρομποτική

Αθήνα, Σεπτέμβριος 2014

[This page intentionally left blank.]

National Technical University of Athens

School of Mechanical Engineering

Control Systems Lab

Master Thesis

Analysis, Modelling and Nonlinear Control Of A Novel Aerial Manipulator

---

Author:

Alexandros Nikou

Supervisor:

Professor Kostas J. Kyriakopoulos

A thesis submitted in partial fulfilment of the requirements for the degree of

Master of Science in Control and Robotic Systems

Athens, September 2014

Progress is impossible without change,
and those who cannot change their minds
cannot change anything.

George Bernard Shaw

Acknowledgements

This dissertation was conducted at Control Systems Lab, in the School of Mechanical Engineering on National Technical University of Athens during the period of 2013-2014.

First and foremost, I would like to thank my advisor Professor Kostas J. Kyriakopoulos, for giving me the opportunity to work in his group and for our excellent collaboration over the last year. He is a very talented professor who, within the difficult current situation in Greece, has managed to make a recognized and fully competitive laboratory with other worldwide. His guidance and deep knowledge of the field of Control Systems and Robotics were crucial for my success. Through this thesis, he gave me the opportunity to participate in high-level research projects. His inspiring and motivational personality as well as his trust in me, strengthened my decision to follow my dream of pursuing a PhD in this field.

Special thanks should be given to the group of the Control Systems Lab, namely Shahab Heshmati, Georgios Gavridis, Georgios Zogopoulos, Zoi Trachana and Nikolaos Kampras for being valuable colleagues and sustaining a creative research work environment.

Last, but not least, I would like to express my gratitude to my friend Areti Tsigkinopoulou, my sister Virginia and my parents Lefteris and Chrysanthi for their faith in me and their priceless moral and emotional support during the period of my studies.

Alexandros Nikou
Athens, September 2014

National Technical University of Athens
School of Mechanical Engineering

Master of Science in Control and Robotic Systems

Analysis, Modelling and Nonlinear Control Of A Novel Aerial Manipulator

by Alexandros Nikou

Abstract

Over the last years a significant scientific research attention has been observed in the aerial robotic field towards aerial manipulation and cooperation in dynamic environments. In this context, a new novel aerial manipulation system will be constructed in the Control Systems Lab at National Technical University of Athens. The proposed integrated system is composed of seven thrusters and an end-effector that can produce the desired actuation forces and torques to the environment. The mechanical design of the aforementioned system has been studied in [1].

Following this work, in this thesis a detailed differential kinematic model that relates the end-effector velocities with the corresponding velocities of the body frame is presented. The geometry specifications and the dynamic analysis are studied in order to describe mathematically the motion of the proposed system in the Cartesian task space. A static analysis is introduced for providing the mathematical relationship of the interaction with the environment. Taking all the above parameters into consideration, a nonlinear robust adaptive backstepping controller is designed in order to ensure robustness against actuator failures, unmodeled dynamics and external disturbances.

Extended numerical simulations were performed in Matlab Environment in order to verify the theoritical results of the this work, to demonstrate the performance of the system and the effectiveness of the controller. Finally, animated videos were created with the aim to observe graphically the motion the proposed system in arbitrary tracking and stabilization manipulation tasks scenarios.

Keywords: Robotics, Aerial Manipulation, Optimization, Kinematics, Dynamics, Statics, Nonlinear Control, Robust Adaptive Backstepping, MATLAB Simulations

Εθνικό Μετσόβιο Πολυτεχνείο
Σχολή Μηχανολόγων Μηχανικών

Μεταπτυχιακό Δίπλωμα Ειδίκευσης στον Αυτόματο Έλεγχο και στη Ρομποτική

Ανάλυση, Μοντελοποίηση, Σχεδίαση και Μη Γραμμικός Έλεγχος Ενός Ιπτάμενου Ρομποτικού Οχήματος

Αλέξανδρος Νίκου

Περίληψη[1]

Τα τελευταία χρόνια μια σημαντική επιστημονική ερευνητική προσοχή έχει παρατηρηθεί στον τομέα της εναέριας ρομποτικής ως προς την κατεύθυνση του εναέριου ρομποτικού χειρισμού και τη συνεργασία σε δυναμικά περιβάλλοντα. Σε αυτό το πλαίσιο, ενας νέος και καινοτόμος ρομποτικός χειριστής πρόκειται να κατασκευαστεί στο Εργαστήριο Αυτομάτου Ελέγχου στο Εθνικό Μετσόβιο Πολυτεχνείο. Το προτεινόμενο ολοκληρωμένο σύστημα αποτελείται από εφτά κινητήρες και ενα τελικό στοιχείο δράσης το οποίο έχει την δυνατότητα να επικοινωνεί με το περιβαλλον και να ασκεί επιθυμητές δυνάμεις και ροπές. Ο μηχανολογικός σχεδιασμός του συστήματος μελετήθηκε στην εργασία [2].

Συνεχίζοντας αυτήν την έρευνα, στην παρούσα εργασία μελετήθηκε λεπτεμερώς το διαφορικό κινηματικό μοντέλο του συστήματος, μέσω του οποίου συσχετίζονται οι ταχύτητες του τελικού σημείου δράσης με τις αντίστοιχες του βασικού σωματόδετου πλαισίου. Μελετήθηκαν τα γεωμετρικά χαρακτηριστικά του συστήματος καθώς και η δυναμική ανάλυση ώστε να περιγραφεί με ένα μαθηματικό μοντέλο η κίνηση του προτεινόμενου συστήματος στον Καρτεσιανό χώρο δράσης. Στη συνέχεια ένα στατικό δυναμικό μοντέλο εισάγεται ώστε να περιγραφεί η μαθηματική σχέση που συνδέει της αλληλεπίδραση του συστήματος με το περιβάλλον.

[1] Λόγω του οτι το πρόβλημα που πραγματεύεται η παρούσα εργασία εμπεριέχει μεγάλο πλήθος από εξειδικευμένους όρους, η μετάφραση των οποίων στα Ελληνικά δεν είναι δόκιμη, κρίθηκε προτιμότερο να γραφτεί εξ ολοκλήρου στα Αγγλικά

[2] G. Gavridis,"Control Oriented Aerodynamic Design Optimization For An Aerial Manipulator", Diploma Thesis, National Technical University of Athens, 2014

Λαμβάνοντας όλα τα προηγούμενα υπόψιν, ένας μη γραμμικός εύρωστος προσαρμοστικός ελεγχτής μέσω αλγορίθμου οπισθοδρόμησης σχεδιάστηκε έτσι ώστε να εγγυηθεί η ευρωστία και η ευστάθεια του συστήματος ενάντια στην παρουσία σφαλμάτων ενεργοποίησης από τους κινητήρες, τις δυνάμεις και ροπές που είναι ανέφικτο να μοντελοποιηθούν καθώς και τις εξωτερικές διαταραχές που επιδρούν στο σύστημα.

Τέλος, πραγματοποιήθηκαν εκτενείς αριθμητικές προσομοιώσεις στο περιβάλλον προγραματισμού του Matlab έτσι ώστε να επιβεβαιωθούν τα θεωρητικά αποτελέσματα της εργασίας και να αποδειχθεί η αποδοτικότητα του προτεινόμενου συστήματος καθώς και του ελεγχτή. Τέλος, δημιουργήθηκαν animation video με στόχο την καλύτερη παρατήρηση της γραφικής κίνησης και του ελέγχου του καινοτόμου συστήματος σε προβλήματα σταθεροποίησης και παρακολούθησης επιθυμητών τροχιών.

Λέξεις Κλειδιά: Ρομποτική, Εναέριος Ρομποτικός Χειρισμός, Κινηματική Ανάλυση, Δυναμική Ανάλυση, Στατική Ανάλυση, Μη Γραμμικός Έλεγχος, Έυρωστος Προσαρμοστικός Ελεγχτής μέσω Οπισθοδρόμισης, Προσομοιώσεις με MATLAB

Contents

List of Figures

List of Tables

Chapter 1

Preface

1.1 Introduction

Aerial manipulation is a new scientific field which has been gaining significant research attention and a wide variety of structures have been proposed in the last years. These manipulation systems possess several features which have lately brought them in the spotlight, with their objective mainly oriented towards performing effectively complex manipulating tasks in unstructured and dynamic environments. Having them include active manipulation as a major functionality, would vastly broaden the applications of these systems, as they move from mere passive observation and sensing to interaction with the environment. Therefore, new scientific applicable horizons will be introduced related to cooperative manipulation, surveillance, industrial inspections, inspection and maintenance of aerial power lines, assisting people in rescue operations, constructing at inaccessible sites by repairing and assembling, with potential applications in object retrieval and improved observation through manipulating barriers, objects or switches. These aerial robots are capable of physically interacting with objects in the environment through a terminal end-effector. Naturally, both designing and controlling aerial manipulators could be considered as nontrivial engineering challenges.

1.2 Literature Review

A wide variety of aerial manipulation systems and aerial robots that can interact with the environment have been studied and proposed in bibliography. In this subsection,

an explanatory and extended literature review for the previous works that has been adopted in this field, is presented.

The first theoretical and experimental results on aerial robots interacting with the environment were derived by a three DOF ducted-fan prototype with a four DOF end-effector (Figure 1.1). This UAV aerial manipulator was within the framework of AIRobots project on 2008-2013. The works in [2, 3, 4, 5, 6] refer to the mechanical design, the mathematical modelling and the control of this system focusing on the interaction with the environment by addressing two different control scenarios, the take-off and the set-stand vertical fixed surfaces. Impedance control problems are also considered. Authors performed ulstrasonic non-destructive testing experiments and versatile tasks at unreachable locations for humans.

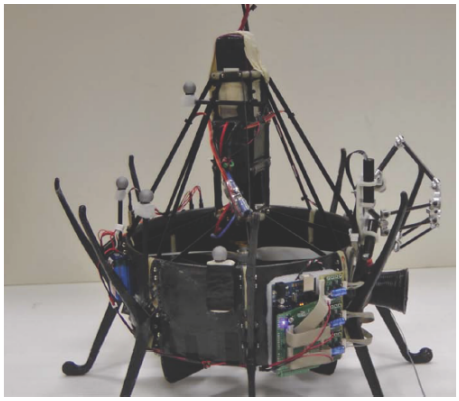

FIGURE 1.1: Ducted Aerial Manipulator from AIRobots Project

The design of a quadrotor (Figure 1.2) capable of applying force to a wall maintaining flight stability is provided in [7]. The basis for the work presented is a quadrotor system which is stabilized with an inertial measurement unit. As new approach an additional actuator was added to generate forces in physical contact while the quadrotor stays horizontal. The performance of the system is proved by several flight tests.

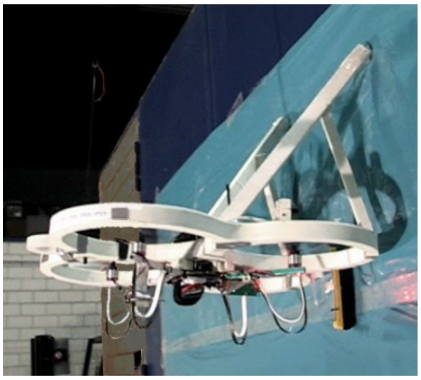

FIGURE 1.2: A quadrotor applying force to a wall [7]

In [8, 9, 10, 11] considerable experimental results at Yale University with a small helicopter with grasping capabilities (Figure 1.3) are shown along with the stability proofs while grasping. Authors demonstrated stable grasping of a range of objects both when landing and while hovering. The dynamic load disturbances introduced by the load mass was rejected by a PID flight controller. The approach employs passive mechanical compliance and adaptive underactuation in the gripper to allow for large positional displacements between the aircraft and the target object.

FIGURE 1.3: The Yale Aerial Manipulator

The authors in [12] present the design of several light-weight, low-complexity grippers that allow quadrotors to grasp and perch on branches or beams and pick up and transport payloads (Figure 1.4). It is showed how the robot can use rigid body dynamic models and sensing to verify a grasp, to estimate the inertial parameters of the grasped object, and to adapt the controller and improve performance during flight. Experimental results with different grippers are also showed.

FIGURE 1.4: A Quadrotor equipped with a gripper from UPEN Grasp Lab [12]

An implementation of autonomous indoor aerial gripping using a low-cost, custom-built quadrotor is provided in [13], [14]. This research extends the typical functionality

of micro air vehicles form passive observation to sensing and to dynamic interaction with the environment. The system utilizes nested PID controllers for attitude stabilization, vision-based navigation and gripping. This quadrotor (Figure 1.5) is able to autonomously navigate, locate and grasp an object using only on-board sensors.

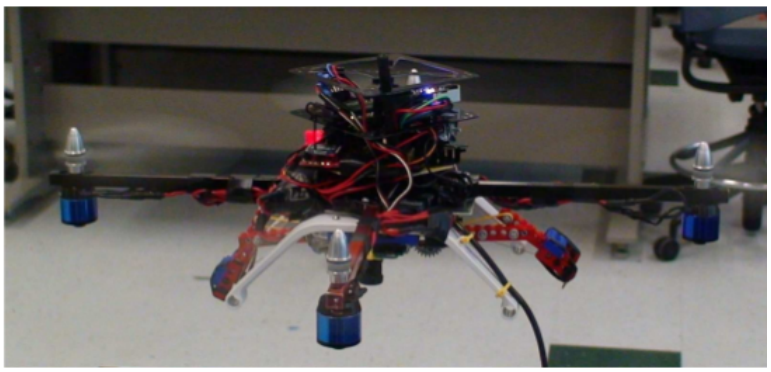

FIGURE 1.5: A quadrotor performing aerial gripping [13]

The authors in [15, 16, 17] considered the problem of controlling multiple quadrotor robots that cooperatively grasp and transport a payload in three dimensions. Quadrotors are modeled (Figure 1.6) both individually and as a group rigidly attached to a payload. Individual robot control laws which are proposed, are defined with respect to the payload that stabilize the payload along three-dimensional trajectories. An experimental study with teams of quadrotors cooperatively grasping, stabilizing and transporting payloads along desired three-dimensional trajectories is presented below.

FIGURE 1.6: Four quadrotors carrying a payload

Another significant work with cooperative quadrotors throwing and catching a ball with a net (Figure 1.7) is presented in [18]. Based on a first-principles model of the net forces, nominal inputs for all involved vehicles are derived from arbitrary target trajectories of the net. Two algorithms that generate open-loop trajectories for

throwing and catching a ball are also introduced. The feasibility methods has been validated in experimental in the ETH Arena.

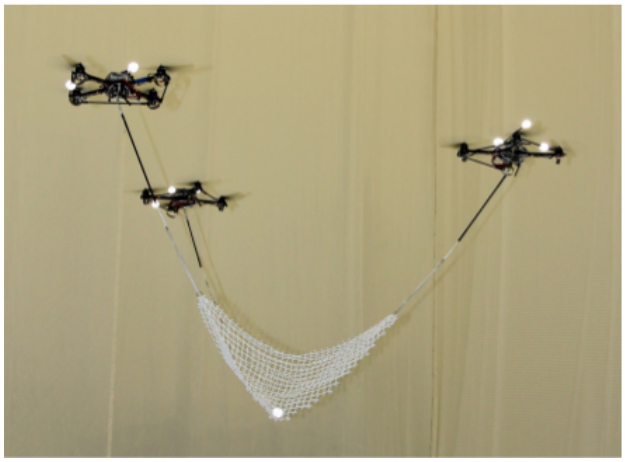

FIGURE 1.7: Three quadrotors attached to a net [18]

A system for aerial manipulation composed of a helicopter platform and a fully actuated seven DOF redundant industrial robotic arm (Figure 1.8) is introduced in [19, 20]. It is shown that the dynamic coupling between helicopter and arm can generate diverging oscillations with very slow frequency. An impedance controller approach is proposed for the whole system. Flights experiments that have been done showed that the system might be used in practically relevant tasks.

FIGURE 1.8: A helicopter equipped with a 7 DOF robotic arm in [19]

A novel dextrous hexrotor platform equipped with a 6 DOF end-effector (Figure 1.9) for interaction with structures has been proposed in [21, 22, 23, 24]. This manipulator can exert arbitrary wrenches in the 6 DOF force/torque space and provides the unique capability of being able to resist any applied wrench, or generalized force/torque. A thrust mapping based on decomposed net force/torque and a control system which allows the pilot to control the position and the orientation separately has been derived.

FIGURE 1.9: A novel dextrous hexrotor manipulator in [21]

A multi-body aerial manipulator composed of a hexarotor main body equipped with a two-link manipulator with a low-cost gripper (Figure 1.10) has been studied in [25]. The proposed approach employed free-flying multi-body dynamics modelling and back-stepping control to develop stabilizing control laws for a class of underactuated systems. Two control methods are developed: coordinate-based and coordinate-free which are both generally applicable to aerial manipulation tasks.

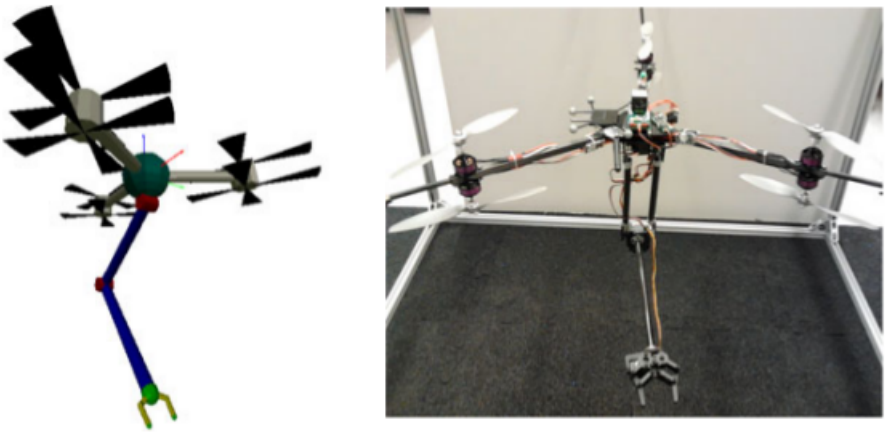

FIGURE 1.10: A helicopter equipped with a two-link manipulator in [25]

A significant experiment using a quadrotor with a two DoF robotic arm (Figure 1.11) can be found in [26]. By considering the quadrotor and the robot arm as a combined system, the kinematic and dynamic models were developed and an adaptive sliding mode controller was designed. With the controller, an autonomous flight experiment was conducted including picking up and delivering an object, which requires accurate control of the quadrotor and the robotic arm.

FIGURE 1.11: A quadrotor with 2 DoF manipulator in [26]

In [27] the challenges in controlling a mobile manipulating UAV using a commercially available aircraft with three light-weight each with 2-DoF robotic arms (Figure 1.12) is investigated. Because of the overall instability of the rotorcraft, a motion capture system was used to build an efficient autopilot. The results indicated that the prototype could be accurately modeled and controlled given significant disturbances when both moving the manipulators and interacting with the ground.

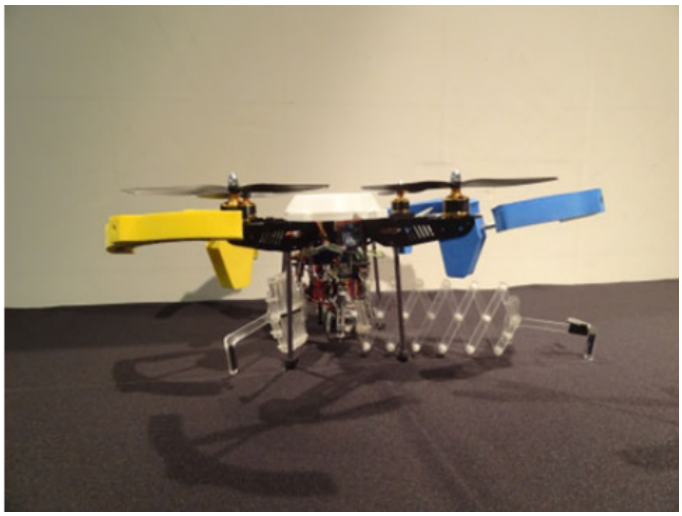

FIGURE 1.12: A quadrotor with three 2-DoF robotic arms in [27]

Finally, theoretical results for modelling and controlling quadrotors equipped with multi DoF robotic arms in order to interact with the environment can be found in [28, 29, 30, 31, 32].

1.3 Problem Statement

In the framework of the development of a completely autonomous aerial manipulation system, the main issues to be resolved are the mechanical design, the kinematic, dynamic and static analysis, the control of the final system aiming to perform advanced manipulation tasks effectively and the final choice of the system's mechanical and hardware components.

The idea of the proposed novelty system was developed at Control Systems Lab on National Technical University of Athens. The proposed system is fully integrated, because is not considered as a commercial aerial robot equipped with an external robotic arm, as many of proposed aerial manipulators in the bibliography introduced above. The system is equipped with seven thrusters in optimal locations that can produce maximum thrust force $\lambda_{\max} = 28N$, without aerodynamic interaction. The mechanical design has been performed in a control-oriented way so that the final system could be controllable and exact feedback linearizable.

The first engineering results of the project can be found in [1] where the mechanical design of the system, which is the result of solving difficult optimization problems, is presented along with an extended review of the suitable system components and hardware. The aim of this thesis was to integrate the primary work with the final pre-manufacturing stage. In this context, the first objective was to provide a well-defined 3D geometry mechanism for the exact study of the motion of the system in the 3D space. This was investigated by the extensive geometry analysis, the thrust force redistribution among the seven actuators, the kinematic differential equations of the end-effector and the dynamic/static force analysis needed for the final motion. The following step was to design a high-level nonlinear controller that would provide accurate trajectory tracking of the end-effector in arbitrary trajectories, by identifying and taking into account the system geometry specifics. The controller should be able to handle possible uncertainties, unmodeled dynamics, actuator failures, external and environmental disturbances. Finally, simulations have been carried out in order to test the performance of the system and to estimate if the proposed system was able to be manufactured, which constituted the last objective.

1.4 Thesis Structure

The rest of this thesis is organized as follows:

- In Chapter 2 a functional description of the proposed aerial robot, the main ideas and principles, the primary work, the mechanical design process via optimization problems and the components that are going to compose the system in the manufacturing stage are discussed.
- In Chapter 3 an analysis is made on the Kinematics of the Aerial Manipulator. At first, several reference frames and relative motions are defined and in the sequel the kinematic tranformations and the basic assumptions are provided. Finally, the differential kinematics equation is derived along with the time derivative of Jacobian.
- In Chapter 4 a mathematical model that captures the proposed system dynamics and govern the behavior of the system is derived with well-known Newton - Euler formalism. All matrices that compose the dynamic analysis are presented explanatory and in the end of the Chapter a static model for the system in interaction with the environment is provided.
- In Chapter 5 the nonlinear model of the system is analyzed with nonlinear control theory tools. Controllability conditions, system's relative degree computation and feedback linearizability conditions are provided. Based on this highly nonlinear model a robust adaptive backstepping control law is designed taking into account the modelling errors, the unmodeled dynamics, the actuator failures, the external and environmental disturbances. The stability proofs are extensively provided.
- In Chapter 6 the performance of the developed kinematic, the dynamic and the controller design analysis is demonstrated through a series of simulation in MATLAB where various aerial manipulation tasks scenarios are considered. MATLAB Figures and animation videos are used for illustrative purposes in order to show the motion of the system and the controller effectiveness.
- Finally, in Chapter 7 an overall description of this work is presented. Moreover, the conclusions of the thesis are summarized and possible suggestions and future directions are provided.

Chapter 2

Mechanical Design

2.1 Introduction

The overall description of the Aerial Manipulator was based on the idea of designing an aerial robot composed of a set number n of similar thrusters and an end-effector in order to interact with objects in the environment. the exact geometry of the structure will be the result of the analysis in this section. The aforementioned mechanical design process is extensively presented in the primary work thesis [1].

2.2 Principles of the Problem

Initially, we will define the Body-Fixed frame $F_B = \{\hat{x}_B, \hat{y}_B, \hat{z}_B\}$ and End-Effector frame $F_E = \{\hat{x}_E, \hat{y}_E, \hat{z}_E\}$. These frames are attached to the rigid body of the aerial manipulator as in Figure 2.1. The vectors $r_i, r_e \in \mathbb{R}^3$ denote the position of each thruster and the position of end-effector respectively with reference to the Body frame. The thruster orientations are given by a unit vector $\hat{F}_i \in \mathbb{R}^3,\ i = 1, ..., n$, the corresponding thrust forces are defined as λ_i and the propulsion vectors are given by $\lambda_i\ \hat{F}_i$. In the rest of the analysis, all forces ant torques acting to the system can be expressed in Body-Fixed frame. At this point, it is assumed that the total system is considered to be a rigid body and without loss of generality the End-Effector frame and the Body frame have the same orientation. Thus, for the actuation force applying to the end-effector is

$$F_{act}\big|_B = F_{act}\big|_E \in \mathbb{R}^3 \tag{2.1}$$

where $\big|_B, \big|_E$, denote the expression to frames F_B, F_E respectively. The corresponding actuation torque is obtained via the formula

$$T_{act}\big|_B = T_{act}\big|_E + r_e \times f_e \tag{2.2}$$

where

$$T_{act}\big|_E = r \times f_e \tag{2.3}$$

is the torque produced by the end-effector. The terms r, f_e are the displacement vector (length of the lever arm) and the vector force that tends to rotate a gripped object from the end-effector.

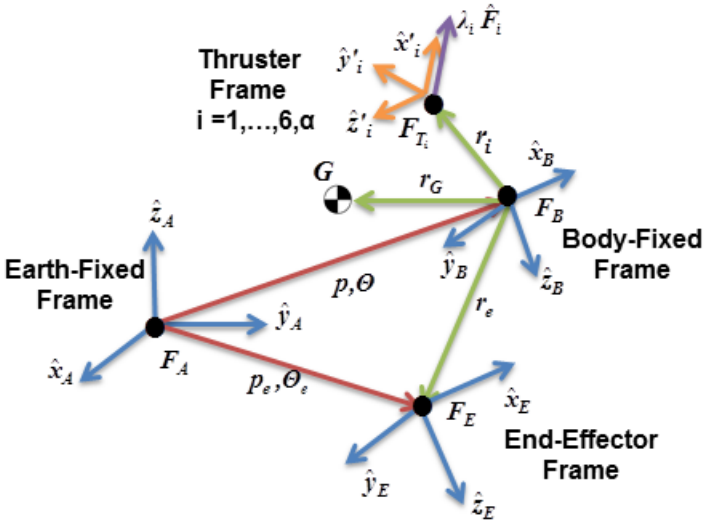

FIGURE 2.1: Aerial Manipulator Configuration Frame System

2.3 Forces and Torques

The forces transmitted essentially through the end-effector are written as

$$\sum_{i=1}^{n}(\lambda_i\ \hat{F}_i) + W = F_{act}\big|_B \tag{2.4}$$

where $W \in \mathbb{R}^3$ is the vector that correspond to the total weight of the system. The weight can be separated as $w_s = W - n\ w$ where $w \in \mathbb{R}^3$ is the weight of each thruster. The separation of weights is made so as to define the necessary number (n) of thrusters in the rest of analysis. Using the previous result and modifying the (2.4) in matrix

form we conclude that

$$F\ \lambda + n\ w + w_s = F_{act}\big|_B \tag{2.5}$$

where

$$\lambda = \begin{bmatrix}\lambda_1 \cdots \lambda_n\end{bmatrix}^\tau \in \mathbb{R}^n \tag{2.6}$$

$$F = \begin{bmatrix}\hat{F}_1 \cdots \hat{F}_n\end{bmatrix}^\tau \in \mathbb{R}^{3\times n} \tag{2.7}$$

Using the matrix

$$\bar{F} = F_{act}\big|_B - n\ w - w_s \tag{2.8}$$

the equation (2.5) can be written as

$$F\ \lambda = \bar{F} \tag{2.9}$$

Similarly, the torque produced from each thruster is

$$T_i = r_i \times (\lambda_i\ \hat{F}_i) = \lambda_i\ S(r_i)\ \hat{F}_i \tag{2.10}$$

using the well-known skew-symmetric matrix $S(\cdot) \in \mathbb{R}^{3\times3}$ such that $a \times b = S(a)\ b$ for the cross-product $\times$ and any vectors $a, b\ \in \mathbb{R}^3$ (explanatory properties of skew-symmetric matrices will be discussed in Chapter 3). The torque due to the weight can be calculated as

$$T_W = r_G \times W = \sum_{i=1}^{n} r_i \times w + r_s \times w_s = \sum_{i=1}^{n} S(r_i)w + S(r_s)w_s$$

where r_G is the center of gravity of the system and r_s is the center of gravity of the total system when omitting the mass of each thruster. The reaction torque of each thruster is $\tau_i = \mu\ (\lambda\ \hat{F}_i)$ where μ is a coefficient that represents the relationship between the thrust force and the reaction torque [33]. Therefore, combining all torques the following equation holds

$$\begin{aligned}
&\sum_{i=1}^{n}\left\{\lambda_i\ S(r_i)\ \hat{F}_i\right\} + \mu\ \sum_{i=1}^{n}\left(\lambda_i\ \hat{F}_i\right) + \sum_{i=1}^{n} S(r_i)\ w + S(r_s)\ w_s = T_{act}\big|_B \\
&\quad\Leftrightarrow \sum_{i=1}^{n}\left\{\lambda_i\ S(r_i)\ \hat{F}_i\right\} + \mu\ F\ \lambda + \sum_{i=1}^{n} S(r_i)\ w + S(r_s)\ w_s = T_{act}\big|_B \\
&\quad\Leftrightarrow \sum_{i=1}^{n}\left\{\lambda_i\ S(r_i)\ \hat{F}_i\right\} + \mu\ \bar{F} + \sum_{i=1}^{n} S(r_i)\ w + S(r_s)\ w_s = T_{act}\big|_B
\end{aligned} \tag{2.11}$$

Using the matrices

$$r = \begin{bmatrix} r_1 & \cdots & r_n \end{bmatrix}^\tau \in \mathbb{R}^{3\times n} \tag{2.12}$$

$$E(r,F) = \begin{bmatrix} S(r_1)\ \hat{F}_1 & \cdots & S(r_n)\ \hat{F}_n \end{bmatrix} \in \mathbb{R}^{3\times n} \tag{2.13}$$

in (2.11) we get

$$\begin{cases} F\ \lambda = \bar{F} \\ E\ \lambda = T_{act}\big|_B - \mu\ \bar{F} - \sum_{i=1}^{n} S(r_i)\ w - S(r_s)\ w_s \end{cases} \tag{2.14}$$

Defining the transformation matrix from actuator space to end-effector space

$$D(r,F) = \begin{bmatrix} F \\ E(r,F) \end{bmatrix} \in \mathbb{R}^{6\times n} \tag{2.15}$$

from the system (2.14) it is implied that

$$D(r,F)\ \lambda = W_R \tag{2.16}$$

where the augmented wrench vector $W_R \in \mathbb{R}^6$ is given by

$$W_R = \begin{bmatrix} \bar{F} \\ T_{act}\big|_B - \mu\bar{F} - \sum_{i=1}^{n} S(r_i)w - S(r_s)w_s \end{bmatrix} \tag{2.17}$$

2.4 Negative Thrust Forces

It is clear that when solving the (2.16), the matrix that corresponds to the propulsion effort λ can obtain any value in $\mathbb{R}^6$. However, the thrusters are optimally designed to produce thrust force towards a specific direction, which we set to correspond to the positive values of λ_i. In order to alleviate the problem of negative thrust forces λ_i, a conservative solution is adopted in this analysis, which will be based on the idea of introducing one additional thruster. Thus, (2.16) is rewritten as

$$\sum_{i=1}^{n} \lambda_i\ t_i = W_R \tag{2.18}$$

where

$$D(r, \hat{F}) = \begin{bmatrix} t_1 & \cdots & t_n \end{bmatrix} \tag{2.19}$$

$$t_i = \begin{bmatrix} \hat{F}_i \\ S(r_i)\ \hat{F}_i \end{bmatrix} \in \mathbb{R}^6 \tag{2.20}$$

for all $i = 1, \ldots, n$. The vector

$$t_a = -\sum_{i=1}^{n} t_i = -\sum_{i=1}^{n} \begin{bmatrix} \hat{F}_i \\ S(r_i)\ \hat{F}_i \end{bmatrix} = \begin{bmatrix} -\sum_{i=1}^{n} \hat{F}_i \\ -\sum_{i=1}^{n} \left\{ S(r_i)\hat{F}_i \right\} \end{bmatrix} = \begin{bmatrix} \hat{F}_a \\ S(r_a)\hat{F}_a \end{bmatrix} \tag{2.21}$$

that corresponds to the additional thruster is introduced. Using (2.21) the position vector r_a and the direction $\hat{F}_a$ of the new thruster should satisfy the equations

$$\hat{F}_a = -\sum_{i=1}^{n} \hat{F}_i \tag{2.22}$$

$$S(\hat{F}_a)\ r_a = -\sum_{i=1}^{n} \left\{ S(\hat{F}_i)\ r_i \right\} \tag{2.23}$$

If we assume at this point, that (2.16) results in some negative thrust forces then the set

$$\sigma_N = \{k : \lambda_k < 0, k = 1, ..., 6\} \tag{2.24}$$

denote the indexes for every negative thrust force and

$$\sigma_P = \{1, 2, 3, 4, 5, 6\} - \sigma_N \tag{2.25}$$

the corresponding set of positive thrust forces. Noticing that

$$\lambda_k < 0 \Leftrightarrow (-\lambda_k) > 0,\ \forall\ k \in \sigma_N \tag{2.26}$$

the equation (2.18) can be separated in

$$\begin{aligned} &\sum_{i \in \sigma_P} \lambda_i\ t_i + \sum_{k \in \sigma_N} \lambda_k\ t_k = W_R \\ \Leftrightarrow &\sum_{i \in \sigma_P} \lambda_i\ t_i + \sum_{k \in \sigma_N} (-\lambda_k)\ (-t_k) = W_R \end{aligned} \tag{2.27}$$

Now, from (2.21) the following can be exported

$$t_a = -\sum_{i=1}^{n} t_i = -\sum_{i\in\sigma_P} t_i - \sum_{j\in\sigma_N} t_j$$
$$\Leftrightarrow -\sum_{j\in\sigma_N} t_j = t_a + \sum_{i\in\sigma_P} t_i \tag{2.28}$$

It is obvious that

$$-\sum_{j\in\sigma_N} t_j = -t_k - \sum_{\substack{j\in\sigma_N \\ j\neq k}} t_j,\ \forall\ k \in \sigma_N \tag{2.29}$$

Combining (2.28), (2.29) we obtain

$$-t_k = t_a + \sum_{i\in\sigma_P} t_i + \sum_{\substack{j\in\sigma_N \\ j\neq k}} t_j,\ \forall\ k \in \sigma_N \tag{2.30}$$

Substituting (2.30) in (2.27) we have

$$\sum_{i\in\sigma_P} \lambda_i\ t_i + \sum_{k\in\sigma_N} (-\lambda_k) \left[t_a + \sum_{i\in\sigma_P} t_i + \sum_{\substack{j\in\sigma_N \\ j\neq k}} t_j\right] = W_R$$
$$\sum_{i\in\sigma_P} \lambda_i\ t_i + \sum_{k\in\sigma_N} (-\lambda_k)\ t_a + \sum_{k\in\sigma_N} (-\lambda_k) \sum_{i\in\sigma_P} t_i + \sum_{k\in\sigma_N} \left[(-\lambda_k) \sum_{\substack{j\in\sigma_N \\ j\neq k}} t_j\right] = W_R \tag{2.31}$$

It is known from basic mathematical summing properties that

$$\sum_{k\in\sigma_N} (-\lambda_k) \sum_{i\in\sigma_P} t_i = \sum_{i\in\sigma_P} \left[\sum_{k\in\sigma_N} (-\lambda_k)\right] t_i \tag{2.32}$$
$$\sum_{k\in\sigma_N} \left[(-\lambda_k) \sum_{\substack{j\in\sigma_N \\ j\neq k}} t_j\right] = \sum_{k\in\sigma_N} \left[\sum_{\substack{j\in\sigma_N \\ j\neq k}} (-\lambda_j)\right] t_k \tag{2.33}$$

Thus, the (2.31) by combining (2.32) and (2.33) can be written as

$$\sum_{i\in\sigma_P} \left[\lambda_i + \sum_{k\in\sigma_N} (-\lambda_k)\right] t_i + \sum_{k\in\sigma_N} \left[\sum_{\substack{j\in\sigma_N \\ j\neq k}} (-\lambda_j)\right] t_k + \left[\sum_{k\in\sigma_N} (-\lambda_k)\right] t_a = W_R \tag{2.34}$$

Defining

$$\Delta = \sum_{k \in \sigma_N} (-\lambda_k) > 0 \tag{2.35}$$

$$E_k = \sum_{\substack{j \in \sigma_N \\ j \neq k}} (-\lambda_j) > 0 \tag{2.36}$$

and substituting it in (2.34) it finally yields

$$\sum_{i \in \sigma_P} (\lambda_i + \Delta)\ t_i + \sum_{k \in \sigma_N} E_k\ t_k + \Delta\ t_a = W_R \tag{2.37}$$

From (2.37) the thruster redistribution among all thrusters after adding the new thruster is provided. It has been proven that the issue of negative thrust forces can be alleviated by adding one extra thruster. This equation can be better analysed in Figure 2.2 in which the thrust redistribution algorithm is depicted. The variables $\lambda', \lambda'_i, \lambda'_k$ denote the initial thrust forces and the other the thrust force after redistribution, plus the additional thrust force λ_a. The $\lambda'_i,\ \forall\ i \in \sigma_P$ denote the initially non-negative thrust forces and the $\lambda'_k,\ \forall\ k \in \sigma_N$ denote the initially negative thrust forces. This means that at every time, six thrust forces (not necessary all positive) are equivalent with seven thrust forces, all positive with redistributed thrust forces as in (2.37).

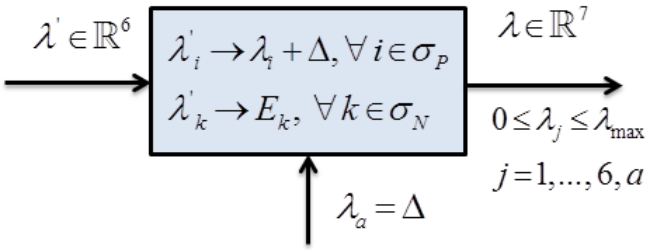

FIGURE 2.2: Thrust Force Equivalence

In order better understand the thrust force redistribution algorithm, an example will be given. Let's assume at in an arbitrary time $t_s \geq 0$, the system needs actuation thrust forces

$$\begin{bmatrix} \lambda'_1(t_s) \\ \lambda'_2(t_s) \\ \lambda'_3(t_s) \\ \lambda'_4(t_s) \\ \lambda'_5(t_s) \\ \lambda'_6(t_s) \end{bmatrix} = \begin{bmatrix} -8 \\ 7 \\ -5 \\ 3 \\ -4 \\ 5 \end{bmatrix} \text{ [Newton]}$$

Then the sets σ_P, σ_N can be easily derived from (2.24), (2.25) as $\sigma_P = \{2, 4, 6\}$, $\sigma_N = \{1, 3, 5\}$. The Δ is given by $\Delta = -(-8) - (-5) - (-4) = 17$. Hence, after the redistribution algorithm the new thrusts are

$$\begin{bmatrix} \lambda'_1(t_s) \\ \lambda'_2(t_s) \\ \lambda'_3(t_s) \\ \lambda'_4(t_s) \\ \lambda'_5(t_s) \\ \lambda'_6(t_s) \\ \lambda_a(t_s) \end{bmatrix} = \begin{bmatrix} 9 \\ 24 \\ 12 \\ 20 \\ 13 \\ 22 \\ 17 \end{bmatrix} \text{ [Newton]}$$

Closing the issue of the negative thrust forces, the additional thruster reforms the (2.12), (2.17) into

$$\bar{F} = F_{act}\big|_B - (n+1)\ w - w_s \tag{2.38}$$

$$W_R = \begin{bmatrix} \bar{F} \\ T_{act}\big|_B - \mu\ \bar{F} - \sum_{i=1}^{n+1} S(r_i)\ w - S(r_s)\ w_s \end{bmatrix} \tag{2.39}$$

where here after n is added the additional thruster for changing the total weight of the system.

2.5 Aerodynamic Interaction

At this point, the aerodynamic interaction between the operating thrusters is investigated. The aerodynamic effects produced by each thruster are based on experiments that took place in Control Systems Lab NTUA on a $8 \times 4.7SF$ APC propeller accompanied with the Neu Motor NEU 1902/2Y - 2035 motor, which produces at 17550 rpm, $\lambda_{\max} = 28N$ thrust force. The surface, corresponding to every thruster, that approximates these effects is a third order equation in (SI). By expressing this surface to body attached thruster coordination frame $F_{T_i} = \{\hat{x}'_i, \hat{y}'_i, \hat{z}'_i\}, i = 1, ..., 6, a$ we get

$$\begin{cases} -0.06 \leq x'_i \leq 0.91 \\ (y'_i)^2 + (z'_i)^2 \leq \left[-1.11(x'_i)^3 + 1.56(x'_i)^2 - 0.31(x'_i) + 0.11\right]^2 \end{cases} \tag{2.40}$$

Hence, the aerodynamic effects of the air flow throughout the rotor are extended from $x = -0.06m$ to $x = 0.91m$ and x axis shows the length of the aerodynamic effect of the exit flow. In order to understand this one should consider the rotor/blade to be positioned at $x = 0$. On the other side, y axis shows the distance of the effect measured from the rotation axis of the blade, where at position $x = 0$, $y = 0.102m$ (SI) is the blade radius in approximation (because the existence of an offset).

The description of an arbitrary point $p = [x\ y\ z]^\tau$ expressed in F_B and the corresponding $p'_i = [x'_i\ y'_i\ z'_i]^\tau$ expressed in F_{T_i}, can be linked by an equation

$$p = \{TR_{F_B}^{F_{T_i}}(r_i, \hat{F}_i)\}\ p'_i \tag{2.41}$$

where $TR_{F_B}^{F_{T_i}}(r_i, \hat{F}_i)$ is the appropriate homogeneous frame transformation corresponding to the translation and orientation vectors $(r_i, \hat{F}_i)$. By combining the coordinates transformation equation with the constraints (2.40), a set of constraints that can be described in matrix form as $G(r_i, \hat{F}_i, p) \leq 0$, is produced. The distance between two such volumes i, j can defined and evaluated via the optimization problem (P_1) of Table 2.1.

(P_1)	$d_{ij}(r_i, \hat{F}_i, r_j, \hat{F}_j) = \min_{p_i, p_j} \|p_i - p_j\|$ $s.t.\quad G(r_i, \hat{F}_i, p_i) \leq 0$ $\quad\quad G(r_i, \hat{F}_i, p_j) \leq 0$
(P_2)	$\min_{r, \hat{F}}\ J(r)$ $s.t.\quad \sigma(D) \geq \epsilon_1$ $\quad\quad d_{ij} \geq \epsilon_2,\ \forall\, i, j = 1, 2, \ldots, n, \alpha$ $\quad\quad d_{ei} \geq R_e,\ \forall\ i = 1, 2, \ldots, n, \alpha$ $\quad\quad \hat{F}_a = -\sum_{i=1}^{n} \hat{F}_i$ $\quad\quad S(\hat{F}_a)\ r_a = -\sum_{i=1}^{n} S(\hat{F}_i)\ r_i$ $\quad\quad 1 \leq \kappa(D) \leq K$

TABLE 2.1: Optimization Problems

2.6 Design Problem

Given a particular structure defined by the matrices $(r,\ F)$, for a set of required actuation forces and torques $(F_{act}\big|_E, T_{act}\big|_E)$ it is necessary to find the associates levels

of the thrust forces λ_i. Since $W_R \in \mathbb{R}^6$, in order for (2.16) to have a solution for $\lambda \in \mathbb{R}^n$, the conditions $\{\text{rank}(D(r,F)) = 6, n \geq 6\}$ are required. The rank condition is adequate from a strict mathematical perspective but from a practical point of view, since the (2.16) leads to the thrust forces values $\lambda \in \mathbb{R}^n$ the sought solutions should not be very sensitive to small deviations. This is partially achieved by using the condition number

$$\kappa(D) = \frac{\sigma_{\max}(D)}{\sigma_{\min}(D)} \tag{2.42}$$

where $\sigma(D) = \sqrt{\text{eig}(D^\tau D)}$ are the singular values of matrix D, eig$(\cdot)$ denotes the eigenvalues of a matrix and $\sigma_{\max}(D), \sigma_{\min}(D)$ are the maximum and minimum singular values of matrix D respectively. Thus, a low condition number $\kappa(D) \geq 1$ is required [34]. Although the condition number is bounded to to take feasible values (not equal to zero/infinity) when $\sigma(D) \to 0$, the matrix $D(r,F)$ might be ill-conditioned and the determinate close to zero ($\det(D(r,F)) \approx 0$). Thus, $\sigma(D) \geq \epsilon_1 > 0$. Furthermore, as it is referred, to avoid fan interaction an other constraint is $d_{ij}(r_i, \hat{F}_i, r_j, \hat{F}_j) \geq \epsilon_2 > 0 \quad \forall i,j = 1,2,\ldots,n,\alpha$. Note that in resemblance to (P_1), it should be introduced to the design problem the position r_e as the avoidance between a sphere, (with R_e radius) that encloses the end-effector, and thrusters. This sphere when expressed to body attached end-effector coordination frame F_E is given by

$$(x'_e)^2 + (y'_e)^2 + (z'_e)^2 \leq R_e^2 \tag{2.43}$$

in correspondence to (2.40). Therefore, $d_{ei}(r_e, r_i) \geq R_e > 0 \quad \forall i = 1,2,\ldots,n,\alpha$. An optimization is also needed to minimize the volume of the system, which is translated with the norm function of the form: $J(r) = \|r\|_2$. Taking all these into account, the design problem is essentially recast to the optimization problem (P_2) from Table 2.1 where the optimization parameters are chosen as $K = 5$, $\epsilon_1 = 10^{-3}$, $\epsilon_2 = 10^{-2}\ m$, $R_e = 10^{-2}\ m$.

2.7 Solving the Optimization Problem

Notice that when solving the optimization problem (P_2) each time should be solved the inside optimization (P_1). But the number of thrusters is seven and in that way the total number of distances to be calculated is twenty one plus seven between the end-effector. The decision variables of the optimization problem will be 45 corresponding to seven position vectors and to seven directional vectors of each thruster and one position vector of the end-effector. That entails the necessity of solving twenty one

optimization problems for each evaluation of the outside problem (P_2). Although the problem (P_2) has smooth objective function the inequality constraints are nonsmooth, nonlinear and discontinuous.

More specifically, the inside optimization problem that refers to the avoidance of the fan interaction is smooth but in terms of the outside (P_2) is nonsmooth and nonlinear. This inside problem has one and only one minimum according to the inputs and that minimum is global. Moreover, both the objective function and the constraints of the problem are continuous. Therefore, it was solved with active-set strategy [35],[36] by using appropriate rotation and transformation matrices.

Since the design problem (P_2) has nonsmooth, discontinuous and nonlinear inequality constraints, it is used a non-gradient-based methodology that searches disjoint feasible regions. Therefore, for the pre search of the design space was chosen the Latin Hypercube (LHS) [37]. This ensures that the points are distributes throughout the search space, and Latin hypercube sampling is known to provide better coverage than simple random sampling, [38]. Following this was used a direct search algorithm called Generalized Pattern Search (GPS) [39],[40].

The thrust force (λ) and momentum (Q) can be computed from [41],[42] as

$$\begin{cases} Q = \pi\rho\ C_Q\ R^5\ \Omega^2 \\ \lambda = \pi\rho\ C_\lambda\ R^4\ \Omega^2 \end{cases} \quad \Leftrightarrow \quad Q = \frac{C_Q}{C_\lambda}\ R\ \lambda \tag{2.44}$$

where the term $\frac{C_Q}{C_\lambda}\ R$ corresponds to the μ coefficient, R is the radius of the rotor and ρ, Ω are the air density and the rotational speed of the rotor respectively. By applying a combination of Blade Element Theory [42] and Momentum Theory [33] and using modified versions proposed in [41], it was calculated in experiments held on CSL for the APC propeller that

$$C_\lambda = 0.008, C_Q = 0.0095, \mu = 0.1473, R = 0124m \tag{2.45}$$

Consequently, by solving the optimization, with the results depicted in Table 2.2, the $D(r, F)$ resulted as a full ranked matrix. For this solution of (P_2), all the constraints were satisfied and produced results that correspond to a low volume body structure with condition number $\kappa(D) = 3.36$. The above raised solution will be the one with which will be evaluated the actuating force and torque the Aerial Manipulator is capable to apply for the specific match of motor and propeller. Therefore, by using the above values and inserting the preferable actuating forces and torques $(F_{act}\big|_E, T_{act}\big|_E)$

the matrix W_R can be determined. Moreover, by using the (2.16) the propulsion effort λ can be identified since the matrix $D(r, F)$ is invertible. In that way, the maximum thrust force and torque the proposed system can apply are approximately $\lambda_{\max} = 28N$ and $3Nm$ respectively. The values of the components, proposed for the Aerial Manipulator are: the motor and propeller 0.12 kg, the frame 0.66 kg, the battery 0.25 kg and the electronic components 0.15 kg. Therefore, the total mass of the proposed system is $m = 1.90\ kg$ and the production of a carefully studied framework was achieved by using 3D CAD package (Solidworks) shown in Figures 2.3,2.4,2.5 and 2.6 based on which the mass and geometry properties of the table 2.2 have been evaluated. Some the parameters that are depicted in 2.2 will be introduced in the next Chapters.

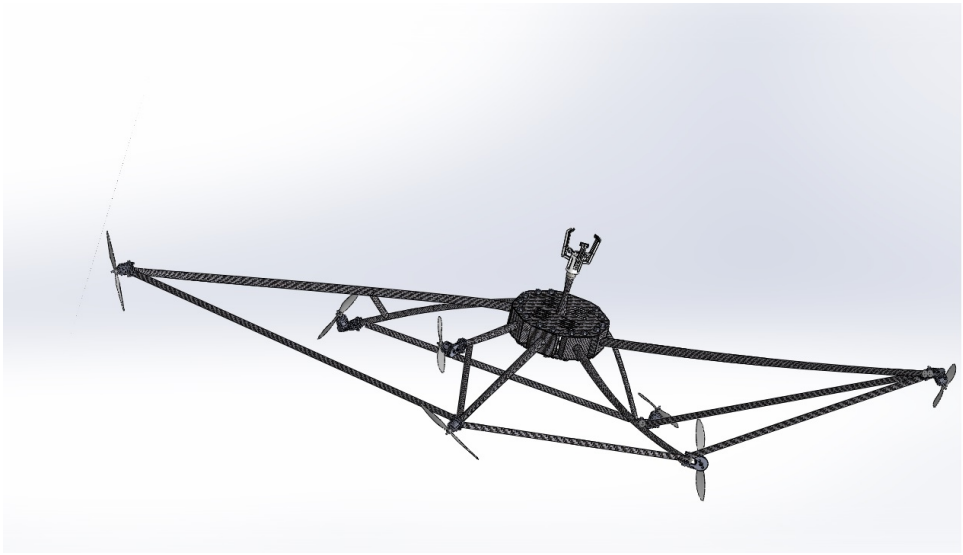

FIGURE 2.3: Aerial Manipulator 3D caption of the framework (1)

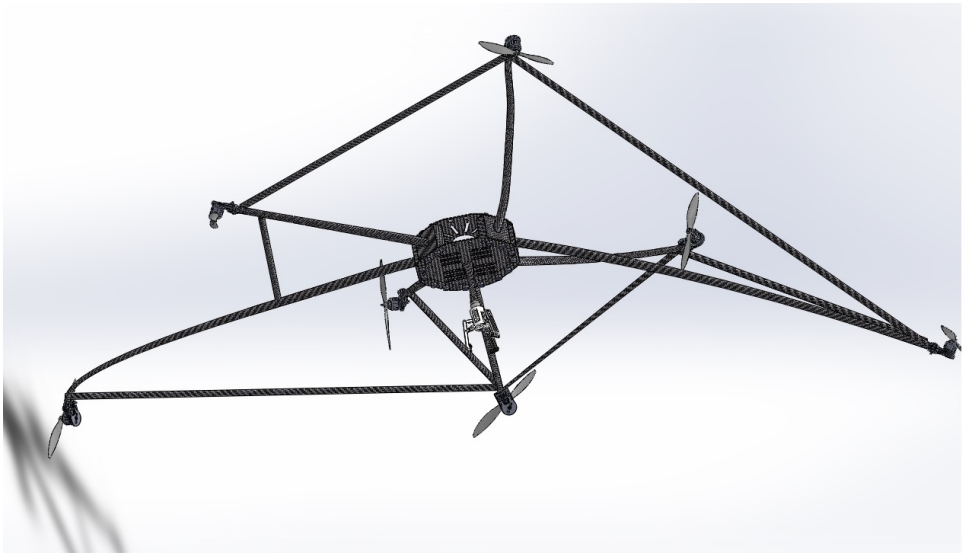

FIGURE 2.4: Aerial Manipulator 3D caption of the framework (2)

FIGURE 2.5: Aerial Manipulator 3D caption of the framework (3)

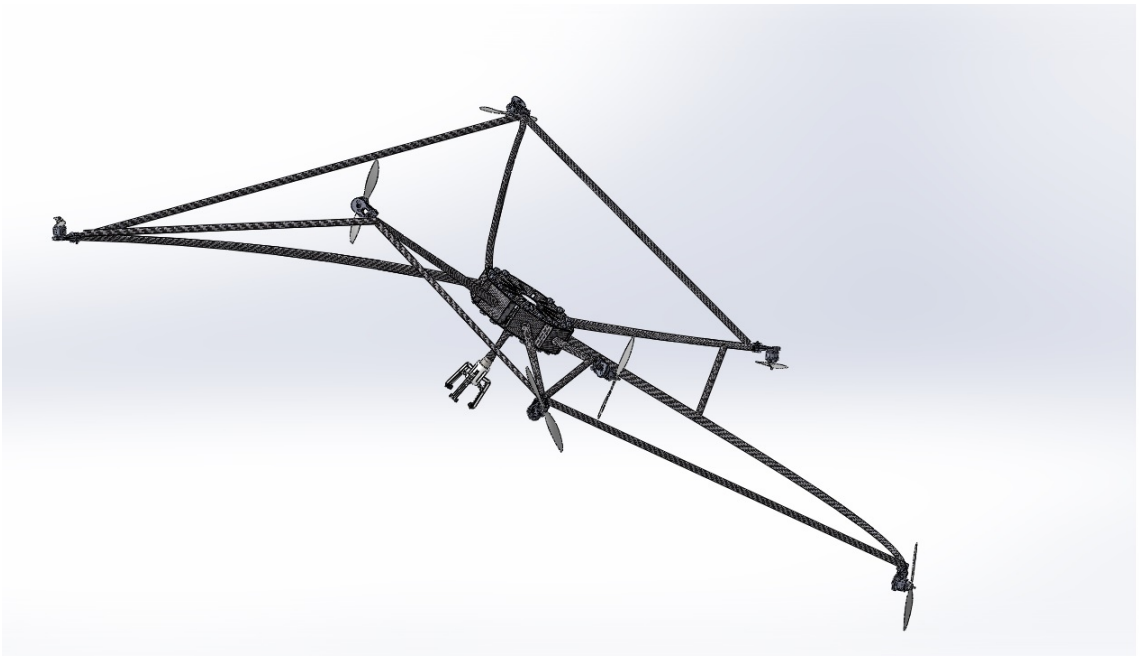

FIGURE 2.6: Aerial Manipulator 3D caption of the framework (4)

Parameters	Description	Value	Units
m	Total Mass	1.90	kg
m_s	Rest of Structure Mass	1.06	kg
m_{thr}	Thruster Mass	0.12	kg
I_G	Moment of Inertia Tensor	$\begin{bmatrix} 0.3488 & 0.0683 & -0.0457 \\ 0.0683 & 0.1588 & 0.0144 \\ -0.0457 & 0.0144 & 0.4081 \end{bmatrix}$	$kg\ m^2$
r_G	Center of Gravity Position	$[0.0737\ 0.0083\ -0.0781]^\tau$	m
r_e	End-Effector Position	$[-0.23\ -0.15\ 0.23]^\tau$	m
r_s	Rest of Structure Center of Gravity	$[0.1267\ -0.0052\ -0.1900]^\tau$	m
$J(r)$	Structure Total Volume	1.80018	m^3
R	Radius of the Rotor	0.124	m
g	Gravitational Acceleration	9.81	m/s^2
r_i	Thruster Positions	$r_1 = [0.43\ -0.15\ -0.44]^\tau$ $r_2 = [0.08\ -0.22\ -0.14]^\tau$ $r_3 = [0.1\ -0.9 - 0.2]^\tau$ $r_4 = [-0.34\ 0.25\ 0.006]^\tau$ $r_5 = [0.184\ 0.359\ -0.254]^\tau$ $r_6 = [-0.22\ -0.44\ -0.04]^\tau$ $r_7 = [0.51\ 0.79\ -0.06]^\tau$	m
$\hat{F}_i$	Thruster Orientations	$\hat{F}_1 = [0.08\ 0.39\ 0.92]^\tau$ $\hat{F}_2 = [-0.33\ -0.90\ 0.29]^\tau$ $\hat{F}_3 = [0.13\ -0.87\ -0.48]^\tau$ $\hat{F}_4 = [0.56\ 0.08\ 0.82]^\tau$ $\hat{F}_5 = [0.83\ 0.11\ -0.55]^\tau$ $\hat{F}_6 = [-0.66\ 0.57\ -0.49]^\tau$ $\hat{F}_7 = [-0.59\ 0.62\ -0.51]^\tau$	

Table 2.2: Aerial Manipulator Parameters

Chapter 3

Kinematic Analysis

3.1 Introduction

In this chapter the differential kinematic analysis of the proposed aerial manipulator system is provided. It is divided into two parts. The first part deals with the differential kinematic analysis of the system rigid body, and the second one deals with the kinematic equations of end-effector of the manipulator. In order to analyze the motion of the proposed system, several reference frames need to be defined. As in all problems in robotics, various quantities are represented in different coordinate frames and there is the need for transformation of them between frames.

3.2 Deriving the Kinematic Equations of the Rigid Body

The aerial manipulator is consisted of the main body, which is assumed to be rigid and the end-effector which provides the contact between the robot system and the environment. The end-effector is rigidly connected to the main body with a link and there are no extra joints. This means that end-effector does not increase the system's Degrees of Freedom (DOF). The analytical mechanical design process of the system was given in previous chapter. The goal here is to derive the kinematic equations for the motion of the system in 3D task space.

Consider the structure in Figure 2.1 of the proposed aerial manipulator system with reference frames. An aerial manipulator moves in six degrees of freedom (DOF). Thus,

to describe its motion, we need to consider three coordinates to define translations and three coordinates to define the orientation. These coordinates are defined using two types of reference frames: the Earth-fixed frame and the Body-Fixed frame. In this chapter, the derivation of the body's motion and velocity transformations are provided. Forces and torques that are produced by the thrusters and gravitational forces will be used in dynamic model. They do not affect the kinematic model. The basic ideas for the analysis in this chapter are discussed in [43], [44], [45]. The goal is to correlate the linear and angular velocity of Body-Fixed frame with the derivatives of position and orientation of the Inertial frame. This correlation is well-known from the robotics as the Analytical Jacobian Matrix [46].

Due to the fact that there are several types of relative positions, orientations and velocities, a strict mathematical formulation will be provided.

To begin the kinematic analysis, first are defined the system reference frames.

- The frame

$$F_A = \{\hat{x}_A \quad \hat{y}_A \quad \hat{z}_A\} \tag{3.1}$$

is the Earth-Fixed frame which is assumed to be an Inertial frame. The origin a of frame F_A is any convenient point on the Earth. We assume that the system moves in near-Earth gravity and the effect of gravity is uniform over the system, thus center of mass coincides with the center of gravity G. It is also well-known in literature as the generalized earth coordination system.

- The moving frame

$$F_B = \{\hat{x}_B \quad \hat{y}_B \quad \hat{z}_B\} \tag{3.2}$$

is conveniently fixed to the body and is called Body-Fixed reference frame. Its origin is the point b and rotates according to the rotation of the rigid body. Note that point b is not coincided with the center of gravity (it is useful for the dynamic analysis in the next chapter). The orientation of the rigid body is defined by the orientation of the Body-Fixed frame. The position and orientation of the flying manipulator should be described relative to the Inertial reference frame F_A while linear and angular velocity of the body should be expressed in the body-fixed coordinate system. In this point, it should be mentioned that the reader should not be confused by the term "resolving a vector to a frame". This term is the same as the bibliographically well-known term "the vector is expressed".

Let $p \in \mathbb{R}^3$

$$p = [x \quad y \quad z]^\tau \tag{3.3}$$

be the position vector of frame F_B relative to the Inertial frame F_A, resolved in frame F_A. The vector $\dot{p} \in \mathbb{R}^3$ is the linear velocity of F_B relative to F_A with respect to F_A, resolved in frame F_A. The vector $v \in \mathbb{R}^3$ is defined as

$$v = [v_x \quad v_y \quad v_z]^\tau \tag{3.4}$$

as the linear velocity of F_B relative to F_A with respect to F_A, resolved in the body-fixed frame F_B. The vector $\dot{v} \in \mathbb{R}^3$ is the linear acceleration of F_B relative to F_A with respect to F_A, resolved in the body-fixed frame F_B.

The Body-Fixed frame is related to the Inertial frame by a $\psi - \theta - \phi$ Euler angle rotation sequence applied to the Inertial frame. The term Euler angles refers to the angles of rotation ψ, θ, ϕ needed to go from one coordinate system to another using the specific sequence of rotations Yaw, Pitch, Roll. These operations yield two intermediate frames, namely

$$F_{A'} = \{\hat{x}_{A'} \quad \hat{y}_{A'} \quad \hat{z}_{A'}\} \tag{3.5}$$

$$F_{A''} = \{\hat{x}_{A''} \quad \hat{y}_{A''} \quad \hat{z}_{A''}\} \tag{3.6}$$

for the rotation from frame F_A to F_B. Therefore, the overal rotations are

$$F_A \xrightarrow[\hat{z}]{\psi} F_{A'} \xrightarrow[\hat{y}]{\theta} F_{A''} \xrightarrow[\hat{x}]{\phi} F_B \tag{3.7}$$

It is generally satisfied for Euler angles that

$$-\frac{\pi}{2} < \theta < \frac{\pi}{2} \tag{3.8}$$

Assumption (3.8) is totally crucial for the rest of the work and will be used many times. This assumption can be likewise found in publications [47], [48]. Let now define $\Theta \in \mathbb{R}^3$

$$\Theta = [\phi \quad \theta \quad \psi]^\tau \tag{3.9}$$

as the Euler angles vector of frame F_B relative to the Inertial frame F_A. The vector $\dot{\Theta} \in \mathbb{R}^3$ is the angular velocity of F_B relative to F_A, resolved in the frame F_A.

The orientation matrices corresponding to the three rotations are given by

$$O_{B/A''} = O_1(\phi) = \begin{bmatrix} 1 & 0 & 0 \\ 0 & c_\phi & s_\phi \\ 0 & -s_\phi & c_\phi \end{bmatrix} \in SO(3) \tag{3.10}$$

$$O_{A''/A'} = O_2(\theta) = \begin{bmatrix} c_\theta & 0 & -s_\theta \\ 0 & 1 & 0 \\ s_\theta & 0 & c_\theta \end{bmatrix} \in SO(3) \tag{3.11}$$

$$O_{A'/A} = O_3(\psi) = \begin{bmatrix} c_\psi & s_\psi & 0 \\ -s_\psi & c_\psi & 0 \\ 0 & 0 & 1 \end{bmatrix} \in SO(3) \tag{3.12}$$

where

$$SO(n) = \left\{ R \in \mathbb{R}^{n \times n} : R\ R^\tau = I_n, \det(R) = \pm 1 \right\} \tag{3.13}$$

is the set of all orthogonal matrices with determinant equal to 1 or -1. Therefore, using formulas (3.10)-(3.12), the orientation of the frame F_A relative to the frame F_B can be calculated as

$$\begin{aligned} O_{A/B} &= \left[O_{B/A}\right]^\tau \\ &= \left[O_{B/A''}\ O_{A''/A'}\ O_{A'/A}\right]^\tau \\ &= \left[O_1(\phi)\ O_2(\theta)\ O_3(\psi)\right]^\tau \\ &= \begin{bmatrix} c_\theta\ c_\psi & s_\phi\ s_\theta\ c_\psi - s_\psi\ c_\phi & s_\theta\ c_\phi\ c_\psi + s_\phi\ s_\psi \\ s_\psi\ c_\theta & s_\phi s_\theta s_\psi + c_\phi c_\psi & s_\theta\ s_\psi\ c_\phi - s_\phi\ c_\psi \\ -s_\theta & s_\phi\ c_\theta & c_\phi\ c_\theta \end{bmatrix} \end{aligned} \tag{3.14}$$

It is defined the Jacobian transformation matrix $J_t(\Theta) \in \mathbb{R}^{3\times3}$ expressing the transformation from the Body-Fixed frame F_B to the Inertial frame F_A as

$$J_t(\Theta) = O_{A/B} \tag{3.15}$$

This matrix is useful for transforming vectors from frame F_B to F_A and is usually denoted in bibliography as ${}^A R_B$.

We define now the position vector of point b relative to point a as

$$\vec{r}_{b/a} = x\ \hat{i}_A + y\ \hat{j}_A + z\ \hat{k}_A \tag{3.16}$$

For the time derivative of the unit vectors $\hat{x}_A, \hat{y}_A, \hat{z}_A$ with reference to frame F_A it holds that

$$\overset{A\bullet}{\hat{x}}_A = \overset{A\bullet}{\hat{y}}_A = \overset{A\bullet}{\hat{z}}_A = 0 \tag{3.17}$$

since the frame vectors of F_A are constant with respect to this frame. Differentiating (3.16) with respect to frame F_A we have

$$\begin{aligned} \overset{A\bullet}{\vec{r}}_{b/a} = \vec{\nu}_{b/a/A} &= \dot{p}_x\ \hat{x}_A + p_x \overset{A\bullet}{\hat{x}}_A + \dot{p}_y\ \hat{y}_A + p_y \overset{A\bullet}{\hat{y}}_A + \dot{p}_z\ \hat{z}_A + p_z \overset{A\bullet}{\hat{z}}_A \\ &= \dot{p}_x\ \hat{x}_A + \dot{p}_y\ \hat{y}_A + \dot{p}_z\ \hat{z}_A \end{aligned} \tag{3.18}$$

and resolving in frame F_A leads to

$$\left.\overset{A\bullet}{\vec{r}}_{b/a}\right|_A = \left.\vec{\nu}_{b/a/A}\right|_A = \dot{p} = [\dot{x} \quad \dot{y} \quad \dot{z}]^\tau \tag{3.19}$$

Using now the definition (3.4) of the vector v we have

$$\vec{\nu}_{b/a/A} = v_x\ \hat{x}_B + v_y\ \hat{y}_B + v_z\ \hat{z}_B \tag{3.20}$$

and thus $\vec{\nu}_{b/a/A}$ resolved in body-fixed frame is given by

$$\left.\vec{\nu}_{b/a/A}\right|_B = [v_x \quad v_y \quad v_z]^\tau = v \tag{3.21}$$

On the other hand, if $\vec{\nu}_{b/a/A}$ is resolved in frame F_A and using the basic formula

$$\left.\vec{x}\right|_A = O_{A/B}\ \left.\vec{x}\right|_B \tag{3.22}$$

for any arbitrary vector $\vec{x}$ from [45], we get

$$\begin{aligned}
\vec{\nu}_{b/a/A}\Big|_A &= v_x\ \hat{x}_B\Big|_A + v_y\ \hat{y}_B\Big|_A + v_z\ \hat{z}_B\Big|_A \\
&= v_x\ O_{A/B}\ \hat{x}_B\Big|_B + v_y\ O_{A/B}\ \hat{y}_B\Big|_B + v_z\ O_{A/B}\ \hat{z}_B\Big|_B \\
&= v_x\ O_{A/B}\ e_1 + v_y\ O_{A/B}\ e_2 + v_z\ O_{A/B}\ e_3 \\
&= O_{A/B}\ \ (v_x\ e_1 + v_y\ e_2 + v_z\ e_3) \\
&= O_{A/B}\ \left(\begin{bmatrix} v_x \\ 0 \\ 0 \end{bmatrix} + \begin{bmatrix} 0 \\ v_y \\ 0 \end{bmatrix} + \begin{bmatrix} 0 \\ 0 \\ v_z \end{bmatrix} \right) \\
&= O_{A/B}\ \begin{bmatrix} v_x \\ v_y \\ v_z \end{bmatrix} \\
\Rightarrow \begin{bmatrix} \dot{x} \\ \dot{y} \\ \dot{z} \end{bmatrix} &= O_{A/B}\ \begin{bmatrix} v_x \\ v_y \\ v_z \end{bmatrix}
\end{aligned} \tag{3.23}$$

where $e_1 = [1\ 0\ 0]^\tau, e_2 = [0\ 1\ 0]^\tau$ and $e_3 = [0\ 0\ 1]^\tau$. Now, by substituting (3.15) in (3.23) the following transformation holds

$$\begin{bmatrix} \dot{x} \\ \dot{y} \\ \dot{z} \end{bmatrix} = J_t(\Theta)\ \begin{bmatrix} v_x \\ v_y \\ v_z \end{bmatrix} \tag{3.24}$$

which denotes the relationship between Earth-Fixed and Body-Fixed linear velocities of the rigid body of the proposed aerial system and can be represented in a more compact form as

$$\dot{p} = J_t(\Theta)\ v \tag{3.25}$$

It should be noted that, any vector in Body-Fixed frame can be expressed in the corresponding Inertial frame with transformation $J_t(\Theta)$. Now, as regards the rigid body's rotation motion, we define $\omega \in \mathbb{R}^3$

$$\omega = [\omega_x \quad \omega_y \quad \omega_z]^\tau \tag{3.26}$$

as the angular velocity of F_B relative to F_A resolved in the body-fixed frame F_B. The vector $\dot{\omega} \in \mathbb{R}^3$ is the angular acceleration of F_B relative to F_A. It is known that (see [45]) if $\hat{n}$ is a unit vector in the direction of the rotation, then the angular velocity is

given by

$$\vec{\omega} = \dot{x}\ \hat{n} \tag{3.27}$$

for an arbitrary angle x. The angular velocity can be easily related to the derivatives of Euler angles. For a $\psi - \theta - \phi$ angle rotation we have the sequence of rotations

$$F_A \xrightarrow[\hat{k}_{A'}]{\psi} F_{A'} \iff \vec{\omega}_{A'/A} = \dot{\psi}\ \hat{z}_{A'} \tag{3.28}$$

$$F_{A'} \xrightarrow[\hat{y}_{A''}]{\theta} F_{A''} \iff \vec{\omega}_{A''/A'} = \dot{\theta}\ \hat{y}_{A''} \tag{3.29}$$

$$F_{A''} \xrightarrow[\hat{x}_B]{\phi} F_B \iff \vec{\omega}_{B/A''} = \dot{\phi}\ \hat{x}_B \tag{3.30}$$

Using the addition theorem for angular velocities and formulas (3.28)-(3.30), the angular velocity of frame F_B relative to F_A is given by

$$\begin{aligned}\vec{\omega}_{B/A} &= \vec{\omega}_{B/A''} + \vec{\omega}_{A''/A'} + \vec{\omega}_{A'/A} \\ &= \dot{\phi}\ \hat{x}_B + \dot{\theta}\ \hat{y}_{A''} + \dot{\psi}\ \hat{z}_{A'}\end{aligned} \tag{3.31}$$

Using the orientation matrices from equations (3.10)-(3.12) the unit vectors of frames $F_{A'}, F_{A''}$ and F_B are related by the transformations

$$\begin{aligned}\begin{bmatrix}\hat{x}_B \\ \hat{y}_B \\ \hat{z}_B\end{bmatrix} &= O_1(\phi) \begin{bmatrix}\hat{x}_{A''} \\ \hat{y}_{A''} \\ \hat{z}_{A''}\end{bmatrix} \\ \iff \begin{bmatrix}\hat{x}_{A''} \\ \hat{y}_{A''} \\ \hat{z}_{A''}\end{bmatrix} = [O_1(\phi)]^\tau \begin{bmatrix}\hat{x}_B \\ \hat{y}_B \\ \hat{z}_B\end{bmatrix} &= \begin{bmatrix}1 & 0 & 0 \\ 0 & c_\phi & -s_\phi \\ 0 & s_\phi & c_\phi\end{bmatrix} \begin{bmatrix}\hat{x}_B \\ \hat{y}_B \\ \hat{z}_B\end{bmatrix}\end{aligned} \tag{3.32}$$

and

$$\begin{aligned}\begin{bmatrix}\hat{x}_{A''} \\ \hat{y}_{A''} \\ \hat{z}_{A''}\end{bmatrix} &= O_2(\theta) \begin{bmatrix}\hat{x}_{A'} \\ \hat{y}_{A'} \\ \hat{z}_{A'}\end{bmatrix} \\ \iff \begin{bmatrix}\hat{x}_{A'} \\ \hat{y}_{A'} \\ \hat{z}_{A'}\end{bmatrix} = [O_2(\theta)]^\tau \begin{bmatrix}\hat{x}_{A''} \\ \hat{y}_{A''} \\ \hat{z}_{A''}\end{bmatrix} &= [O_2(\theta)]^\tau\ [O_1(\phi)]^\tau \begin{bmatrix}\hat{x}_B \\ \hat{y}_B \\ \hat{z}_B\end{bmatrix} \\ &= \begin{bmatrix}c_\theta & s_\phi s_\theta & s_y c_\phi \\ 0 & c_\phi & -s_\phi \\ -s_\theta & s_\phi c_\theta & c_\phi c_\theta\end{bmatrix} \begin{bmatrix}\hat{x}_B \\ \hat{y}_B \\ \hat{z}_B\end{bmatrix}\end{aligned} \tag{3.33}$$

Substituting (3.32), (3.33) in (3.31) the following equation

$$\begin{aligned}\vec{\omega}_{B/A} &= \dot{\phi}\ \hat{x}_B + \dot{\theta}\ [c_\phi\ \hat{y}_B - s_\phi\ \hat{z}_B] \\ &\quad + \dot{\psi}\ [-s_\theta\ \hat{x}_B + s_\phi c_\theta\ \hat{y}_B + c_\phi c_\theta\ \hat{z}_B] \\ &= \left[\dot{\phi} - s_\theta\ \dot{\psi}\right]\ \hat{x}_B + \left[c_\phi\ \dot{\theta} + s_\phi c_\theta\ \dot{\psi}\right]\ \hat{y}_B \\ &\quad + \left[c_\phi c_\theta\ \dot{\psi} - s_\phi\ \dot{\theta}\right]\ \hat{z}_B \end{aligned} \tag{3.34}$$

is obtained. Resolving (3.34) in frame F_B yields

$$\vec{\omega}_{B/A}\Big|_B = \begin{bmatrix} \dot{\phi} - s_\theta\ \dot{\psi} \\ c_\phi\ \dot{\theta} + s_\phi c_\theta\ \dot{\psi} \\ c_\phi c_\theta\ \dot{\psi} - s_\phi\ \dot{\theta} \end{bmatrix} = \begin{bmatrix} 1 & 0 & -s_\theta \\ 0 & c_\phi & s_\phi c_\theta \\ 0 & -s_\phi & c_\phi c_\theta \end{bmatrix} \begin{bmatrix} \dot{\phi} \\ \dot{\theta} \\ \dot{\psi} \end{bmatrix} \tag{3.35}$$

By the definition (3.26) of the vector ω we have

$$\vec{\omega}_{B/A}\Big|_B = \omega = [\omega_x \quad \omega_y \quad \omega_z]^\tau \tag{3.36}$$

Comparing equations (3.35), (3.36) we have

$$\begin{bmatrix} \omega_x \\ \omega_y \\ \omega_z \end{bmatrix} = \begin{bmatrix} 1 & 0 & -s_\theta \\ 0 & c_\phi & s_\phi c_\theta \\ 0 & -s_\phi & c_\phi c_\theta \end{bmatrix} \begin{bmatrix} \dot{\phi} \\ \dot{\theta} \\ \dot{\psi} \end{bmatrix} \tag{3.37}$$

Now by computing the inverse matrix we get

$$\begin{bmatrix} \dot{\phi} \\ \dot{\theta} \\ \dot{\psi} \end{bmatrix} = \begin{bmatrix} 1 & s_\phi t_\theta & c_\phi t_\theta \\ 0 & c_\phi & -s_\phi \\ 0 & \frac{s_\phi}{c_\theta} & \frac{c_\phi}{c_\theta} \end{bmatrix} \begin{bmatrix} \omega_x \\ \omega_y \\ \omega_z \end{bmatrix} \tag{3.38}$$

This relationship can be represented in compact form as

$$\dot{\Theta} = J_r(\Theta)\ \omega \tag{3.39}$$

where $J_r(\Theta) \in \mathbb{R}^{3\times 3}$ is denoted as

$$J_r(\Theta) = \begin{bmatrix} 1 & s_\phi\ t_\theta & c_\phi\ t_\theta \\ 0 & c_\phi & -s_\phi \\ 0 & \dfrac{s_\phi}{c_\theta} & \dfrac{c_\phi}{c_\theta} \end{bmatrix} \tag{3.40}$$

Collecting the equations (3.15), (3.40) in 6 dimensional matrix forms we have the kinematic differential model for the rigid body of the proposed system

$$\dot{\xi} = \begin{bmatrix} \dot{p} \\ \dot{\Theta} \end{bmatrix} = \underbrace{\begin{bmatrix} J_t(\Theta) & O_{(3\times3)} \\ O_{(3\times3)} & J_r(\Theta) \end{bmatrix}}_{J_o(\Theta)} \begin{bmatrix} v \\ \omega \end{bmatrix} \tag{3.41}$$

where $\xi \in \mathbb{R}^6$ is the augmented position and orientation vector expressed in Earth-Fixed frame. Matrix $J_t(\Theta) \in SO(3)$ transforms a vector from the Body-Fixed frame to the Inertial coordination and the matrix $J_r(\Theta) \in \mathbb{R}^{3\times3}$ denotes the relation in the rate of change of the Euler-Angles and the Body-Fixed angular velocities of the rigid body of the proposed system. If needed the overall analytic form, this is

$$\begin{bmatrix} \dot{x} \\ \dot{y} \\ \dot{z} \\ \dot{\phi} \\ \dot{\theta} \\ \dot{\psi} \end{bmatrix} = \begin{bmatrix} c_\theta\ c_\psi & s_\phi\ s_\theta\ c_\psi - s_\psi\ c_\phi & s_\theta\ c_\phi\ c_\psi + s_\phi\ s_\psi & 0 & 0 & 0 \\ s_\psi\ c_\theta & s_\phi s_\theta s_\psi + c_\phi c_\psi & s_\theta\ s_\psi\ c_\phi - s_\phi\ c_\psi & 0 & 0 & 0 \\ -s_\theta & s_\phi\ c_\theta & c_\phi\ c_\theta & 0 & 0 & 0 \\ 0 & 0 & 0 & 1 & s_\phi\ t_\theta & c_\phi\ t_\theta \\ 0 & 0 & 0 & 0 & c_\phi & -s_\phi \\ 0 & 0 & 0 & 0 & \frac{s_\phi}{c_\theta} & \frac{c_\phi}{c_\theta} \end{bmatrix} \begin{bmatrix} v_x \\ v_y \\ v_z \\ \omega_x \\ \omega_y \\ \omega_z \end{bmatrix} \tag{3.42}$$

One issue that is general confused in bibliography is that the vector $\dot{\Theta} = [\dot{\phi} \quad \dot{\theta} \quad \dot{\psi}]^\tau$ is the time derivative (rate of change) of Euler angles, not the angular velocity of the body with reference to to Inertial frame. In order to find the relation between the time derivative of Euler angles and the angular velocity expressed in Inertial we can apply the following procedure.

Using transformation (3.25) obviously the angular velocity in Body-Fixed and Inertial frame respectively is given by the relation

$$\begin{aligned} \vec{\omega}_{B/A}\Big|_A &= J_t(\Theta)\ \vec{\omega}_{B/A}\Big|_B \\ \Leftrightarrow \vec{\omega}_{B/A}\Big|_A &= J_t(\Theta)\ \omega \end{aligned} \tag{3.43}$$

By computing the inverse transformation from equation (3.39) the following equation holds

$$\omega = (J_r(\Theta))^{-1}\ \dot{\Theta} \tag{3.44}$$

Combining the previous equations (3.43), (3.44) we have

$$\begin{aligned}
\vec{\omega}_{B/A}\Big|_A &= J_t(\Theta)\ \ (J_r(\Theta))^{-1}\ \ \dot{\Theta} \\
\Leftrightarrow \dot{\Theta} &= \left(J_t(\Theta)\ \ (J_r(\Theta))^{-1}\right)^{-1}\ \ \vec{\omega}_{B/A}\Big|_A \\
\Leftrightarrow \dot{\Theta} &= (J_r(\Theta))^{-1}\ \ (J_t(\Theta))^{-1}\ \ \vec{\omega}_{B/A}\Big|_A \\
\Leftrightarrow \dot{\Theta} &= J_r(\Theta)\ \ (J_t(\Theta))^{-1}\ \ \vec{\omega}_{B/A}\Big|_A
\end{aligned} \tag{3.45}$$

The matrix $J_t(\Theta) \in SO(3)$ is orthogonal, hence

$$J_t^{-1}(\Theta) = J_t^{\tau}(\Theta) \tag{3.46}$$

Therefore, combining equations (3.45), (3.46) finally results in

$$\dot{\Theta} = J_r(\Theta)\ \ (J_t(\Theta))^{\tau}\ \ \vec{\omega}_{B/A}\Big|_A \tag{3.47}$$

The last equation denotes the transformation between the rate of change of Euler angles and the angular velocity of the body expressed in Earth-Fixed frame, terms that are confused in many books.

3.3 Deriving the Kinematic Equations of the End-Effector

The tasks for the proposed manipulation system require the knowledge of the absolute position and orientation of end-effector with reference to the Earth-Fixed frame. The aim here is to correlate the velocities of end-effector in Cartesian $\mathbb{R}^6$ space with the translational and angular velocity of the rigid body. To begin with, let

$$F_E = \{\hat{x}_E \quad \hat{y}_E \quad \hat{z}_E\} \tag{3.48}$$

be a frame that is attached to the end-effector. The vector $r_e \in \mathbb{R}^3$ is defined as

$$r_e = [r_e^x \quad r_e^y \quad r_e^z]^{\tau} = \vec{r}_{e/b}\Big|_B \tag{3.49}$$

as the position of the end-effector point e with reference to the point b, expressed in Body-Fixed frame. Let $p_e \in \mathbb{R}^3$

$$p_e = [x_e \quad y_e \quad z_e]^\tau \tag{3.50}$$

be the position vector of end-effector relative to the Inertial frame F_A, resolved in frame F_A. The vector $\dot{p}_e \in \mathbb{R}^3$ is the linear velocity of F_E relative to F_A, resolved in frame F_A. The Euler angles vector $\Theta_e = [\phi \quad \theta \quad \psi]^\tau \in \mathbb{R}^3$ of frame F_B relative to the Inertial frame F_A and the vector $\dot{\Theta}_e \in \mathbb{R}^3$ as the angular velocity of F_B relative to F_A, resolved in the frame F_A are also defined.

In the rest of the thesis the issue of skew-symmetric matrix $S(\cdot)$ will be used several times. Skew-symmetric matrices are very important for 3D Kinematic and Dynamic analysis. These properties will be crucial in this thesis, therefore the main properties are presented below. We define the skew-symmetric matrix

$$S(\omega) = \begin{bmatrix} 0 & -\omega_z & \omega_y \\ \omega_z & 0 & -\omega_x \\ -\omega_y & \omega_x & 0 \end{bmatrix}, S \in SS(3) \tag{3.51}$$

for all arbitrary vectors $\omega = [\omega_x \;\; \omega_y \;\; \omega_z]^\tau \in \mathbb{R}^3$ where

$$SS(n) = \left\{ R \in \mathbb{R}^{n \times n} : R = -R^\tau \right\} \tag{3.52}$$

is the set of all skew-symmetric matrices. The basic properties of skew-symmetric matrices are

- Any cross product can be written in matrix form as

$$\omega_1 \times \omega_2 = S(\omega_1)\, \omega_2 = -S(\omega_2)\, \omega_1, \quad \forall\, \omega_1, \omega_2 \in \mathbb{R}^3 \tag{3.53}$$

- The determinant of a skew-symmetric matrix follows the formula

$$\mathbf{det}(S) = 0, \; \forall\, S \in SS(3) \tag{3.54}$$

- Multiplication with rotation matrices

$$S(R\, \omega) = R\, S(\omega)\, R^\tau, \; \forall\, S \in SS(3), \; \forall\, R \in SO(3), \; \forall\, \omega \in \mathbb{R}^3 \tag{3.55}$$

Continuing the previous analysis, the position of F_E with respect to F_A is given by

$$\vec{r}_{e/a} = \vec{r}_{b/a} + \vec{r}_{e/b} \tag{3.56}$$

Resoling in frame F_A the following equations hold

$$\begin{aligned}
&\vec{r}_{e/a}\Big|_A = \vec{r}_{b/a}\Big|_A + \vec{r}_{e/b}\Big|_A \\
&\Leftrightarrow p_e = p + O_{A/B}\ \vec{r}_{e/b}\ \Big|_B \\
&\Leftrightarrow p_e = p + O_{A/B}\ r_e \\
&\Leftrightarrow p_e = p + J_t(\Theta)\ r_e
\end{aligned} \tag{3.57}$$

Differentiating (3.57) and using the basic formula $\dot{J}_t(\Theta) = J_t(\Theta)\ S(\omega)$ from [47] we have

$$\begin{aligned}
\dot{p}_e &= \dot{p} + \dot{J}_t(\Theta)\ r_e + J_t(\theta)\ \dot{r}_e \\
&= J_t(\Theta)\ v + \dot{J}_t(\Theta)\ r_e + J_t(\theta)\ \dot{r}_e \\
&= J_t(\Theta)\ v + J_t(\Theta)\ S(\omega)\ r_e + J_t(\theta)\ \dot{r}_e \\
&= J_t(\Theta)\ v - J_t(\Theta)\ S(r_e)\ \omega + J_t(\theta)\ \dot{r}_e
\end{aligned} \tag{3.58}$$

It should be noted here that the end-effector is not moving with reference to the rigid body because of there are no extra joints between end-effector and the rigid body. Two points attached to rigid body remain fixed with respect to each other for all $t \geq 0$. Thus, a relative motion between the end-effector and the rigid-body does not exist. Invoking this result, we have that the vector r_e is constant in time i.e.

$$\dot{r}_e = 0 \tag{3.59}$$

and the angular velocity of frame F_E relative to F_B is

$$\vec{\omega}_{E/B} = 0 \tag{3.60}$$

The equation (3.58) is modified as

$$\dot{p}_e = J_t(\Theta)\ v - J_t(\Theta)\ S(r_e)\ \omega \tag{3.61}$$

The angular velocity of frame F_E relative to F_A is given by

$$\vec{\omega}_{E/A} = \vec{\omega}_{E/B} + \vec{\omega}_{B/A} = \vec{\omega}_{B/A} \tag{3.62}$$

Resolving in frame F_B we get

$$\vec{\omega}_{E/A}\Big|_B = \vec{\omega}_{B/A}\Big|_B = \omega \tag{3.63}$$

Using the corresponding transformation (3.39) for the end-effector it holds that

$$\begin{aligned} \dot{\Theta}_e &= J_r(\Theta_e)\ \vec{\omega}_{E/A}\Big|_E \\ &= J_r(\Theta_e)\ O_{E/B}\ \vec{\omega}_{E/A}\Big|_B \\ &= J_r(\Theta_e)\ O_{E/B}\ \omega \end{aligned} \tag{3.64}$$

As mentioned in Chapter 2 the Body-Fixed and the End-Effector frame have the same orientation with reference to the Inertial frame. Thus,

$$O_{E/B} = I_3 \tag{3.65}$$

$$\Theta_e = \Theta \tag{3.66}$$

where I_3 is the 3×3 identity matrix and the (3.64) is modified as

$$\dot{\Theta}_e = J_r(\Theta_e)\ O_{E/B}\ \omega \Leftrightarrow \dot{\Theta} = J_r(\Theta)\ \omega \tag{3.67}$$

Combining the last result with equation (3.61) it eventually follows that

$$\dot{\xi}_e = \begin{bmatrix} \dot{p}_e \\ \dot{\Theta} \end{bmatrix} = \underbrace{\begin{bmatrix} J_t(\Theta) & -J_t(\Theta)\ S(r_e) \\ O_{(3\times3)} & J_r(\Theta) \end{bmatrix}}_{J_e(\Theta)} \begin{bmatrix} v \\ \omega \end{bmatrix} \tag{3.68}$$

where $\xi_e \in \mathbb{R}^6$, $p = [x_e\ y_e\ z_e]^\tau \in \mathbb{R}^3$ denotes the position of the end-effector expressed in the Earth-Fixed frame, r_e is the position of end-effector with reference to Body-Fixed frame. Equation (3.68) is the total differential kinematic equation of the proposed system and the main objective of the chapter is achieved. The Jacobian matrix of the system is given by

$$J_e(\Theta) = \begin{bmatrix} J_t(\Theta) & -J_t(\Theta)\ S(r_e) \\ O_{(3\times3)} & J_r(\Theta) \end{bmatrix} \tag{3.69}$$

where

$$
\begin{aligned}
&- J_t(\Theta)\ S(r_e) = \\
&= \begin{bmatrix}
r_e^y(s_\phi s_\psi + c_\phi c_\psi s_\theta) + r_e^z(c_\phi s_\psi - c_\psi s_\phi s_\theta) & r_e^z c_\psi c_\theta - r_e^x(s_\phi s_\psi + c_\phi c_\psi s_\theta) & -r_e^x(c_\phi s_\psi - c_\psi s_\phi s_\theta) - r_e^y c_\psi c_\theta) \\
-r_e^y(c_\psi s_\phi - c_\phi s_\psi s_\theta) - r_e^z(c_\phi c_\psi + s_\phi s_\psi s_\theta) & r_e^x(c_\psi s_\phi - c_\phi s_\psi s_\theta) + r_e^z c_\theta s_\psi & r_e^x(c_\phi c_\psi + s_\phi s_\psi s_\theta) - r_e^y c_\theta s_\psi \\
{r_e}^y c_\phi c_\theta - r_e^z c_\theta s_\phi & -r_e^z s_\theta - r_e^x c_\phi c_\theta & r_e^y s_\theta + r_e^x c_\theta s_\phi
\end{bmatrix}
\end{aligned}
\tag{3.70}
$$

The Jacobian transformation matrix $J_e(\Theta) \in \mathbb{R}^{6\times 6}$ relates in a straightforward way the linear velocity $\dot{p}_e$ and the rate of change in the Euler Angles $\dot{\Theta}$ of the end-effector expressed in F_A with the Body-Fixed velocities v, ω.

3.4 Kinematic Singularities

During the kinematic analysis in this section there are transformations that need to be invertible due to inverse kinematic processes and the control of the structure that is introduced in Chapter 6. Thus, transformation matrices $J_t(\Theta), J_r(\Theta), J_o(\Theta)$ and $J_t(\Theta)$ in equations (3.25), (3.39), (3.41) and (3.68) should be for all $t \geq 0$ nonsingular. Matrix $J_t(\Theta)$ is nonsingular since $\mathbf{det}(J_t(\Theta)) = 1$. The other three matrices are square, hence it can be shown that they are nonsingular by computing the corresponding determinants as

$$
\begin{cases}
\mathbf{det}(J_r(\Theta)) &= \dfrac{1}{\cos(\theta)} \\
\mathbf{det}(J_o(\Theta)) &= \dfrac{1}{\cos(\theta)} \\
\mathbf{det}(J_e(\Theta)) &= \dfrac{1}{\cos(\theta)}
\end{cases}
\tag{3.71}
$$

Using the basic assumption (3.8) we conclude that all transformation matrices are always nonsingular since the following hold

$$
\begin{cases}
\mathbf{det}(J_r(\Theta)) \neq 0 \\
\mathbf{det}(J_o(\Theta)) \neq 0 \\
\mathbf{det}(J_e(\Theta)) \neq 0
\end{cases}
\quad , \quad \forall\ -\frac{\pi}{2} < \theta < \frac{\pi}{2}
\tag{3.72}
$$

3.5 Time Derivative of the Jacobian Matrix

One important issue of the control of proposed aerial manipulator is the time derivative of the Jacobian matrix. In this section the analytical form of the time derivative of

the Jacobian matrix will be given, which is useful for the controller design in Chapter 6. Differentiating the equation (3.69) it is obtained that

$$\dot{J}_e(\Theta) = \begin{bmatrix} \dot{J}_t(\Theta) & -\dot{J}_t(\Theta)\ S(r_e) \\ O_{(3\times3)} & \dot{J}_r(\Theta) \end{bmatrix} \tag{3.73}$$

since

$$\dot{r}_e = 0 \Leftrightarrow \frac{d}{dt}(S(r_e)) = 0 \tag{3.74}$$

where

$$\begin{aligned}
&\dot{J}_t(\Theta) \\
&= \frac{\partial J_t}{\partial \phi}\ \dot{\phi} + \frac{\partial J_t}{\partial \theta}\ \dot{\theta} + \frac{\partial J_t}{\partial \psi}\ \dot{\psi} \\
&= J_t(\Theta)\ S(\omega) \\
&= J_t(\Theta)\ S((J_r(\Theta))^{-1}\ \dot{\Theta}) \\
&= \begin{bmatrix} -\dot{\psi}\ c_\theta s_\psi - \dot{\theta}\ c_\psi s_\theta & \dot{\phi}(s_\phi s_\psi + c_\phi c_\psi s_\theta) - \dot{\psi}(c_\phi c_\psi + s_\phi s_\psi s_\theta) + \dot{\theta} c_\psi c_\theta s_\phi & \dot{\phi}(c_\phi s_\psi - c_\psi s_\phi s_\theta) + \dot{\psi}(c_\psi s_\phi - c_\phi s_\psi s_\theta) + \dot{\theta} c_\phi c_\psi c_\theta \\ \dot{\psi}\ c_\psi\ c_\theta - \dot{\theta}\ s_\psi s_\theta & \dot{\theta} c_\theta s_\phi s_\psi - \dot{\psi}(c_\phi s_{psi} - c_\psi s_\phi s_\theta) - \dot{\phi}(c_\psi s_\phi - c_\phi s_\psi s_\theta) & \dot{\psi}(s_\phi s_\psi + c_\phi c_\psi s_\theta) - \dot{\phi}(c_\phi c_\psi + s_\phi s_\psi s_\theta) + \dot{\theta} c_\phi c_\theta s_\psi \\ -\dot{\theta}\ c_\theta & \dot{\phi}\ c_\phi c_\theta - \dot{\theta}\ s_\phi s_\theta & -\dot{\phi}\ c_\theta s_\phi - \dot{\theta}\ c_\phi s_\theta \end{bmatrix}
\end{aligned} \tag{3.75}$$

and

$$\begin{aligned}
\dot{J}_r(\Theta) &= \frac{\partial J_r}{\partial \phi}\ \dot{\phi} + \frac{\partial J_r}{\partial \theta}\ \dot{\theta} \\
&= \begin{bmatrix} 0 & \dfrac{\dot{\theta}\ s_\phi + \dot{\phi}\ c_\phi c_\theta s_\theta}{c_\theta^2} & \dfrac{\dot{\theta}\ c_\phi - \dot{\phi}\ c_\theta s_\phi s_\theta}{c_\theta^2} \\ 0 & -\dot{\phi}\ s_\phi & -\dot{\phi}\ c_\phi \\ 0 & \dfrac{\dot{\phi}\ c_\phi c_\theta + \dot{\theta}\ s_\phi s_\theta}{c_\theta^2} & -\dfrac{\dot{\phi}\ c_\theta s_\phi - \dot{\theta}\ c_\phi s_\theta}{c_\theta^2} \end{bmatrix}
\end{aligned} \tag{3.76}$$

Chapter 4

Dynamic Analysis

4.1 Introduction

This chapter presents the dynamic equations of motion of the proposed aerial robot using Newton-Euler formalism. The dynamic analysis of the system will be investigated assuming that the system is moving freely without interaction forces and torques with the environment. This analysis is crucial in order to provide a mechanism that shows the way the thrust forces from the actuators affect the behavior of system in the Cartesian space. In the end of the Chapter, the static force analysis is also provided.

4.2 Basic Assumptions

As assumed in the previous Chapter the vehicle is considered as rigid body. The aerodynamic forces and torques on the body come from two basic sources: the pressure distribution over the body surface and the shear stress distribution over the body surface. As discussed in [1], the proposed aerial manipulation system is supposed to be a low altitude flying vehicle, operating low speed flights with aerodynamic effects having low impact on it. These aspects lead to reduced gyroscopic effects from the propellers and, without loss of generality, to neglected aerodynamic frictions. Taking into account all previous issues, in this Chapter the actuation forces/torques, the gravitational forces/torques and the reaction type torques will be investigated. The unmodeled dynamics could be considered in the robust adaptive control analysis as unknown disturbances affecting the dynamic model of the system. In the next Chapter

it will be proven that the proposed system is able to follow arbitrary trajectories irrespectively of these disturbances.

4.3 Deriving Dynamic Equations of Motion with Newton-Euler Formalism

In the previous chapter, the kinematic analysis of the aerial manipulator was performed resulting in Figure 2.1. The structure is composed of a number of n thrusters and the end-effector. The dynamic analysis of the aerial manipulator depends on the effects of total forces and torques acting on the body. The n thrusters produce forces and torques on the system.

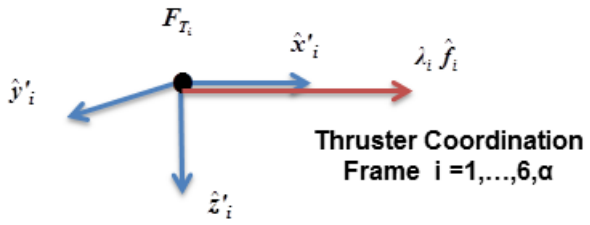

FIGURE 4.1: Local thruster coordination system

We assume that every thruster is attached to its own coordinate system, which is Body-Fixed as in Figure 4.1. For convenience, the Body-Fixed coordinate frame of each thruster is written as

$$F_{T_i} = \{\hat{x}_i, \hat{y}_i, \hat{z}_i\}, \ i = 1, ..., n \tag{4.1}$$

The frames F_{T_i} are orthogonal, right-handed and fixed to the body of the aerial robot. Each frame origin is at the point $\tau_i, i = 1, ..., n$. Points $\tau_i, i = 1, ..., n$ are essentially the points on which the thrust force is applied. Basically, the thrusters are thrust actuators that produce thrust forces for the system. From the analysis of the Chapter 2, the aerial robot is equipped with seven thrusters that actuate the system. The first $i = 1, ..., 6$ are the main thrusters and the n-th is the additional one used from the system in order to alleviate the problem of negative thrust forces.

Let

$$\hat{f}_i = f_{x,i}\ \hat{x}_i + f_{y,i}\ \hat{y}_i + f_{z,i}\ \hat{z}_i,\ \ i = 1, ..., n \tag{4.2}$$

be the unit vector of each thruster in its own coordination frame. Using the basic property of unit vectors, from (4.2) the following holds

$$\|\hat{f}_i\| = 1,\ \ i = 1, ..., n \iff (f_{x,i})^2 + (f_{y,i})^2 + (f_{z,i})^2 = 1,\ \ i = 1, ..., n \tag{4.3}$$

Unit vector $\hat{f}_i$ defines the orientation of thruster i. It is well-known that each thruster can produce thrust force only in one direction. We assume that this direction is parallel to the unit vector $\hat{x}_i,\ \ i = 1, ..., n$ (see mechanical design in [1]). We assume that thruster unit vectors $\hat{f}_i$ have only one component, parallel to unit vector $\hat{x}_i$. Thruster i produces thrust force only in the direction of vector $\hat{x}_i$. Thus, we result in

$$f_{x,i} = 1, f_{y,i} = f_{z,i} = 0,\ \ i = 1, ..., n \tag{4.4}$$

The combination of equations (4.2) and (4.4) leads to

$$\hat{f}_i = \hat{x}_i,\ \ i = 1, ..., n \tag{4.5}$$

Expressing all unit vectors $\hat{f}_i$ in its coordination frame F_{T_i} for $i = 1, .., n$ respectively, results in

$$\hat{f}_i\Big|_{T_i} = \hat{x}_i\Big|_{T_i} = \begin{bmatrix} 1 \\ 0 \\ 0 \end{bmatrix} = e_1, i = 1, ..., n \tag{4.6}$$

Where e_i is the i-th column of the identity matrix I_3. Note that the vectors $\hat{f}_i$ are the unit orientation vectors. We define

$$\vec{f}_{pr,i} = \lambda_i\ \hat{f}_i = \lambda_i\ \hat{x}_i,\ \ i = 1, ..., n \tag{4.7}$$

as the propulsion vector of each thruster and $\lambda_i,\ \ i = 1, ..., n$ the thruster force magnitude of its thruster. The total thrust force that is applied to the system is

$$\vec{f}_{pr,tot} = \sum_{i=1}^{n} \left(\vec{f}_{pr,i}\right) \overset{(4.7)}{=} \sum_{i=1}^{n} (\lambda_i\ \hat{x}_i) \tag{4.8}$$

The information and the technical details for the thrusters that will compose the final structure can be found in [1].

At this point, the total force on the aerial manipulator due to gravity, is investigated.

The gravity is supposed to be uniform in near Earth flights. It is obvious that all the gravitational forces are parallel to the Inertial unit vector $\hat{z}_A$. Furthermore, it is assumed that the total system is consisted of the n thrusters and the rest of the structure and since the fact that all the thrusters are similar, they have the same mass. Let m_{thr} be the mass of each thruster, and m_s the mass of the rest of structure. The total mass m is given by

$$m = n\ m_{thr} + m_s \tag{4.9}$$

It will be assumed that the mass is constant in time, hence

$$\dot{m} = 0 \tag{4.10}$$

The total gravitational force $\vec{f}_{gr}$ acting on the rigid body (essentially is acting in the Body-Fixed frame) is given by

$$\begin{aligned} \vec{f}_{gr,tot} &= m\ \vec{g} \\ &= m\ (-g\ \vec{z}_A) \\ &= (m\ g)\ (-\vec{z}_A) \end{aligned} \tag{4.11}$$

where $\vec{g} = g\ (-\hat{z}_A)$ is the acceleration due to the gravity and $m\ \vec{g}$ is the total weight of the structure.

The total force acting on the vehicle in the Body-Fixed frame can be calculated as follows

$$\begin{aligned} \vec{f}_B &= \vec{f}_{pr,tot} + \vec{f}_{gr,tot} \\ &\overset{(4.8),(4.11)}{=} \sum_{i=1}^{n} (\lambda_i\ \hat{x}_i) + m\ g\ (-\vec{z}_A) \end{aligned} \tag{4.12}$$

The overall force acting on the vehicle in the Body-Fixed can be derived by resolving the vector $\vec{f}_B$ in Body-Fixed frame F_B as

$$\begin{aligned} F_B &= \left(\sum_{i=1}^{n} (\lambda_i\ \hat{x}_i) \right) \Big|_B + (m\ g\ (-\vec{z}_A)) \Big|_B \\ &= \sum_{i=1}^{n} \left\{ (\lambda_i\ \hat{x}_i) \Big|_B \right\} + m\ g\ \left(-\vec{z}_A \Big|_B \right) \\ &= \sum_{i=1}^{n} \left\{ \lambda_i\ \left(\hat{x}_i \Big|_B \right) \right\} + m\ g\ \left(-\vec{z}_A \Big|_B \right) \end{aligned} \tag{4.13}$$

By resolving unit vectors $\hat{k}_A,\ \hat{x}_i, i = 1, ..., n$ in frame F_B it is obtained

$$\hat{z}_A\Big|_B = O_{B/A}\ \hat{z}_A\Big|_A = \left(O_{A/B}\right)^{\tau}\ \hat{z}_A\Big|_A = J_t^{\tau}(\Theta)\ \begin{bmatrix}0\\0\\1\end{bmatrix} = J_t^{\tau}(\Theta)\ e_3 \tag{4.14}$$

$$\hat{i}_{T_i}\Big|_B = O_{B/T_i}\ \hat{x}_i\Big|_{T_i} = O_{B/T_i}\ \begin{bmatrix}1\\0\\0\end{bmatrix} = O_{B/T_i}\ e_1 = F_i,\ \forall\ i = 1, ..., n \tag{4.15}$$

where O_{B/T_i} is the orientation matrix of the frame F_B relative to thruster frames $F_{T_i},\ i = 1, ..., n$. Using the definition of the orientation matrix [45], simply yields

$$O_{B/T_i}\ e_1 = \begin{bmatrix} cos(\theta_{\hat{x}_B/\hat{x}_{T_i}})\\ cos(\theta_{\hat{y}_B/\hat{x}_{T_i}})\\ cos(\theta_{\hat{z}_B/\hat{x}_{T_i}})\end{bmatrix}, i = 1, ..., n \tag{4.16}$$

where $\theta_{\hat{x}_\bullet/\hat{y}_\times} \in [0, \pi]$ denotes the angle between vectors $\hat{x}_\bullet, \hat{y}_\times$.

Substituting equations (4.14), (4.15) in (4.13) leads to

$$F_B = \underbrace{\sum_{i=1}^{n}\left(\lambda_i\ O_{B/T_i}\ e_1\right)}_{\text{thruster propulsion forces}} - \underbrace{m\ g\ J_t^{\tau}(\Theta)\ e_3}_{\text{gravitational forces}} \tag{4.17}$$

Equation (4.17) shows that the total force acting on the vehicle in Body-Fixed frame is consisted of the propulsion efforts from the thrusters and the gravitational forces.

Writing equation (4.17) in matrix form we have

$$\begin{aligned} F_B &= \begin{bmatrix} O_{B/T_1}\ e_1 & \vdots & \cdots & \vdots & O_{B/T_n}\ e_1\end{bmatrix}\begin{bmatrix}\lambda_1\\ \lambda_2\\ \vdots\\ \lambda_n\end{bmatrix} - m\ g\ J_t^{\tau}(\Theta)\ e_3 \\ &= F\ \lambda - m\ g\ J_t^{\tau}(\Theta)\ e_3 \end{aligned} \tag{4.18}$$

Where the matrix

$$\begin{aligned} F &= \begin{bmatrix} F_1 & \vdots & \cdots & \vdots & F_n\end{bmatrix} \\ &= \begin{bmatrix} O_{B/T_1}\ e_1 & \vdots & \cdots & \vdots & O_{B/T_n}\ e_1\end{bmatrix} \in \mathbb{R}^{3\times n} \end{aligned} \tag{4.19}$$

denotes the transformation from the actuator space to Body space (i.e. from every thruster frames F_{T_i} to the the Body-Fixed frame F_B) and the vector

$$\lambda = [\lambda_1 \quad \cdots \quad \lambda_n] \in \mathbb{R}^n \tag{4.20}$$

denotes the vector of all thrust forces.

We are proceeding now with the computation of torques that are applied in Body-Fixed frame. We the position vectors of each thruster relative to the Body-Fixed frame as

$$\vec{r}_{\tau_i/b} = r_{x,i}\ \hat{x}_B + r_{y,i}\ \hat{y}_B + r_{z,i}\ \hat{z}_B,\ i = 1, ..., n \tag{4.21}$$

For notation convenience we define $r_i \in \mathbb{R}^3$ as

$$r_i = \vec{r}_{\tau_i/b}\Big|_B = \begin{bmatrix} r_{x,i} \\ r_{y,i} \\ r_{z,i} \end{bmatrix},\ i = 1, ..., n \tag{4.22}$$

The next step is to take into consideration the thruster torques. It is well known that each thruster, due to its own rotation produces a reaction torque which is given by

$$\vec{M}_{react,i} = \mu\ \vec{f}_{pr,i} = \mu\ (\lambda_i\ \hat{f}_i) = (\mu\ \lambda_i)\ \hat{x}_i,\ i = 1, ..., n \tag{4.23}$$

where μ is an aerodynamic coefficient which is related by the type of the thruster introduced in Chapter 2. Note that the coefficient μ is the same for all thrusters of the system. The total reaction torque which is produced from all the thrusters is

$$\vec{M}_{react,tot} = \sum_{i=1}^{n} \left(\vec{M}_{react,i}\right) \overset{(4.23)}{=} \sum_{i=1}^{n} \{(\mu\ \lambda_i)\ \hat{x}_i\} = \mu\ \left\{\sum_{i=1}^{n} (\lambda_i\ \hat{x}_i)\right\} \tag{4.24}$$

We define

$$\vec{M}_{\tau_i/b} = \vec{r}_{\tau_i/b} \times \vec{f}_{pr,i}\ ,\ i = 1, ..., n \tag{4.25}$$

as the torque that is produced from each thruster. The total torque acting on vehicle in Body-Fixed frame due to the thruster propulsion is given by

$$\begin{aligned}\vec{M}_{thr,tot} &= \sum_{i=1}^{n}\left(\vec{M}_{\tau_i/b}\right)\\ &= \sum_{i=1}^{n}\left(\vec{r}_{\tau_i/b}\times\vec{f}_{pr,i}\right)\\ &\overset{(4.7)}{=} \sum_{i=1}^{n}\left\{\vec{r}_{\tau_i/b}\times(\lambda_i\ \hat{x}_i)\right\}\\ &= \sum_{i=1}^{n}\left\{\lambda_i\ \left(\vec{r}_{\tau_i/b}\times\hat{x}_i\right)\right\}\end{aligned} \tag{4.26}$$

Consider now the total torque that is acting in body-fixed frame due to the fact of gravity. We define $r_G \in \mathbb{R}^3$

$$\begin{aligned}&\vec{r}_{G/b} = r_{Gx}\ \hat{x}_B + r_{Gy}\ \hat{y}_B + r_{Gz}\ \hat{z}_B\\ \Leftrightarrow\ &r_G = \vec{r}_{G/b}\Big|_B = \begin{bmatrix} r_{Gx}\\ r_{Gy}\\ r_{Gz}\end{bmatrix}\end{aligned} \tag{4.27}$$

as the position of the center of gravity of the total system. The torque that is applied by the gravitational force is given by

$$\begin{aligned}\vec{M}_{gr,tot} &= \vec{r}_{G/b}\times\vec{f}_{gr,tot}\\ &\overset{(4.11)}{=} \vec{r}_{G/b}\times(m\ g\ (-\hat{z}_A))\\ &= -\left(m\ g\right)\left(\vec{r}_{G/b}\times\hat{z}_A\right)\end{aligned} \tag{4.28}$$

The total torque acting on vehicle in Body-Fixed frame can be computed using equations (4.26), (4.24) and (4.28) as

$$\begin{aligned}\vec{M}_B &= \vec{M}_{thr,tot} + \vec{M}_{react,tot} + \vec{M}_{gr,tot}\\ &= \sum_{i=1}^{n}\left\{\lambda_i\ \left(\vec{r}_{\tau_i/b}\times\hat{x}_i\right)\right\} + \mu\ \left\{\sum_{i=1}^{n}\left(\lambda_i\ \hat{x}_i\right)\right\} - \left(m\ g\right)\left(\vec{r}_{G/b}\times\hat{z}_A\right)\end{aligned} \tag{4.29}$$

By resolving the equation (4.29) in Body-Fixed frame gives

$$\begin{aligned} M_B &= \left\{ \sum_{i=1}^{n} \left\{ \lambda_i \ \left(\vec{r}_{\tau_i/b} \times \hat{x}_i \right) \right\} \right\} \Big|_B + \left\{ \mu \ \left\{ \sum_{i=1}^{n} \left(\lambda_i \ \hat{x}_i \right) \right\} \right\} \Big|_B \\ &\quad - \left\{ (m \ g) \left(\vec{r}_{G/b} \times \hat{z}_A \right) \right\} \Big|_B \\ &= \sum_{i=1}^{n} \left\{ \lambda_i \ \left(\vec{r}_{\tau_i/b} \times \hat{x}_i \right) \Big|_B \right\} + \mu \ \left\{ \sum_{i=1}^{n} \left(\lambda_i \ \hat{x}_i \right) \Big|_B \right\} \\ &\quad - (m \ g) \left(\vec{r}_{G/b} \times \hat{z}_A \right) \Big|_B \\ &= \sum_{i=1}^{n} \left\{ \lambda_i \ \left(\vec{r}_{\tau_i/b} \Big|_B \right) \times \left(\hat{x}_i \Big|_B \right) \right\} + \mu \ \left\{ \sum_{i=1}^{n} \lambda_i \ \left(\hat{x}_i \Big|_B \right) \right\} \\ &\quad - (m \ g) \left(\vec{r}_{G/b} \Big|_B \right) \times \left(\hat{z}_A \Big|_B \right) \end{aligned} \tag{4.30}$$

Substituting the (4.14), (4.15), (4.22), (4.27) in the equation (4.30) we have

$$\begin{aligned} M_B &= \sum_{i=1}^{n} \left\{ \lambda_i \ \left(r_i \times O_{B/T_i} \ e_1 \right) \right\} + \mu \ \left\{ \sum_{i=1}^{n} \left(\lambda_i \ O_{B/T_i} \ e_1 \right) \right\} \\ &\quad - (m \ g) \left(r_G \times J_t^{\tau}(\Theta) \ e_3 \right) \\ &\overset{(3.53)}{=} \sum_{i=1}^{n} \left[\lambda_i \ S(r_i) \ O_{B/T_i} \ e_1 \right] + \mu \ \left\{ \sum_{i=1}^{n} \left(\lambda_i \ O_{B/T_i} \ e_1 \right) \right\} \\ &\quad - (m \ g) \left[S(r_G) \ J_t^{\tau}(\Theta) \ e_3 \right] \\ &= \underbrace{\sum_{i=1}^{n} \left[\lambda_i \ S(r_i) \ O_{B/T_i} \ e_1 \right]}_{\text{thruster propulsion torques}} + \underbrace{\mu \ \left\{ \sum_{i=1}^{n} \left(\lambda_i \ O_{B/T_i} \ e_1 \right) \right\}}_{\text{thruster reaction torques}} \\ &\quad - \underbrace{m \ g \ S(r_G) \ J_t^{\tau}(\Theta) \ e_3}_{\text{gravitational torques}} \end{aligned} \tag{4.31}$$

Equation (4.31) implies that the total torque acting on the vehicle in the Body-Fixed frame is consisted of the propulsion thrust torques, the gravitational torques and the torques due to thruster own rotation.

Writing equation (4.31) in matrix form we get

$$\begin{aligned} M_B = &\begin{bmatrix} S(r_1)\ O_{B/T_1}\ e_1 & \vdots & \cdots & \vdots & S(r_n)\ O_{B/T_n}\ e_1 \end{bmatrix} \begin{bmatrix} \lambda_1 \\ \lambda_2 \\ \vdots \\ \lambda_n \end{bmatrix} \\ &+ \mu \begin{bmatrix} O_{B/T_1}\ e_1 & \vdots & \cdots & \vdots & O_{B/T_n}\ e_1 \end{bmatrix} \begin{bmatrix} \lambda_1 \\ \lambda_2 \\ \vdots \\ \lambda_n \end{bmatrix} \\ &- m\ g\ S(r_G)\ J_t^{\tau}(\Theta)\ e_3 \\ = &\ E\ \lambda + \mu\ F\ \lambda - m\ g\ S(r_G)\ J_t^{\tau}(\Theta)\ e_3 \end{aligned} \tag{4.32}$$

Where

$$\begin{aligned} E &= \begin{bmatrix} E_1 & \vdots & \cdots & \vdots & E_n \end{bmatrix} \\ &= \begin{bmatrix} S(r_1)\ O_{B/T_1}\ e_1 & \vdots & \cdots & \vdots & S(r_n)\ O_{B/T_n}\ e_1 \end{bmatrix} \in \mathbb{R}^{3\times n} \end{aligned} \tag{4.33}$$

and F, λ as in (4.19), (4.20). Combining equation (4.18) and (4.32) we have the generalized vector $\Lambda_B \in \mathbb{R}^6$ of forces and torques acting on aerial robot in Body-Fixed frame is obtained as

$$\begin{aligned} \Lambda_B &= \begin{bmatrix} F_B \\ M_B \end{bmatrix} \\ &= \begin{bmatrix} F\ \lambda - m\ g\ J_t^{\tau}(\Theta)\ e_3 \\ (E + \mu\ F)\ \lambda - m\ g\ S(r_G)\ J_t^{\tau}(\eta)\ e_3 \end{bmatrix} \\ &= \begin{bmatrix} F\ \lambda \\ (E + \mu\ F)\ \lambda \end{bmatrix} - \begin{bmatrix} m\ g\ J_t^{\tau}(\Theta)\ e_3 \\ m\ g\ S(r_G)\ J_t^{\tau}(\Theta)\ e_3 \end{bmatrix} \\ &= \begin{bmatrix} F \\ E + \mu\ F \end{bmatrix} \lambda - \begin{bmatrix} m\ g\ I_{(3\times 3)} \\ m\ g\ S(r_G) \end{bmatrix} J_t^{\tau}(\Theta)\ e_3 \\ &= \begin{bmatrix} F \\ E \end{bmatrix} \lambda + \begin{bmatrix} O_{(3\times 6)} \\ \mu\ F \end{bmatrix} \lambda - m\ g \begin{bmatrix} I_{(3\times 3)} \\ S(r_G) \end{bmatrix} J_t^{\tau}(\Theta)\ e_3 \end{aligned}$$

$$= \underbrace{\begin{bmatrix} F \\ E \end{bmatrix} \lambda}_{\text{propulsion forces/torques}} + \underbrace{\begin{bmatrix} O_{(3\times 6)} \\ \mu\ F \end{bmatrix} \lambda}_{\text{reaction torques}} - \underbrace{m\ g \begin{bmatrix} I_{(3\times 3)} \\ S(r_G) \end{bmatrix} J_t^\tau(\Theta)\ e_3}_{\text{gravitational forces/torques}}$$

$$= \bar{N}\ \lambda - m\ g \begin{bmatrix} I_{(3\times 3)} \\ S(r_G) \end{bmatrix} J_t^\tau(\Theta)\ e_3 \tag{4.34}$$

where here the matrix $\bar{N}$ is given by

$$\bar{N} = \begin{bmatrix} F \\ E + \mu\ F \end{bmatrix} \in \mathbb{R}^{6\times 6} \tag{4.35}$$

The matrix $\bar{N} \in \mathbb{R}^6$ is known in bibliography as actuator configuration matrix or thruster allocation matrix.

There are several techniques which can be used to derive the equations of motions of a rigid body with 6 DOF. The Newton-Euler formalism has been adopted to this work. The dynamic equations with respect to the Body-Fixed frame can be conveniently written (main ideas are discussed extensively in [44], [45]) as

$$\begin{aligned} & M \begin{bmatrix} \dot{v} \\ \dot{\omega} \end{bmatrix} + C(\nu) \begin{bmatrix} v \\ \omega \end{bmatrix} = \Lambda_B \\ \Leftrightarrow\ & M \begin{bmatrix} \dot{v} \\ \dot{\omega} \end{bmatrix} + C(\nu) \begin{bmatrix} v \\ \omega \end{bmatrix} = \begin{bmatrix} F_B \\ M_B \end{bmatrix} \\ \Leftrightarrow\ & M \begin{bmatrix} \dot{v} \\ \dot{\omega} \end{bmatrix} + C(\nu) \begin{bmatrix} v \\ \omega \end{bmatrix} = \begin{bmatrix} F \\ E + \mu\ F \end{bmatrix} \lambda - m\ g \begin{bmatrix} I_{(3\times 3)} \\ S(r_G) \end{bmatrix} J_t^\tau(\Theta)\ e_3 \end{aligned} \tag{4.36}$$

where

$$M = \begin{bmatrix} m\ I_3 & -m\ S(r_G) \\ m\ S(r_G) & I_B \end{bmatrix} \tag{4.37}$$

is the inertia matrix,

$$C(\nu) = \begin{bmatrix} m\ S(\omega) & -m\ S(\omega)\ S(r_G) \\ m\ S(r_G)\ S(\omega) & -S(I_B\ \omega) \end{bmatrix} \tag{4.38}$$

is the Coriolis-Centipetal matrix, $\nu = [v^\tau\ \omega^\tau]^\tau \in \mathbb{R}^6$ is the vector of Body-Fixed velocities. The term I_B denotes the well-known inertia tensor matrix expressed in F_B. Using the parallel axis theorem (also well known as Steiners theorem) from [43] we

have

$$I_B = I_G - m\ S(r_G)\ S(r_G) \tag{4.39}$$

where I_G is the inertia tensor relative to the body's center of gravity.

Solving equation (4.36) with respect to $[\dot{v}^\tau\ \dot{\omega}^\tau]^\tau$ we get

$$\begin{bmatrix} \dot{v} \\ \dot{\omega} \end{bmatrix} = -M^{-1}C(\nu) \begin{bmatrix} v \\ \omega \end{bmatrix} + M^{-1} \begin{bmatrix} F \\ E + \mu\ F \end{bmatrix} \lambda - m\ g\ M^{-1} \begin{bmatrix} I_3 \\ S(r_G) \end{bmatrix} J_t^\tau(\Theta)\ e_3 \tag{4.40}$$

The (4.40) can be written in a more convenient matrix form as

$$\begin{aligned} \dot{\nu} &= H(\nu) + G(\xi_e) + N\ \lambda \\ \Leftrightarrow \dot{\nu} &= B(\xi_e, \nu) + N\ \lambda \end{aligned} \tag{4.41}$$

where the matrices in (4.41) are defined as

$$H(\nu) = -M^{-1}\ C(\nu)\ \nu \tag{4.42}$$

$$N = M^{-1} \begin{bmatrix} F \\ E + \mu\ F \end{bmatrix} \tag{4.43}$$

$$G(\xi_e) = -m\ g\ M^{-1} \begin{bmatrix} I_{(3\times3)} \\ S(r_G) \end{bmatrix} J_t^\tau(\Theta) e_3 \tag{4.44}$$

$$B(\xi_e, \nu) = H(\nu) + G(\xi_e),\ B : \mathbb{R}^6 \times \mathbb{R}^6 \to \mathbb{R}^6 \tag{4.45}$$

Equation (4.41) constitutes the final dynamic equation of motion in matrix form of the proposed system. Combining the kinematic model from (3.68) with the dynamic model (4.41) the aerial manipulator model including kinematics and dynamics can be written as

$$(S) : \begin{cases} \dot{\xi}_e = J(\xi_e)\ \nu \\ \dot{\nu} = B(\xi_e, \nu) + N\ \lambda \end{cases} \tag{4.46}$$

This convenient final form is appropriate for the nonlinear controller design that will be introduced in Chapter 6. All the parameters that appear in the (4.46) can be found in Table 2.2. The dynamic model (4.46) is highly nonlinear with coupling between the translational and rotational dynamics. Additionally, there is coupling between inputs and output channels in which the nonlinearity of the system makes the control design of the proposed system a real challenge. On the other hand, if we consider

the control problem of the aerial manipulator to be position tracking with attitude regulating, then the system is square in which with six actuators and six outputs (3D position and three attitude angles). This highlights the positive aspect of the proposed configuration in terms of controller design compared to other systems that are in general underactuated systems.

The matrix M can be written in 6 column as

$$M = \begin{bmatrix} m\ I_{(3\times3)} & -m\ S(r_G) \\ m\ S(r_G) & I_B \end{bmatrix}$$

$$= \begin{bmatrix} m & 0 & 0 & 0 & mr_{Gz} & -mr_{Gy} \\ 0 & m & 0 & -mr_{Gz} & 0 & mr_{Gx} \\ 0 & 0 & m & mr_{Gy} & -m\ r_{Gx} & 0 \\ 0 & -mr_{Gz} & mr_{Gy} & c_{xx} & I_{xy} - mr_{Gx}r_{Gy} & I_{xz} - mr_{Gx}r_{Gz} \\ mr_{Gz} & 0 & -mr_{Gx} & I_{xy} - mr_{Gx}r_{Gy} & c_{yy} & I_{xz} - mr_{Gx}r_{Gz} \\ -mr_{Gy} & mr_{Gx} & 0 & I_{xz} - mr_{Gx}r_{Gz} & I_{yz} - mr_{Gy}r_{Gz} & c_{zz} \end{bmatrix}$$

where

$$c_{xx} = I_{xx} + mr_{Gy}^2 + mr_{Gz}^2 \tag{4.47}$$

$$c_{yy} = I_{yy} + mr_{Gx}^2 + mr_{Gz}^2 \tag{4.48}$$

$$c_{zz} = I_{zz} + mr_{Gx}^2 + mr_{Gy}^2 \tag{4.49}$$

4.4 Properties of the Matrices in the Dynamic Analysis

In this section some important properties of the matrices that are involved in the dynamic model of the proposed system will be given. These properties are important since they affect the controller design in Chapter 6 crucially.

To begin with, matrix $C(\nu)$ is time dependent and matrices M, I_G are time independent, hence we have that

$$\dot{M} = \dot{I}_G = 0, \dot{C}(\nu) \neq 0 \tag{4.50}$$

Continuing the analysis, the determinants of matrices M and I_G can be easily calculated by Symbolic MATLAB Toolbox. The corresponding determinants satisfy the

formula

$$\mathbf{det}(M) = m^3 \, \mathbf{det}(I_G) \tag{4.51}$$

This formula shows that the singularity of matrix M depends on the correspond of matrix I_G. Nevertheless, from the mechanical design in Chapter 2 we have that $I_G > 0$, $\mathbf{cond}(I_G) = 3.25$. Therefore, matrix M is nonsingular with

$$M > 0, \ \mathbf{cond}(M) = 9.5 \tag{4.52}$$

For the Coriolis/Centipetal matrix it can be easily shown that

$$C(\nu) = -C^{\tau}(\nu) \tag{4.53}$$

The matrix N is positive definite with small condition number

$$N > 0, \ \mathbf{cond}(N) = 6.63 \tag{4.54}$$

which is the main result of Chapter 2 and [1] and the control-oriented optimization that the system was mainly designed.

4.5 Static Force Analysis

We assume now that the proposed aerial robot is needed to contact with the environment for accomplishing different tasks. In this situation, the aerial manipulator is in contact with an object and is assumed to be stationary. Consequently, static equations must be provided. In this situation forces and torques are applied to the end-effector from the environment. These forces and torques acts in the whole system, thus the dynamic equation is modified and the force/torque transformations between the reference frames of the system must be provided.

The principle of virtual work yields a set of linear equations that relate the resultant force-torque six vector, called a wrench, that acts on the end-effector, to the joint torques of the robot. If the end-effector wrench is known, then a direct calculation yields the joint torques.

The inverse statics problem seeks the end-effector wrench associated with a given set of joint torques, and requires the inverse of the Jacobian matrix. As in the case of inverse velocity analysis, at singular configurations this problem cannot be solved.

When the system is in contact with the environment (actually the end-effector is in contact with the environment) forces and torques are applied at the tip of the manipulator. In this case, there are interaction forces and torques that are applied to the end-effector. Consequently, in the dynamic equation of the system, forces and torques that will be resolved in the Body-Fixed frame will appear. Remember that all the vectors appearing in the dynamic equation are expressed in Body-Fixed frame. With all these considerations, the dynamic equations of motion with system interaction with the environment are modified as

$$M \begin{bmatrix} \dot{v} \\ \dot{\omega} \end{bmatrix} + C(\nu) \begin{bmatrix} v \\ \omega \end{bmatrix} = \begin{bmatrix} F \\ E + \mu\ F \end{bmatrix} \lambda - m\ g \begin{bmatrix} I_{(3\times 3)} \\ S(r_G) \end{bmatrix} J_t^{\tau}(\Theta)\ e_3 - \begin{bmatrix} f_e \\ M_e \end{bmatrix} \tag{4.55}$$

where $f_e, M_e \in \mathbb{R}^3$ are the magnitude of the contact force and torque respectively that are exerted by the manipulator's end-effector on the environment expressed in the Body-Fixed frame. The minus (-) in the right part of the equation denotes the reaction force/torque that is applied from the environment to the system (Newton's Third Law) [46], [49]. Using the notation from the previous chapters, it is clear that

$$f_e = \vec{f_e}\Big|_B \tag{4.56}$$

$$M_e = \vec{M_e}\Big|_B \tag{4.57}$$

Note that in (4.55) all the vectors are expressed in Body-Fixed frame. It is well-known from the robotics [43, 46], the manipulator wrench vector

$$h_e = \begin{bmatrix} f_e\big|_A \\ M_e\big|_A \end{bmatrix} \in \mathbb{R}^6 \tag{4.58}$$

where $\vec{f_e}\Big|_A, \vec{M_e}\Big|_A$ are the interaction force and torque respectively that applied at the end-effector expressed in Inertial frame. The wrench vector is expressed in the Inertial frame, thus the transformation from Body-Fixed frame to the Inertial must be provided. This can be done using the well-known kineto-statics duality from [43, 46].

Hence, we get

$$\begin{aligned}
&\begin{bmatrix} \vec{f}_e|_B \\ \vec{M}_e|_B \end{bmatrix} = J^\tau(\xi_e) \begin{bmatrix} f_e|_A \\ M_e|_A \end{bmatrix} \\
\Leftrightarrow &\begin{bmatrix} \vec{f}_e|_B \\ \vec{M}_e|_B \end{bmatrix} = \begin{bmatrix} J_t(\Theta) & -J_t(\Theta)\ S(r_e) \\ O_{(3\times3)} & J_r(\Theta) \end{bmatrix}^\tau h_e \\
\Leftrightarrow &\begin{bmatrix} \vec{f}_e|_B \\ \vec{M}_e|_B \end{bmatrix} = \begin{bmatrix} (J_t(\Theta))^\tau & O_{(3\times3)} \\ S(r_e)\ (J_t(\Theta))^\tau & (J_r(\Theta))^\tau \end{bmatrix} h_e
\end{aligned} \tag{4.59}$$

where the formula $(S(r_e))^\tau = -S(r_e)$ was invoked. Substituting the (4.59) in the dynamic equation (4.55) the following equation holds

$$M \begin{bmatrix} \dot{v} \\ \dot{\omega} \end{bmatrix} + C \begin{bmatrix} v \\ \omega \end{bmatrix} = \begin{bmatrix} F \\ E + \mu\ F \end{bmatrix} \lambda - m\ g \begin{bmatrix} I_{(3\times3)} \\ S(r_G) \end{bmatrix} J_t^\tau(\Theta)\ e_3 - J(\xi_e)^\tau\ h_e \tag{4.60}$$

Under the assumption that the aerial manipulator is stationary while it is applying a force/moment h_e to an object, the dynamics can reduced to statics. Thus, considering that $v = \dot{v} = \omega = \dot{\omega} = 0$ the following statics equation is delivered from (4.60)

$$\begin{aligned}
0 = &\begin{bmatrix} F \\ E + \mu\ F \end{bmatrix} \lambda - m\ g \begin{bmatrix} I_{(3\times3)} \\ S(r_G) \end{bmatrix} J_t^\tau(\Theta)\ e_3 - J^\tau(\xi_e)\ h_e \\
\Leftrightarrow &\begin{bmatrix} F \\ E + \mu\ F \end{bmatrix} \lambda = m\ g \begin{bmatrix} I_{(3\times3)} \\ S(r_G) \end{bmatrix} J_t^\tau(\Theta)\ e_3 + J^\tau(\xi_e)\ h_e
\end{aligned} \tag{4.61}$$

The equation (4.61) is the static force equation when the aerial manipulator is in interaction with the environment. This equation will be widely used in the case of the force/torque control which will not be investigated in this thesis.

Chapter 5

Nonlinear Control of The Aerial Manipulator

5.1 Introduction

In this chapter we will attempt to control the motion of the system in the case where there are no interaction forces and torques from the environment applied to the system. Firstly, we will conduct a complete analysis using nonlinear geometry control tools in order to study the controllability and the feedback linearizability of the system. Following this, a backstepping control will be designed in order to control the absolute position and orientation of the end-effector. Due to the fact that the system is in the presence of actuator failures, unmodeled dynamics and external disturbances, the controller needs to be adaptive and robust to improve the performance of the system.

5.2 Basic Definitions from Nonlinear Control Theory

Before proceeding with the analysis some important definitions will be presented. Vector signals are time varying vector functions, defined for nonnegative time as $x(t) : \{0\} \cup \mathbb{R}_+ \rightarrow \mathbb{R}$, where t denotes the time. Consider a vector signal $x(t) = [x_1(t) \ \cdots \ x_n(t)]^\tau \in \mathbb{R}^n$. At any time t, $x(t)$ is a vector. As t changes, $x(t)$ represents a vector field. A function is called smooth, if its every component has continuous partial derivatives of all orders. A vector field $f : \mathbb{R}^n \rightarrow \mathbb{R}^n$ is a function which assigns

a n-dinemnsional vector to every point in the n-dimensional space $\mathbb{R}^n$. Having two smooth vector fields $f, g : \mathbb{R}^n \to \mathbb{R}^n$ and a smooth scalar function $h : \mathbb{R}^n \to \mathbb{R}$, the Lie derivative of h with respect to the vector field f is a new function $L_f h : \mathbb{R}^n \to \mathbb{R}$ given by

$$L_f^{(0)}\ h = h \tag{5.1}$$
$$L_f^{(1)}\ h = \nabla h\ f \tag{5.2}$$
$$L_f^{(k)}\ h = L_f\ L_f^{(k-1)}\ h, k = 1, 2, ... \tag{5.3}$$
$$L_g L_f\ h = \nabla(L_f h)\ g = \nabla(\nabla h\ f)\ g \tag{5.4}$$

where the function $\nabla h(x)$ denotes the gradient of scalar function $h(x)$ and it is denoted as a $1 \times n$ row vector

$$\nabla h(x) = \frac{\partial h}{\partial x} = \begin{bmatrix} \frac{\partial h}{\partial x_1} & \vdots & \cdots & \vdots & \frac{\partial h}{\partial x_n} \end{bmatrix} \tag{5.5}$$

Similarly, given a vector field $f(x) = [f_1(x)\ \cdots\ f_n(x)]^\tau$, the Jacobian of $f(x)$ is denoted by $\nabla f(x)$ and is a $n \times n$ matrix

$$\nabla f(x) = \begin{bmatrix} \frac{\partial f_1}{\partial x_1} & \cdots & \frac{\partial f_1}{\partial x_n} \\ \vdots & \ddots & \vdots \\ \frac{\partial f_n}{\partial x_1} & \cdots & \frac{\partial f_n}{\partial x_n} \end{bmatrix} \tag{5.6}$$

Let us now define two smooth vector fields $f, g : \mathbb{R}^n \to \mathbb{R}^n$. The Lie Bracket of f and g is a third vector field defined recursively by

$$[f, g]^{(0)} = g \tag{5.7}$$
$$[f, g]^{(1)} = \nabla g\ f - \nabla f\ g \tag{5.8}$$
$$[f, g]^{(k)} = \left[f, [f, g]^{(k-1)}\right], k = 1, 2, ... \tag{5.9}$$

A signal $x(t) = [x_1(t)\ \cdots x_n(t)\ ]^\tau \in \mathbb{R}^n$ is bounded if $x(t) \in \mathcal{L}_\infty$, that is, $||x(t)||_\infty \leq K,\ \forall t \geq 0$, for some $K > 0$ where

$$||x(t)||_\infty = \max_{1 \leq i \leq n} |x_i(t)| \tag{5.10}$$

5.3 Controllability Conditions

Consider now the overall system model from (4.46)

$$(S): \begin{cases} \dot{\xi}_e = J(\xi_e)\ \nu \\ \dot{\nu} = B(\xi_e, \nu) + N\ \lambda \end{cases} \tag{5.11}$$

The state vector of the model is defined as

$$x = \begin{bmatrix} \xi_e \\ \nu \end{bmatrix} \in \mathbb{R}^{12} \tag{5.12}$$

and let

$$u = \lambda = \begin{bmatrix} u_1 & \cdots & u_6 \end{bmatrix} \in \mathbb{R}^6 \tag{5.13}$$

be the control input, namely the thrust forces from actuators as alluded in the previous Chapter. System (5.11) can be written in the well-known nonlinear control affine form [50]

$$\dot{x} = f(x) + \sum_{i=1}^{6} g_i\ u_i \tag{5.14}$$

where the smooth vector field $f : \mathbb{R}^{12} \to \mathbb{R}^{12}$ is given by

$$f(x) = \begin{bmatrix} J(\xi_e) \\ B(\xi_e, \nu) \end{bmatrix} \tag{5.15}$$

and is called drift vector field. The smooth vector fields $g_i : \mathbb{R}^{12} \to \mathbb{R}^{12},\ i = 1, ..., 6$ are defined as

$$g_i = \begin{bmatrix} O_{(6\times 6)} \\ N \end{bmatrix}_{(i)} \tag{5.16}$$

where the notation $X_{(i)}$ denote the ith column of matrix X. The vector fields $g_i, i = 1, ..., 6$ are called control input vector fields. The accessibility distribution is defined as

$$G(x) = \mathbf{span}\left\{g_1, ..., g_6, [f, g_1], ..., [f, g_6]\right\} \tag{5.17}$$

The dimension of the distribution $G(x)$ can be calculated from [51] as

$$\mathbf{dim}(G(x)) = \mathbf{rank}\left[g_1, ..., g_6, [f, g_1], ..., [f, g_6]\right] \tag{5.18}$$

By computing the lie brackets

$$\nabla g_i = 0, \ \forall \ i = 1, ..., 6 \tag{5.19}$$

$$[f, g_i] = \nabla g_i \ f - \nabla f \ g_i = -\nabla f \ g_i, \ i = 1, ..., 6 \tag{5.20}$$

the following conditions hold

$$\mathbf{rank}\left[g_1, ..., g_6, [f, g_1], ..., [f, g_6]\right] = 12 = n, \quad \forall \ x \in \mathbb{R}^{12}, x_5 \neq \pm\frac{\pi}{2} \tag{5.21}$$

$$\mathbf{det}\left[g_1, ..., g_6, [f, g_1], ..., [f, g_6]\right] = 30.78 \ \cos(\theta) \neq 0, \ \forall \ x \in \mathbb{R}^{12}, x_5 \neq \pm\frac{\pi}{2} \tag{5.22}$$

The (5.22) holds due to the assumption (3.8) that $-\frac{\pi}{2} < \theta < \frac{\pi}{2}$. The (5.21), (5.22) result in $\mathbf{dim}(G(x)) = 12 = n, \ \forall \ x \in \mathbb{R}^{12}, x_5 \neq \pm\frac{\pi}{2}$ and the system is locally controllable from any $x_0 \in \mathbb{R}^{12}, x_5 \neq \pm\frac{\pi}{2}$. Further analysis for nonlinear controllability is discussed in [50], [52].

5.4 Feedback Linearization Conditions

Feedback linearization is an approach to nonlinear control design which has attracted a great deal of research interest in recent years (see [51, 53, 54, 55]). The central idea of the approach is to algebraically transform a nonlinear system dynamics into a linear and controllable one so that the linear control techniques can be applied. The basic assumption for this methodology is the exact knowledge of the nonlinear model of the system. In this section the mathematical conditions to prove that the system is exact feedback linearizable are provided.

Let

$$\begin{aligned} h(t) &= [h_1(t) \ \cdots \ h_6(t) \ ]^\tau \\ &= [x(t) \ y(t) \ z(t) \ \phi(t) \ \theta(t) \ \psi(t)]^\tau \end{aligned} \tag{5.23}$$

be the desired output of the system. System (5.14) has a vector relative degree at a point $x_0 \in \mathbb{R}^{12}$

$$\begin{aligned} r &= \begin{bmatrix} r_1 & r_2 & r_3 & r_4 & r_5 & r_6 \end{bmatrix} \\ &= \begin{bmatrix} 2 & 2 & 2 & 2 & 2 & 2 \end{bmatrix} \end{aligned} \tag{5.24}$$

since

$$L_{g_j}\ L_f^{(0)} h_i(x_0) = 0,\ \forall\ 1 \leq i \leq 6,\ \forall\ 1 \leq j \leq 6 \tag{5.25}$$

$$L_{g_j}\ L_f^{(1)} h_i(x_0) \neq 0,\ \text{for at least one } 1 \leq j \leq 6 \tag{5.26}$$

for all x in a neighborhood of x_0 and the 6×6 matrix

$$\begin{aligned} A(x_0) &= \begin{bmatrix} L_{g_1}\ L_f^{(r_1-1)}\ h_1 & L_{g_2}\ L_f^{(r_1-1)}\ h_1 & \cdots & L_{g_6}\ L_f^{(r_1-1)}\ h_1 \\ L_{g_1}\ L_f^{(r_2-1)}\ h_2 & L_{g_2}\ L_f^{(r_2-1)}\ h_2 & \cdots & L_{g_6}\ L_f^{(r_2-1)}\ h_2 \\ \vdots & \vdots & \ddots & \vdots \\ L_{g_1}\ L_f^{(r_6-1)}\ h_6 & L_{g_2}\ L_f^{(r_6-1)}\ h_6 & \cdots & L_{g_6}\ L_f^{(r_6-1)}\ h_6 \end{bmatrix} \\ &= \begin{bmatrix} L_{g_1}\ L_f\ h_1 & L_{g_2}\ L_f\ h_1 & \cdots & L_{g_6}\ L_f\ h_1 \\ L_{g_1}\ L_f\ h_2 & L_{g_2}\ L_f\ h_2 & \cdots & L_{g_6}\ L_f\ h_2 \\ \vdots & \vdots & \ddots & \vdots \\ L_{g_1}\ L_f\ h_6 & L_{g_2}\ L_f\ h_6 & \cdots & L_{g_6}\ L_f\ h_6 \end{bmatrix} \end{aligned} \tag{5.27}$$

is nonsingular at x_0 since $\mathbf{rank}(A(x_0)) = 6$ and $\mathbf{det}(A(x_0)) = -55.47\ \cos(\theta) = -55.47\ \cos(x_5),\ \forall x_5 \neq \pm\frac{\pi}{2}$.

By defining the distributions

$$\Delta_i(x) = \mathbf{span}\{\ [f, g_j]^{(k)}\ : i = 0, \ldots, 5,\ j = 1, \ldots, 6,\ k = 1, \ldots, i\ \} \tag{5.28}$$

the system (5.11) is full state space exact feedback linerizable (see [51, 55]) since the following conditions holds

- $\sum_{i=1}^{6} r_i = 12$
- $\mathbf{rank}(g) = 6$
- $\mathbf{dim}[\ \Delta_i(x)\ ] = 6,\ i = 0, ..., 5$
- All the distributions $\Delta_i,\ i = 0, ..., 4$ are involutive

5.5 Controller Design

In this section, we will proceed with the controller design. A backstepping controller design is adopted. Integrator backstepping is a nonlinear control design technique that

employs Lyapunov synthesis to recursively determine controllers for systems satisfying a particular cascaded structure called “strict feedback form”.

Backstepping has become a very popular control design method for nonlinear control systems because can guarantee global stability, tracking and transient performance for strict-feedback systems. It is a recursive controller design methodology, in which the construction of both feedback control laws and the associated Lyapunov functions is systematic, following a step-by-step algorithm.

Strong properties of global or regional stability and tracking are built into the system in a number of steps, which is never higher than the system order. While feedback linearization methods require precise models and often cancel some useful nonlinearities, backstepping designs offer a choice of design tools for accommodation of uncertain nonlinearities and can avoid wasteful cancellations. Backstepping designs are more flexible and do not force the designed system to appear linear. They can avoid cancellations of useful nonlinearities and ofted introduce additional nonlinear terms to improve transient performance.

In contrast to feedback linearization technique which stipulates the cancellation of all nonlinearities including useful ones, backstepping affords the control engineer not only the choice of retaining all beneficial nonlinearities, but also great freedom in selecting the final control law. Furthermore, backstepping can accommodate, by explicitly accounting for, large nonlinearities and uncertainties in the system’s model, ignored dynamics, input and measurement disturbances.

Another advantage is that the backstepping controller can be used to relax the matching conditions, which are blocked in the traditional Lyapunov design. By matching condition we mean that the nonlinearity enter the system at the same point as the control input, thus it can be canceled. Therefore, backstepping require no matching conditions. Backstepping is a well known technique extensively used in nonlinear control with applications in helicopters, quadrotors and other aerial systems. The technique was comprehensively addresed by Krstic, Kanellakopoulos and Kokotovic in [56].

The idea of Backstepping is to design a controller for the nonlinear system recursively by considering some of the state variables as “virtual controls” and designing intermediate control laws for them. It starts with a subsystem which is stabilizable with a known feedback law for a known Lyapunov function, and then adds to its input an integrator. For the augmented subsystem a new stabilizing feedback law is explicitly

designed and shown to be stabilizing for a new Lyapunov function. The process continues till the explicit construction of the controller and the Lyapunov function for the complete system.

We will now recall the nonlinear system model from (5.11). The system (5.11) is a cascaded highly nonlinear system in the well-known ([57], [58]) strict feedback form. This form is defined in general as

$$(S_1): \begin{cases} \dot{x}_1 = f_0(x_1) + g_0(x_1)\ x_2 \\ \dot{x}_2 = f_1(x_1, x_2) + g_1(x_1, x_2)\ u \end{cases} \tag{5.29}$$

By comparing equations (5.11), (5.29) we get

$$x_1 = \xi_e,\ x_2 = \nu,\ f_0 = 0,\ g_0 = J(\xi_e),\ f_1 = B(\xi_e, \nu),\ g_1 = N \tag{5.30}$$

This particular form of the nonlinear system of the aerial manipulator is appropriate for applying the backstepping recursive controller design method.

A manipulation task is usually given in terms of desired position and orientation of the end-effector. The objective of this section is to design a controller of the proposed aerial manipulator ensuring that the position $p_e(t)$ and the orientation $\Theta(t)$ of the end-effector tracks the desired Cartesian trajectory

$$\xi_{\text{des}}(t) = \begin{bmatrix} x_{\text{des}}(t) & y_{\text{des}}(t) & z_{\text{des}}(t) & \phi_{\text{des}}(t) & \theta_{\text{des}}(t) & \psi_{\text{des}}(t) \end{bmatrix}^\tau \in \mathbb{R}^6 \tag{5.31}$$

asymptotically. Thus, a nonlinear controller $\lambda(\xi_e, \nu)$ should be designed in order to guarantee that

$$\lim_{t\to\infty} \|\xi_e(t) - \xi_{\text{des}}\| = 0 \tag{5.32}$$

and all closed loop signals required in controller design should remain bounded for all $t \geq 0$.

The system (5.11) is separated in kinematic and dynamic model. The objective of the kinematic control is to find suitable vehicle trajectories $\nu(t)$ that correspond to a desired end-effector trajectory $\xi_e(t)$. The objective of the dynamic controller is to find suitable control inputs $\lambda_i(t),\ i = 1, .., 6$ to drive the desired velocities $\nu(t)$ from kinematic controller.

It is generally known in control theory that due to imperfect modelling, the system dynamics are in presence of parameters uncertainties, actuation failures, unmodeled dynamics, modelling errors and external disturbances. All this parameters, may decrease the performance of the closed loop system and cause system instabilities. Therefore, the nonlinear controller should be designed in such a way that are taken into consideration and are tackled these problems in order to increase closed loop efficiency.

The reasons which made us to take into consideration of the uncertainties and the disturbances in the system dynamic model (5.11) are the imperfect mathematical modeling from Chapters 3, 4 and the unpredictable changes in the physical environment. Control techniques, such as robust control, can yield good performance for these cases. It is possible to determine the bounds on the system uncertainties and design a robust control scheme, which guarantees stable control of the system as long as the uncertainties stay within these bounds. However, robust control does not enhance its performance with time. When a certain amount of error is present in a robust control system, the error gets carried on even in a repetitive task. The solution to this problem is the use of adaptive control methods.

Mathematical modelling is the central point in almost all control system design methods. However, no physical system can be perfectly modeled and there is a mismatch between the model and the physical system. Even if an exact model of the physical system is available, one type of uncertainty may still arise from some exogenous disturbances which might affect the control system via imperfect measurement of state or output. On the other hand, other types of uncertainties may be present due to the lack of knowledge about the physical system. Even if the model is qualitatively correct, i.e. the structure of the model is exact, the actual parameter values of the physical system could hardly be obtained exactly.

Robustness of a control system determines the capability of the controller to be unaffected by the uncertainties. Since uncertainties will always be present, robustness is always a desired property when designing control systems.

Another problem is the change of system dynamics due to changes in the environment in an unexpected manner. For example, although the exact mathematical model of the aerial manipulator is usually available, there may be abrupt changes in the loads that the manipulator handles. This kind of unknown changes in the dynamics lead to an inexact model and create difficulties in its control.

Additionally, the controller should be able to handle problems such as battery drains, miscalculated mechanical properties, measurement bias and noise. To cope with these

uncertainties, the controller needs to be adaptive. The Adaptive Control tries to remove the effects of the uncertainties in the system model. Te objective of the adaptive control is to provide a mechanism such that the model parameters converge to the true values, even if the actual system parameters change unexpectedly.

Due to the fact that the model plan is in presence of uncertainties, an adaptive backstepping controller is the best solution. The uncertain plant parameters will be estimated on-line since the adaptive controller is a dynamic system with an online parameter estimation. The stability analysis will be held with the well-known Lyapunov Stability Theory.

Taking all the above issues into consideration a robust adaptive backstepping controller will be designed in order to tackle them. Firstly, we consider the system as

$$(S): \begin{cases} \dot{\xi} = J(\xi_e)\ \nu \\ \dot{\nu} = B(\xi_e, \nu) + N\ \theta_\lambda^\star\ \lambda + d(\xi_e, \nu, t) \end{cases} \tag{5.33}$$

where $\theta_\lambda^\star = \mathbf{diag}\{\theta_1^\star,\ \dots\ ,\ \theta_6^\star\} \in \mathbb{R}^{6\times 6}$. The uncertainty in $\theta_\lambda^\star$ is introduced to model the control actuation failures and the modelling errors, in the sense that there may exist uncertain control gains or the designer may have incorrectly estimated the system control effectiveness. The entries $\theta_\lambda^\star$ are bounded in the set $[\theta_{\min}, \theta_{\max}] = [0.1, 1]$. This means that if for example $\theta_i^\star = 0.5$ for an arbitrary $i = 1, \dots, 6$ then the i-th acuator has 50 % controller effectiveness reduction. For Multi Input-Multi Output systems, such as the proposed system in the aerospace engineering field, it is usually useful to simultaneously estimate and adapt to differences between the real and design actuator effectiveness. The system is in the presence of disturbance $d(\xi_e, \nu, t) : \mathbb{R}^6 \times \mathbb{R}^6 \times \mathbb{R}_+ \to \mathbb{R}^6$ with

$$d(\xi_e, \nu, t) = \begin{bmatrix} d_1(\xi_e, \nu, t) & d_2(\xi_e, \nu, t) & \cdots & d_6(\xi_e, \nu, t) \end{bmatrix}^\tau \tag{5.34}$$

where d_i are continuous functions on (ξ_e, ν) and piecewise continuous on $t \geq 0$ representing the disturbances of the system. The disturbances might be time-dependent noise, constant disturbances, time varying disturbances, unmodeled nonlinear dynamics and external or environmental disturbances.

It is assumed for the disturbances that there are unknown positive constants $\Delta_i,\ i = 1, ..., 6$ such that

$$|d_i(\xi_e, \nu, t)| \leq \Delta_i\ \delta_i(\xi_e, \nu),\ i = 1, ..., 6 \tag{5.35}$$

where $\delta_i(\xi_e, \nu) : \mathbb{R}^6 \times \mathbb{R}^6 \to \mathbb{R}^6$ are known continuous and differentiable positive functions. This assumption is very crucial since ensures that the disturbances $d(\xi_e, \nu, t)$ will

not become unbounded for all $t \geq 0$. The matrix of unknown disturbance constants is defined as

$$\Delta = \begin{bmatrix} \Delta_1 & \Delta_2 & \cdots & \Delta_6 \end{bmatrix}^\tau \in \mathbb{R}^6 \tag{5.36}$$

Since the matrix Δ and the constants Δ_i are unknown they should be estimated online through the adaptation parameter updates laws. Let

$$\hat{\Delta} = \begin{bmatrix} \hat{\Delta}_1 & \hat{\Delta}_2 & \cdots & \hat{\Delta}_6 \end{bmatrix}^\tau \in \mathbb{R}^6 \tag{5.37}$$

$$\hat{\theta}_\lambda = \mathbf{diag}\{\hat{\theta}_1 \dots \hat{\theta}_6\} \in \mathbb{R}^{6\times 6} \tag{5.38}$$

denote the matrix of estimations of the unknown parameters. The matrix of the parameter estimations errors are given by

$$\tilde{\Delta} = \begin{bmatrix} \tilde{\Delta}_1 & \tilde{\Delta}_2 & \cdots & \tilde{\Delta}_6 \end{bmatrix}^\tau \in \mathbb{R}^6 \tag{5.39}$$

$$\tilde{\theta}_\lambda = \mathbf{diag}\{\tilde{\theta}_1 \dots \tilde{\theta}_6\} \in \mathbb{R}^{6\times 6} \tag{5.40}$$

Obviously, we have

$$\tilde{\Delta} = \hat{\Delta} - \Delta \tag{5.41}$$

The value of $\tilde{\Delta}$ will generally be unknown. However, it is not required by the control law (only the estimations $\hat{\Delta}$ are required), it is used only in the Lyapunov design process. We are proceeding now with the controller design suitable for the proposed system.

In order to design the controller of the system (5.33), the following assumptions are required:

Assumption 1: The states of the system ξ_e, ν are available for measurement $\forall\ t \geq 0$ for the following control development.

Assumption 2: The desired trajectories ξ_{des} are known bounded functions of time ($\xi_{\text{des}} \in \mathcal{L}_\infty$) with known and bounded derivatives ($\dot{\xi}_{\text{des}}, \ddot{\xi}_{\text{des}} \in \mathcal{L}_\infty$).

Assumption 3: It is assumed for all $t \geq 0$ that $-\frac{\pi}{2} < \theta(t) < \frac{\pi}{2}$. This ensures that the Jacobian matrix is nonsingular since $\det(J(\xi_e)) = 1/c_\theta$. This assumption is likewise utilized in [47], [48].

• ***Step 1:*** To begin with the backstepping controller design, let the position-orientation error of the end-effector $z_1 \in \mathbb{R}^6$ be given by

$$z_1 = \xi_e - \xi_{\text{des}} \tag{5.42}$$

By differentiating (5.42) and using (3.68) we get

$$\begin{aligned}\dot{z}_1 &= \dot{\xi}_e - \dot{\xi}_{\text{des}} \\ &= J(\xi_e)\ \nu - \dot{\xi}_{\text{des}}\end{aligned} \tag{5.43}$$

We view ν as a control variable and we define a virtual control law for (5.43), say $\nu_{\text{des}} \in \mathbb{R}^6$, and let $z_2 \in \mathbb{R}^6$ be an error signal representing the difference between the virtual and actual controls of (5.43) as

$$\begin{aligned}z_2 &= \nu - \nu_{\text{des}} \\ \Leftrightarrow \nu &= \nu_{\text{des}} + z_2\end{aligned} \tag{5.44}$$

Thus, in terms of the new state variable, (5.43) can be rewritten as

$$\begin{aligned}\dot{z}_1 &= J(\xi_e)\ (\nu_{\text{des}} + z_2) - \dot{\xi}_{\text{des}} \\ &= J(\xi_e)\ \nu_{\text{des}} + J(\xi_e)\ z_2 - \dot{\xi}_{\text{des}}\end{aligned} \tag{5.45}$$

Consider now a positive definite and radially unbounded ($V(z_1) \to \infty,\ \text{as}\ \|z_1\| \to \infty$) candidate Lyapunov function as the squared norm of error z_1

$$V_1(z_1) = \frac{1}{2}\|z_1\|^2 = \frac{1}{2} z_1^\tau z_1 \tag{5.46}$$

Its time derivative is

$$\dot{V}_1(z_1) = \frac{1}{2}\dot{z}_1^\tau z_1 + \frac{1}{2} z_1^\tau \dot{z}_1 \tag{5.47}$$

Noting that

$$\dot{z}_1^\tau z_1 = z_1^\tau \dot{z}_1 \tag{5.48}$$

we arrive at

$$\begin{aligned}\dot{V}_1(z_1) &= 2\ \frac{1}{2}\ z_1^\tau \dot{z}_1 \\ &= z_1^\tau \left\{ J(\xi_e)\ \nu_{\text{des}} + J(\xi_e)\ z_2 - \dot{\xi}_{\text{des}} \right\} \\ &= z_1^\tau \left\{ J(\xi_e)\ \nu_{\text{des}} - \dot{\xi}_{\text{des}} \right\} + z_1^\tau J(\xi_e) z_2\end{aligned} \tag{5.49}$$

The stabilization of z_1 can be obtained by designing an appropriate virtual control law

$$\nu_{\text{des}} = J^{-1}(\xi_e)\ \left\{ \dot{\xi}_{\text{des}} - K_1 z_1 \right\} \tag{5.50}$$

where matrix $K_1 \in \mathbb{R}^{6\times6}, K_1 = K_1^\tau > 0$ is diagonal, positive definite and represents the first controller gain to be designed. Hence, the time derivative of V_1 becomes

$$\dot{V}_1 = -z_1^\tau K_1 z_1 + z_1^\tau J(\xi_e) z_2 \tag{5.51}$$

The first term on the right-hand side in (5.51) is stable, and the second term will be canceled at the next step.

• ***Step 2:*** For the second step, we take into consideration the time derivative of error (5.44)

$$\dot{z}_2 = \dot{\nu} - \dot{\nu}_{\text{des}} \tag{5.52}$$

$$= B(\xi_e, \nu) + N\ \theta_\lambda^\star\ \lambda + d(\xi_e, \nu, t) - \dot{\nu}_{\text{des}} \tag{5.53}$$

Choosing the augmented radial unbounded Lyapunov function as

$$V_2(z_1, z_2, \tilde{\Delta}, \tilde{\theta}_\lambda) = V_1 + \frac{1}{2}\|z_2\|^2 + \frac{1}{2}\tilde{\Delta}^\tau\ \Gamma_\Delta^{-1}\ \tilde{\Delta} + \frac{1}{2}\mathbf{tr}(\tilde{\theta}_\lambda^\tau\ \Gamma_\theta^{-1}\ \tilde{\theta}_\lambda) \tag{5.54}$$

where $\Gamma_\Delta = \Gamma_\Delta^\tau > 0, \Gamma_\Delta \in \mathbb{R}^{6\times6}, \Gamma_\theta = \Gamma_\theta^\tau > 0, \Gamma_\theta \in \mathbb{R}^{6\times6}$ are diagonal adaptation gain matrices. The notation $\mathbf{tr}(\cdot)$ denotes the matrix trace. The adaptive parameters will be adjusted in the adaptive control that are given below. The time derivative of the constant parameter estimation errors are

$$\dot{\tilde{\Delta}} = \dot{\hat{\Delta}} - \dot{\Delta} = \dot{\hat{\Delta}} \in \mathbb{R}^6 \tag{5.55}$$

$$\dot{\tilde{\theta}}_i = \dot{\hat{\theta}}_i - \dot{\theta}_i^\star = \dot{\hat{\theta}}_i,\ \forall i = 1, \ldots, 6 \tag{5.56}$$

The time derivative of the augmented Lyapunov (5.54) can be calculated by

$$\begin{aligned}\dot{V}_2(z_1, z_2, \tilde{\Delta}, \tilde{\theta}_\lambda) &= \dot{V}_1(z_1) + z_2^\tau \dot{z}_2 + \frac{1}{2}\dot{\tilde{\Delta}}^\tau\ \Gamma_\Delta^{-1}\ \tilde{\Delta} + \frac{1}{2}\tilde{\Delta}^\tau\ \Gamma_\Delta^{-1}\ \dot{\tilde{\Delta}} + \frac{1}{2}\mathbf{tr}(\dot{\tilde{\theta}}_\lambda^\tau\ \Gamma_\theta^{-1}\ \tilde{\theta}_\lambda) \\ &\qquad + \frac{1}{2}\mathbf{tr}(\tilde{\theta}_\lambda^\tau\ \Gamma_\theta^{-1}\ \dot{\tilde{\theta}}_\lambda) \\ &= -z_1^\tau K_1 z_1 + z_1^\tau J(\xi_e) z_2 + z_2^\tau \dot{z}_2 + 2\ \frac{1}{2}\ \tilde{\Delta}^\tau\ \Gamma_\Delta^{-1}\ \dot{\tilde{\Delta}} + 2\ \frac{1}{2}\mathbf{tr}(\tilde{\theta}_\lambda^\tau\ \Gamma_\theta^{-1}\ \dot{\tilde{\theta}}_\lambda) \\ &= -z_1^\tau K_1 z_1 + z_1^\tau J(\xi_e) z_2 + z_2^\tau \dot{z}_2 + \tilde{\Delta}^\tau\ \Gamma_\Delta^{-1}\ \dot{\tilde{\Delta}} + \mathbf{tr}(\tilde{\theta}_\lambda^\tau\ \Gamma_\theta^{-1}\ \dot{\tilde{\theta}}_\lambda)\end{aligned} \tag{5.57}$$

It should be noted that

$$z_1^\tau J(\xi_e) z_2 = z_2^\tau J^\tau(\xi_e) z_1 \tag{5.58}$$

By substituting the last equation in (5.57) we have

$$\begin{aligned}
\dot{V}_2(z_1, z_2, \tilde{\Delta}, \tilde{\theta}_\lambda) &= -z_1^\tau K_1 z_1 + z_2^\tau J^\tau(\xi_e) z_1 + z_2^\tau \dot{z}_2 + \tilde{\Delta}^\tau \ \Gamma_\Delta^{-1} \ \dot{\tilde{\Delta}} + \mathbf{tr}(\tilde{\theta}_\lambda^\tau \ \Gamma_\theta^{-1} \ \dot{\tilde{\theta}}_\lambda) \\
&= -z_1^\tau K_1 z_1 + z_2^\tau \left\{ J^\tau(\xi_e) z_1 + \dot{z}_2 \right\} + \tilde{\Delta}^\tau \ \Gamma_\Delta^{-1} \ \dot{\tilde{\Delta}} + \mathbf{tr}(\tilde{\theta}_\lambda^\tau \ \Gamma_\theta^{-1} \ \dot{\tilde{\theta}}_\lambda) \\
&= -z_1^\tau K_1 z_1 + z_2^\tau \left\{ J^\tau(\xi_e) z_1 + B(\xi_e, \nu) + N \ \theta_\lambda^\star \ \lambda + d(\xi_e, \nu, t) - \dot{\nu}_{\text{des}} \right\} \\
&\qquad + \tilde{\Delta}^\tau \ \Gamma_\Delta^{-1} \ \dot{\tilde{\Delta}} + \mathbf{tr}(\tilde{\theta}_\lambda^\tau \ \Gamma_\theta^{-1} \ \dot{\tilde{\theta}}_\lambda) \\
&= -z_1^\tau K_1 z_1 + z_2^\tau \left\{ J^\tau(\xi_e) z_1 + B(\xi_e, \nu) + N \ \theta_\lambda^\star \ \lambda - \dot{\nu}_{\text{des}} \right\} \\
&\qquad + z_2^\tau \ d(\xi_e, \nu, t) + \tilde{\Delta}^\tau \ \Gamma_\Delta^{-1} \ \dot{\tilde{\Delta}} + \mathbf{tr}(\tilde{\theta}_\lambda^\tau \ \Gamma_\theta^{-1} \ \dot{\tilde{\theta}}_\lambda)
\end{aligned} \tag{5.59}$$

Writing vector z_2 as

$$z_2 = \begin{bmatrix} z_{2,1} & \cdots & z_{2,6} \end{bmatrix}^\tau \in \mathbb{R}^6 \tag{5.60}$$

and using basic mathematic inequalities properties the following statements hold

$$\begin{aligned}
z_2^\tau \ d(\xi_e, \nu, t) &= \begin{bmatrix} z_{2,1} & \cdots & z_{2,6} \end{bmatrix} \begin{bmatrix} d_1(\xi_e, \nu, t) \\ \vdots \\ d_6(\xi_e, \nu, t) \end{bmatrix} = \sum_{i=1}^{6} z_{2,i} \ d_i(\xi_e, \nu, t) \\
&\leq \sum_{i=1}^{6} |z_{2,i} \ d_i(\xi_e, \nu, t)| \leq \sum_{i=1}^{6} |z_{2,i}| \ |d_i(\xi_e, \nu, t)| \\
&\leq \sum_{i=1}^{6} |z_{2,i}| \ \Delta_i \ \delta_i(\xi_e, \nu, t) \\
&= \begin{bmatrix} |z_{2,1}| & \cdots & |z_{2,6}| \end{bmatrix} \begin{bmatrix} \Delta_1 \ \delta_1(\xi_e, \nu, t) \\ \vdots \\ \Delta_6 \ \delta_6(\xi_e, \nu, t) \end{bmatrix} \\
&= \{ \mathbf{sgn}(z_2) \ z_2 \}^\tau \begin{bmatrix} \Delta_1 \ \delta_1(\xi_e, \nu, t) \\ \vdots \\ \Delta_6 \ \delta_6(\xi_e, \nu, t) \end{bmatrix} \\
&= z_2^\tau \ \{ \mathbf{sgn}(z_2) \}^\tau \begin{bmatrix} \Delta_1 \ \delta_1(\xi_e, \nu, t) \\ \vdots \\ \Delta_6 \ \delta_6(\xi_e, \nu, t) \end{bmatrix} \\
&= z_2^\tau \ \mathbf{sgn}(z_2) \begin{bmatrix} \Delta_1 \ \delta_1(\xi_e, \nu, t) \\ \vdots \\ \Delta_6 \ \delta_6(\xi_e, \nu, t) \end{bmatrix}
\end{aligned} \tag{5.61}$$

where

$$\mathbf{sgn}(x) = \begin{cases} 1, & \text{if } x > 0 \\ 0, & \text{if } x = 0 \\ -1, & \text{if } x < 0 \end{cases} \tag{5.62}$$

$$\mathbf{sgn}(z_2) = \{\mathbf{sgn}(z_2)\}^\tau = \mathbf{diag}\{\mathbf{sgn}(z_{2,1}),\ \dots\ , \mathbf{sgn}(z_{2,6})\} \in \mathbb{R}^{6\times 6} \tag{5.63}$$

By adding and subtracting the terms $\hat{\Delta}_i\ \delta_i(\xi_e, \nu), i = 1, ..., 6$ in the equation (5.61) we obtain

$$\begin{aligned}
z_2^\tau\ d(\xi_e, \nu, t) &\leq z_2^\tau\ \mathbf{sgn}(z_2) \begin{bmatrix} \Delta_1\ \delta_1(\xi_e, \nu) \pm \hat{\Delta}_1\ \delta_1(\xi_e, \nu) \\ \vdots \\ \Delta_6\ \delta_6(\xi_e, \nu) \pm \hat{\Delta}_6\ \delta_6(\xi_e, \nu) \end{bmatrix} \\
&= z_2^\tau\ \mathbf{sgn}(z_2) \begin{bmatrix} (\Delta_1 - \hat{\Delta}_1)\ \delta_1(\xi_e, \nu) + \hat{\Delta}_1\ \delta_1(\xi_e, \nu) \\ \vdots \\ (\Delta_6 - \hat{\Delta}_6)\ \delta_6(\xi_e, \nu) + \hat{\Delta}_6\ \delta_6(\xi_e, \nu) \end{bmatrix} \\
&= z_2^\tau\ \mathbf{sgn}(z_2) \begin{bmatrix} -\tilde{\Delta}_1\ \delta_1(\xi_e, \nu) + \hat{\Delta}_1\ \delta_1(\xi_e, \nu) \\ \vdots \\ -\tilde{\Delta}_6\ \delta_6(\xi_e, \nu) + \hat{\Delta}_6\ \delta_6(\xi_e, \nu) \end{bmatrix} \\
&= -z_2^\tau\ \mathbf{sgn}(z_2) \begin{bmatrix} \tilde{\Delta}_1\ \delta_1(\xi_e, \nu) \\ \vdots \\ \tilde{\Delta}_6\ \delta_6(\xi_e, \nu) \end{bmatrix} + z_2^\tau\ \mathbf{sgn}(z_2) \begin{bmatrix} \hat{\Delta}_1\ \delta_1(\xi_e, \nu) \\ \vdots \\ \hat{\Delta}_6\ \delta_6(\xi_e, \nu) \end{bmatrix} \\
&= -z_2^\tau\ \mathbf{sgn}(z_2)\ \epsilon(\xi_e, \nu)\ \tilde{\Delta} + z_2^\tau\ \mathbf{sgn}(z_2)\ \epsilon(\xi_e, \nu)\ \hat{\Delta}
\end{aligned} \tag{5.64}$$

where

$$\epsilon(\xi_e, \nu) = \{\epsilon(\xi_e, \nu)\}^\tau = \mathbf{diag}\{\delta_1(\xi_e, \nu),\ \dots\ , \delta_6(\xi_e, \nu)\} \tag{5.65}$$

Using inequality (5.64) the Lyapunov function (5.59) becomes

$$\begin{aligned}
&\dot{V}_2(z_1, z_2, \tilde{\Delta}, \tilde{\theta}_\lambda) \\
&\leq -z_1^\tau K_1 z_1 + z_2^\tau \{J^\tau(\xi_e) z_1 + B(\xi_e, \nu) + N\ \theta_\lambda^\star\ \lambda - \dot{\nu}_{\text{des}}\} \\
&+ z_2^\tau\ \mathbf{sgn}(z_2)\ \epsilon(\xi_e, \nu)\ \hat{\Delta} - z_2^\tau\ \mathbf{sgn}(z_2)\ \epsilon(\xi_e, \nu)\ \tilde{\Delta} + \tilde{\Delta}^\tau\ \Gamma_\Delta^{-1}\ \dot{\hat{\Delta}} + \mathbf{tr}(\tilde{\theta}_\lambda^\tau\ \Gamma_\theta^{-1}\ \dot{\hat{\theta}}_\lambda) \\
&= -z_1^\tau K_1 z_1 + z_2^\tau \left\{ J^\tau(\xi_e) z_1 + B(\xi_e, \nu) + N\ \theta_\lambda^\star\ \lambda - \dot{\nu}_{\text{des}} + \mathbf{sgn}(z_2)\ \epsilon(\xi_e, \nu)\ \hat{\Delta} \right\} \\
&- z_2^\tau\ \mathbf{sgn}(z_2)\ \epsilon(\xi_e, \nu)\ \tilde{\Delta} + \tilde{\Delta}^\tau\ \Gamma_\Delta^{-1}\ \dot{\hat{\Delta}} + \mathbf{tr}(\tilde{\theta}_\lambda^\tau\ \Gamma_\theta^{-1}\ \dot{\hat{\theta}}_\lambda)
\end{aligned} \tag{5.66}$$

Invoking the property

$$\begin{aligned} z_2^\tau\ \mathbf{sgn}(z_2)\ \epsilon(\xi_e,\nu)\ \tilde{\Delta} &= \tilde{\Delta}^\tau\ \{\mathbf{sgn}(z_2)\ \epsilon(\xi_e,\nu)\}^\tau\ z_2 \\ &= \tilde{\Delta}^\tau\ \{\epsilon(\xi_e,\nu)\}^\tau\{\mathbf{sgn}(z_2)\}^\tau\ z_2 \\ &= \tilde{\Delta}^\tau\ \epsilon(\xi_e,\nu)\ \mathbf{sgn}(z_2)\ z_2 \end{aligned} \tag{5.67}$$

the Lyapunov function (5.66) becomes

$$\begin{aligned} &\dot{V}_2(z_1,z_2,\tilde{\Delta},\tilde{\theta}_\lambda) \\ &\leq -z_1^\tau K_1 z_1 + z_2^\tau \left\{ J^\tau(\xi_e) z_1 + B(\xi_e,\nu) + N\ \theta_\lambda^\star\ \lambda - \dot{\nu}_{\text{des}} + \mathbf{sgn}(z_2)\ \epsilon(\xi_e,\nu)\ \hat{\Delta} \right\} \\ &\quad - \tilde{\Delta}^\tau\ \epsilon(\xi_e,\nu)\ \mathbf{sgn}(z_2)\ z_2 + \tilde{\Delta}^\tau\ \Gamma_\Delta^{-1}\ \dot{\tilde{\Delta}} + \mathbf{tr}(\tilde{\theta}_\lambda^\tau\ \Gamma_\theta^{-1}\ \dot{\tilde{\theta}}_\lambda) \\ &= -z_1^\tau K_1 z_1 + z_2^\tau \left\{ J^\tau(\xi_e) z_1 + B(\xi_e,\nu) + N\ \theta_\lambda^\star\ \lambda - \dot{\nu}_{\text{des}} + \mathbf{sgn}(z_2)\ \epsilon(\xi_e,\nu)\ \hat{\Delta} \right\} \\ &\quad + \tilde{\Delta}^\tau\ \{\Gamma_\Delta^{-1}\ \dot{\tilde{\Delta}} - \epsilon(\xi_e,\nu)\ \mathbf{sgn}(z_2)\ z_2\} + \mathbf{tr}(\tilde{\theta}_\lambda^\tau\ \Gamma_\theta^{-1}\ \dot{\tilde{\theta}}_\lambda) \end{aligned} \tag{5.68}$$

By adding and subtracting the terms $z_2^\tau\ N\ \hat{\theta}_\lambda\ \lambda$ in the equation (5.68) we get

$$\begin{aligned} &\dot{V}_2(z_1,z_2,\tilde{\Delta},\tilde{\theta}_\lambda) \\ &\leq -z_1^\tau K_1 z_1 + z_2^\tau \left\{ J^\tau(\xi_e) z_1 + B(\xi_e,\nu) + N\ \theta_\lambda^\star\ \lambda \pm N\ \hat{\theta}_\lambda\ \lambda - \dot{\nu}_{\text{des}} + \mathbf{sgn}(z_2)\ \epsilon(\xi_e,\nu)\ \hat{\Delta} \right\} \\ &\quad + \tilde{\Delta}^\tau\ \{\Gamma_\Delta^{-1}\ \dot{\tilde{\Delta}} - \epsilon(\xi_e,\nu)\ \mathbf{sgn}(z_2)\ z_2\} + \mathbf{tr}(\tilde{\theta}_\lambda^\tau\ \Gamma_\theta^{-1}\ \dot{\tilde{\theta}}_\lambda) \\ &\leq -z_1^\tau K_1 z_1 + z_2^\tau \left\{ J^\tau(\xi_e) z_1 + B(\xi_e,\nu) + N\ \hat{\theta}_\lambda\ \lambda - \dot{\nu}_{\text{des}} + \mathbf{sgn}(z_2)\ \epsilon(\xi_e,\nu)\ \hat{\Delta} \right\} \\ &\quad - z_2^\tau\ N\ \tilde{\theta}_\lambda\ \lambda + \tilde{\Delta}^\tau\ \{\Gamma_\Delta^{-1}\ \dot{\tilde{\Delta}} - \epsilon(\xi_e,\nu)\ \mathbf{sgn}(z_2)\ z_2\} + \mathbf{tr}(\tilde{\theta}_\lambda^\tau\ \Gamma_\theta^{-1}\ \dot{\tilde{\theta}}_\lambda) \end{aligned} \tag{5.69}$$

Invoking the basic property $a^\tau\ b = \mathbf{tr}(b\ a^\tau),\ \forall\ a, b \in \mathbb{R}^n$ the following holds

$$\begin{aligned} -z_2^\tau\ N\ \tilde{\theta}_\lambda\ \lambda &= -\lambda^\tau\ \{N\ \tilde{\theta}_\lambda\}^\tau\ z_2 \\ &= -\lambda^\tau\ \tilde{\theta}^\tau\ N^\tau\ z_2 \\ &= -\underbrace{\lambda^\tau}_{a^\tau}\ \underbrace{\tilde{\theta}_\lambda^\tau\ N^\tau\ z_2}_{b} \\ &= -\mathbf{tr}(\tilde{\theta}_\lambda^\tau\ N^\tau\ z_2\ \lambda^\tau) \end{aligned} \tag{5.70}$$

By substituting the (5.70) in (5.69) we get

$$\begin{aligned}
&\dot{V}_2(z_1, z_2, \tilde{\Delta}, \tilde{\theta}_\lambda) \\
&\leq -z_1^\tau K_1 z_1 + z_2^\tau \left\{ J^\tau(\xi_e) z_1 + B(\xi_e, \nu) + N\ \hat{\theta}_\lambda\ \lambda - \dot{\nu}_{\text{des}} + \mathbf{sgn}(z_2)\ \epsilon(\xi_e, \nu)\ \hat{\Delta} \right\} \\
&\quad - \mathbf{tr}(\tilde{\theta}_\lambda^\tau\ N^\tau\ z_2\ \lambda^\tau) + \tilde{\Delta}^\tau\ \{\Gamma_\Delta^{-1}\ \dot{\hat{\Delta}} - \epsilon(\xi_e, \nu)\ \mathbf{sgn}(z_2)\ z_2\} + \mathbf{tr}(\tilde{\theta}_\lambda^\tau\ \Gamma_\theta^{-1}\ \dot{\hat{\theta}}_\lambda) \\
&= -z_1^\tau K_1 z_1 + z_2^\tau \left\{ J^\tau(\xi_e) z_1 + B(\xi_e, \nu) + N\ \hat{\theta}_\lambda\ \lambda - \dot{\nu}_{\text{des}} + \mathbf{sgn}(z_2)\ \epsilon(\xi_e, \nu)\ \hat{\Delta} \right\} \\
&\quad + \tilde{\Delta}^\tau\ \{\Gamma_\Delta^{-1}\ \dot{\hat{\Delta}} - \epsilon(\xi_e, \nu)\ \mathbf{sgn}(z_2)\ z_2\} + \mathbf{tr}\{\tilde{\theta}_\lambda^\tau(\Gamma_\theta^{-1}\ \dot{\hat{\theta}}_\lambda - N^\tau\ z_2\ \lambda^\tau)\}
\end{aligned} \tag{5.71}$$

Aiming to reinforce robustness of the system, a σ-Modification adaptive control design method will be introduced for the parameter estimation update law $\dot{\hat{\Delta}}$ in order to compensate the unknown disturbances effectively. This method is discussed extensively in [59], [60]. Given the form of $\dot{V}_2$ from (5.71), the adaptive control law for the nonlinear system (S) to be designed is

$$\lambda(\xi_e, \nu, \hat{\Delta}, \hat{\theta}_\lambda) = (\hat{\theta}_\lambda)^{-1}\ N^{-1} \left\{ \dot{\nu}_{\text{des}} - J^\tau(\xi_e) z_1 - B(\xi_e, \nu) - \mathbf{sgn}(z_2)\ \epsilon(\xi_e, \nu)\ \hat{\Delta} - K_2\ z_2 \right\} \tag{5.72}$$

and the corresponding parameter estimator update law with σ-Modification method is

$$\dot{\hat{\Delta}} = \Gamma_\Delta \{\epsilon(\xi_e, \nu)\ \mathbf{sgn}(z_2)\ z_2 - \sigma\ \hat{\Delta}\} \tag{5.73}$$

The $K_2 \in \mathbb{R}^{6\times 6}$, $K_2 = K_2^\tau > 0$ is diagonal, positive definite second controller gain matrix to be designed and $\sigma > 0$ is the σ-modification parameter to prevent the parameter drift (see [59], [60]).

Substituting the control laws (5.72), (5.73) in Lyapunov equation (5.71) we obtain

$$\dot{V}_2(z_1, z_2, \tilde{\Delta}) \leq -z_1^\tau K_1 z_1 - z_2^\tau K_2 z_2 - \sigma\ \tilde{\Delta}^\tau\ \hat{\Delta} + \mathbf{tr}\{\tilde{\theta}_\lambda^\tau(\Gamma_\theta^{-1}\ \dot{\hat{\theta}}_\lambda - N^\tau\ z_2\ \lambda^\tau)\} \tag{5.74}$$

At this point, a projection operator method (see [61]) for the parameter update law $\dot{\hat{\theta}}_\lambda$ will be introduced. Projection methods are well-known algorithms in adaptive control theory that can guarantee fast adaptation, can improve robustness of the adaptive backstepping design and can ensure that the estimation parameters remain bounded in compact sets for all time. The parameter adaptation law should be chosen to ensure three rules. The first rule is to ensure that

$$\mathbf{tr}\{\tilde{\theta}_\lambda^\tau(\Gamma_\theta^{-1}\ \dot{\hat{\theta}}_\lambda - N^\tau\ z_2\ \lambda^\tau)\} \leq 0 \tag{5.75}$$

in order to guarantee that the Lyapunov function will not be increasing. The second is

to guarantee that the estimation of the unknown parameters $\hat{\theta}_\lambda$ should remain bounded for all $t \geq 0$. The last rule is to avoid singularity of the term $(\hat{\theta}_\lambda)^{-1}$ from (5.72). Taking all these into consideration, the parameter update law is designed as

$$\dot{\hat{\theta}}_\lambda = \Gamma_\theta \ \mathbf{Proj}(\hat{\theta}_\lambda, N^\tau \ z_2 \ \lambda^\tau) \tag{5.76}$$

where by defining the sets

$$\Omega = \{\theta_i \in \mathbb{R} : \theta_{\max} \leq \theta_i \leq \theta_{\max}, \ \forall \ i = 1, \ldots, 6\} \tag{5.77}$$

$$\Omega_\delta = \{\theta_i \in \mathbb{R} : \theta_{\max} - \delta \leq \theta_i \leq \theta_{\max} + \delta, \ \forall \ i = 1, \ldots, 6\} \tag{5.78}$$

the projection operator is defined as

$$\Big[\mathbf{Proj}(\hat{\theta}_\lambda, y)\Big]_{(ij)} = \begin{cases} \left[1 + \frac{\theta_{\max} - \hat{\theta}_{ij}}{\delta}\right] \ y_{ij}, & \text{if } \hat{\theta}_{ij} > \theta_{\max} \text{ and } y_{ij} > 0 \\ \left[1 + \frac{\hat{\theta}_{ij} - \theta_{\min}}{\delta}\right] \ y_{ij}, & \text{if } \hat{\theta}_{ij} < \theta_{\min} \text{ and } y_{ij} < 0 \\ y_{ij}, & \text{else} \end{cases} \tag{5.79}$$

for every element $(ij), \ i = 1, \ldots, 6, \ j = 1, \ldots, 6$ of the matrices $\hat{\theta}_\lambda, y$ where

$$y = N^\tau \ z_2 \ \lambda^\tau \tag{5.80}$$

The parameter $\delta > 0$ is to be designed. The projection operator (5.79) by definition ensures that

$$\begin{aligned} & \mathbf{tr}\{\tilde{\theta}_\lambda^\tau(\Gamma_\theta^{-1} \ \dot{\hat{\theta}}_\lambda - N^\tau \ z_2 \ \lambda^\tau)\} \leq 0 \\ \Leftrightarrow \ & \mathbf{tr}\{\tilde{\theta}_\lambda^\tau(\mathbf{Proj}(\hat{\theta}_\lambda, N^\tau \ z_2 \ \lambda^\tau) - N^\tau \ z_2 \ \lambda^\tau)\} \leq 0 \\ \Leftrightarrow \ & \mathbf{tr}\{\tilde{\theta}_\lambda^\tau(\mathbf{Proj}(\hat{\theta}_\lambda, y) - y)\} \leq 0 \end{aligned} \tag{5.81}$$

which means that the projection operator contributes to the negative semi-nagativeness of the Lyapunov function. Furthermore in can be verified that this rule satisfies

$$\hat{\theta}_i(0) \in \Omega \Rightarrow \hat{\theta}_i(t) \in \Omega_\delta, \ \forall t \geq 0 \tag{5.82}$$

hence, $\hat{\theta}_\lambda$ remains bounded for all $t \geq 0$ and the term $(\hat{\theta}_\lambda)^{-1}$ in (5.72) is protected away from singularity.

Therefore, using the projection operator property (5.81) the Lyapunov function results in

$$\dot{V}_2(z_1, z_2, \tilde{\Delta}, \tilde{\theta}_\lambda) \leq -z_1^\tau K_1 z_1 - z_2^\tau K_2 z_2 - \sigma\ \tilde{\Delta}^\tau\ \hat{\Delta} \tag{5.83}$$

Now invoking the Rayleigh-Ritz theorem from [59], [62]

$$\begin{aligned} \lambda_{\min}(P)\|x\|^2 \leq x^\tau P x \leq \lambda_{\max}(P)\|x\|^2 \\ \forall x \in \mathbb{R}^n,\ \forall\ P \in \mathbb{R}^{n\times n},\ P = P^\tau > 0 \end{aligned} \tag{5.84}$$

where $\lambda_{\mathbf{min}}(P), \lambda_{\mathbf{max}}(P)$ denote the minimum and the maximum eigenvalue of the matrix P, we have that

$$-z_1^\tau K_1 z_1 \leq -\lambda_{\min}(K_1)\|z_1\|^2 \tag{5.85}$$

$$-z_2^\tau K_2 z_2 \leq -\lambda_{\min}(K_2)\|z_2\|^2 \tag{5.86}$$

where obviously is $\lambda_{\min}(K_1), \lambda_{\min}(K_2) > 0$. Using (5.85), (5.86) in (5.83) we have

$$\dot{V}_2(z_1, z_2, \tilde{\Delta}) \leq -\lambda_{\min}(K_1)\|z_1\|^2 - \lambda_{\min}(K_2)\|z_2\|^2 - \sigma\ \tilde{\Delta}^\tau\ \hat{\Delta} \tag{5.87}$$

A significant property in the adaptive control theory is that for every $\tilde{\theta}, \hat{\theta}, \theta \in \mathbb{R}^p$, the following equality holds

$$\tilde{\theta}^\tau \hat{\theta} = \frac{1}{2}\|\tilde{\theta}\|^2 + \frac{1}{2}\|\hat{\theta}\|^2 - \frac{1}{2}\|\theta\|^2 \tag{5.88}$$

Using this property in (5.87) the Lyapunov function results in

$$\begin{aligned} \dot{V}_2(z_1, z_2, \tilde{\Delta}, \tilde{\theta}_\lambda) &\leq -\lambda_{\min}(K_1)\|z_1\|^2 - \lambda_{\min}(K_2)\|z_2\|^2 \\ &\quad - \sigma\ \{\frac{1}{2}\|\tilde{\Delta}\|^2 + \frac{1}{2}\|\hat{\Delta}\|^2 - \frac{1}{2}\|\Delta\|^2\} \\ &\leq -\lambda_{\min}(K_1)\|z_1\|^2 - \lambda_{\min}(K_2)\|z_2\|^2 \\ &\quad - \frac{\sigma}{2}\|\tilde{\Delta}\|^2 - \frac{\sigma}{2}\|\hat{\Delta}\|^2 + \frac{\sigma}{2}\|\Delta\|^2 \end{aligned} \tag{5.89}$$

It is obvious that the following inequality holds

$$-\frac{\sigma}{2}\|\tilde{\Delta}\|^2 - \frac{\sigma}{2}\|\hat{\Delta}\|^2 + \frac{\sigma}{2}\|\Delta\|^2 \leq -\frac{\sigma}{2}\|\tilde{\Delta}\|^2 + \frac{\sigma}{2}\|\Delta\|^2 \tag{5.90}$$

Then, (5.89) finally results in

$$\dot{V}_2(z_1, z_2, \tilde{\Delta}) \leq -\lambda_{\min}(K_1)\|z_1\|^2 - \lambda_{\min}(K_2)\|z_2\|^2 - \frac{\sigma}{2}\|\tilde{\Delta}\|^2 + \bar{w} \tag{5.91}$$

where $\bar{w}$ is the strictly positive term

$$w = \frac{\sigma}{2}\|\Delta\|^2 > 0 \tag{5.92}$$

From (5.91) it follows that $\dot{V}_2(z_1, z_2, \tilde{\Delta}) \leq 0$ when

$$\|z_2\| > \sqrt{\frac{\bar{w}}{\lambda_{\min}(K_1)}} \tag{5.93}$$

$$\textbf{or} \qquad \|z_2\| > \sqrt{\frac{\bar{w}}{\lambda_{\min}(K_2)}} \tag{5.94}$$

$$\textbf{or} \qquad \|\tilde{\Delta}\| > \sqrt{\frac{2\ \bar{w}}{\sigma}} \tag{5.95}$$

Thus, both the errors z_1, z_2 and the parameter estimation error $\tilde{\Delta}$ are uniformly ultimately bounded (see [59]) with respect to the sets

$$\Omega_1 = \left\{ z_1 \in \mathbb{R}^6 : \|z_1\| \leq \sqrt{\frac{w}{\lambda_{\min}(K_1)}} \right\} \tag{5.96}$$

$$\Omega_2 = \left\{ z_2 \in \mathbb{R}^6 : \|z_2\| \leq \sqrt{\frac{w}{\lambda_{\min}(K_2)}} \right\} \tag{5.97}$$

$$\Omega_\Delta = \left\{ \tilde{\Delta} \in \mathbb{R}^6 : \|\tilde{\Delta}\| \leq \sqrt{\frac{2\ w}{\sigma}} \right\} \tag{5.98}$$

One important issue associated with the controller design is the analytical form of the time derivative of the Jacobian matrix $J(\xi_e)$ and the virtual control vector ν_{des}. The time derivative of the Jacobian $J(\xi_e)$ was derived in Chapter 3 from the equation (3.73). The $\dot{\nu}_{\text{des}}$ can be calculated from (5.50) as

$$\begin{aligned} \nu_{\text{des}} &= J^{-1}(\xi_e)\ \left\{ \dot{\xi}_{\text{des}} - K_1 z_1 \right\} \\ \Leftrightarrow J(\xi_e)\ \nu_{\text{des}} &= \dot{\xi}_{\text{des}} - K_1 z_1 \\ \Leftrightarrow \dot{J}(\xi_e)\ \nu_{\text{des}} + J(\xi_e)\ \dot{\nu}_{\text{des}} &= \ddot{\xi}_{\text{des}} - K_1 \dot{z}_1 \\ \Leftrightarrow \dot{\nu}_{\text{des}} &= J^{-1}(\xi_e)\{\ddot{\xi}_{\text{des}} - \dot{J}(\xi_e)\ \nu_{\text{des}} - K_1 \dot{z}_1\} \end{aligned} \tag{5.99}$$

Invoking from the last results that the z_1, z_2 are bounded in the sets Ω_1, Ω_2 and $\xi_{\text{des}}, \nu_{\text{des}} \in \mathcal{L}_\infty$ from assumption 1, then $\xi_e, \nu \in \mathcal{L}_\infty$. Since $\tilde{\Delta}, \Delta, \hat{\theta}_\lambda, \theta_\lambda^\star$ are bounded then $\hat{\Delta}, \tilde{\theta}_\lambda \in \mathcal{L}_\infty$. Using (5.99) yields that $\dot{\nu}_{\text{des}} \in \mathcal{L}_\infty$ and invoking this, from (5.72) yields that $\lambda \in \mathcal{L}_\infty$. Therefore, it was proven that all closed loop signals are bounded.

The resulting closed-loop error dynamics system for new states $z1, z2 \in \mathbb{R}^6$, with all signals having been proven to be bounded, can be depicted in matrix form as

$$\begin{bmatrix} \dot{z}_1 \\ \dot{z}_2 \end{bmatrix} = \begin{bmatrix} -K_1 & J(\xi_e) \\ -J^\tau(\xi_e) & -K_2 \end{bmatrix} \begin{bmatrix} z_1 \\ z_2 \end{bmatrix} + \begin{bmatrix} O_{(6\times 1)} \\ d(\xi_e, \nu, t) - \mathbf{sgn}(z_2)\ \epsilon(\xi_e, \nu)\ \hat{\Delta} \end{bmatrix} \tag{5.100}$$

$$\dot{\hat{\Delta}} = \Gamma_\Delta \{\epsilon(\xi_e, \nu)\ \mathbf{sgn}(z_2)\ z_2 - \sigma\ \hat{\Delta}\} \tag{5.101}$$

$$\dot{\hat{\theta}}_\lambda = \Gamma_\theta\ \mathbf{Proj}(\hat{\theta}_\lambda, N^\tau\ z_2\ \lambda^\tau) \tag{5.102}$$

Although it is written in a linear-like form, this system is highly nonlinear.

The aforementioned analysis of the controller design in this section could be summarized by the following theorem.

Theorem: Given the dynamic model (5.33) utilized with parameters from Table (2.2), under the assuptions 1-3, the control law (5.72) and the adaptive parameters update laws (5.73), (5.76), all closed signals are bounded and asymptotic tracking

$$\lim_{t\to\infty} \|\xi_e - \xi_{\text{des}}\| = 0 \tag{5.103}$$

is achieved.

While observing the controller design procedure, it should be noted that the only loss of controllability of the proposed system is due to the singularity of matrices $J(\xi_e)$ and N. The first was discussed in Chapter 3, thus due to assumption (3.8) is well-defined and the second matrix has full rank with well-defined and small condition number which is a vital result for the control oriented optimization from [1].

Chapter 6

Simulation Results

In this chapter, the results of extended numerical simulations performed in computer with the MATLAB/Simulink Environment are presented in order to demonstrate the flight performance of the proposed framework for the aerial robot in dynamic environments. Consequently, the effectiveness of the control law designed in Chapter 6 can be verified. The dynamic model in (5.33) is utilized with system parameters which are depicted in Table 2.2.

A task for the proposed system modeled in the previous Chapters is usually specified in terms of a desired trajectory for the end-effector Cartesian position $p_e(t) = [x_e(t) \;\; y_e(t) \;\; z_e(t)]^\tau$ and corresponding Cartesian orientation $\Theta(t) = [\phi(t) \;\; \theta(t) \;\; \psi(t)]^\tau$. The proposed aerial robot is required to move from the Earth-Fixed Frame to a desired position-orientation in 3D Cartesian space, namely Stabilization Scenario, or to track a desired position-orientation trajectory, namely trajectory tracking Scenario.

Each Scenario is accompanied with two Figures with the position/orientation errors and the required thrust forces respectively. The simulations parameters are depicted in the corresponding Tables. The 3D animation simulations (videos in .avi file format) for the proposed system demonstrated with Matlab Software and the video files are available with the CD included with the printed version of this thesis. The geometric transformations and the frame graphics animation were carried out using the Corke MATLAB Toolbox [63].

Scenario 1: In this scenario the end-effector of the proposed aerial manipulator is forced to stabilize at the position $p_{\text{e,des}} = [-2 \ -2 \ 5]^\tau$ with regulated desired orientation $\Theta(t) = [0 \ 0 \ 0]^\tau$ with reference to Earth-Fixed frame and 10 % controller effectiveness reduction. The parameters for this simulation are depicted in Table 6.1 and the corresponding simulation results in Figures 6.1,6.2.

Parameter	Description	Value
$\xi_e(0)$	Initial End-Effector Position/Orientation	$[-0.23 \ 0.015 \ 0.23 \ 0 \ 0 \ 0]^\tau$
$p(0)$	Initial Body-Frame Position	$[0 \ 0 \ 0]^\tau$
$\nu(0)$	Initial Body-Fixed Velocities	$[0 \ 0 \ 0 \ 0 \ 0 \ 0]^\tau$
$\hat{\theta}(0)$	Initial Parameter Estimation Conditions	0.7 **diag**$\{1, 1, 1, 1, 1, 1\}$
$\hat{\Delta}(0)$	Initial Parameter Estimation Conditions	$[0, 0, 0, 0, 0, 0]^\tau$
K_1	Gain of kinematic Controller	0.3 **diag**$\{1, 1, 1, 1, 1, 1\}$
K_2	Gain of Dynamic Controller	8 **diag**$\{1, 1, 1, 1, 1, 1\}$
$\theta^\star_\lambda$	Unknown Actuator Parameters	0.9 **diag**$\{1, 1, 1, 1, 1, 1\}$
Γ_θ	Adaptation Gain Matrix	0.1 **diag**$\{1, 1, 1, 1, 1, 1\}$
Γ_Δ	Adaptation Gain Matrix	13 **diag**$\{1, 1, 1, 1, 1, 1\}$
σ	σ-Modificatioon Gain	0.3
$d(t)$	Disturbance	$[2\sin(t) \ 0.1 \ 0.2 \ 0.5 \ 0.7 \ 2\cos(t)]^\tau$
δ	Projection Parameter	0.05

TABLE 6.1: Simulation Parameters for Scenario 1

Scenario 2: In this scenario the end-effector of the proposed aerial manipulator is forced to stabilize at the position $p_{\text{e,des}} = [2 \ 3 \ 2]^\tau$ with regulated desired orientation $\Theta(t) = \left[\frac{\pi}{4} \ -\frac{\pi}{3} \ \frac{\pi}{6}\right]^\tau$ with reference to Earth-Fixed frame and 20 % controller effectiveness reduction. The parameters for this simulation are depicted in Table 6.2 and the corresponding simulation results in Figures 6.3,6.4.

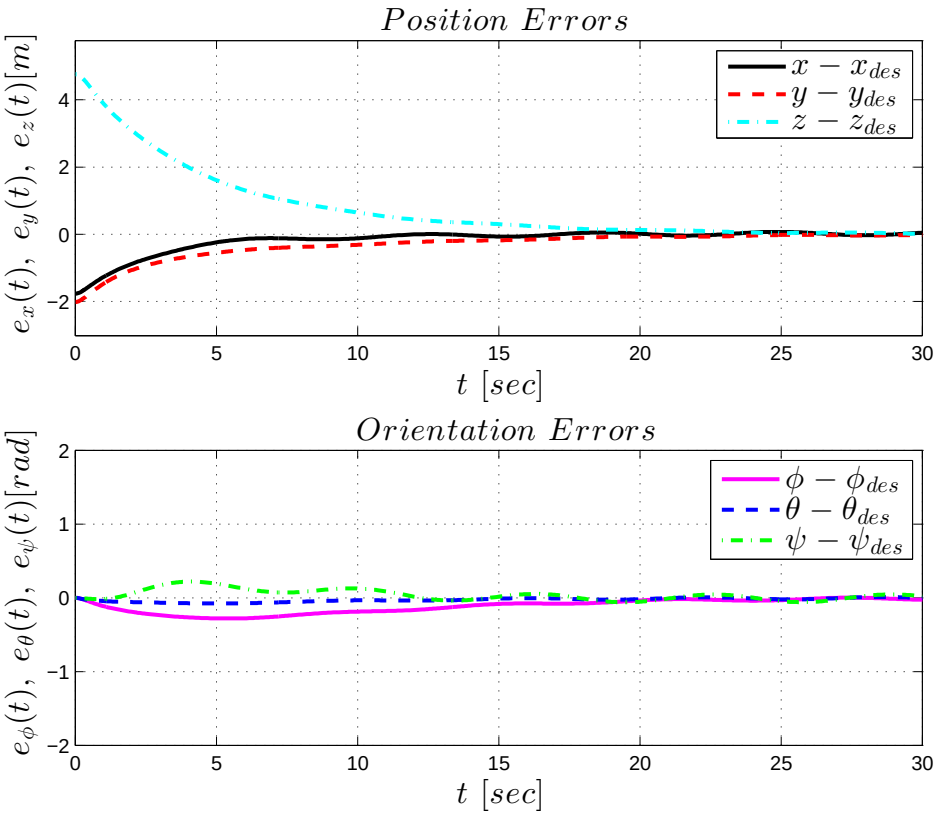

FIGURE 6.1: Position and Orientation Errors in Scenario 1

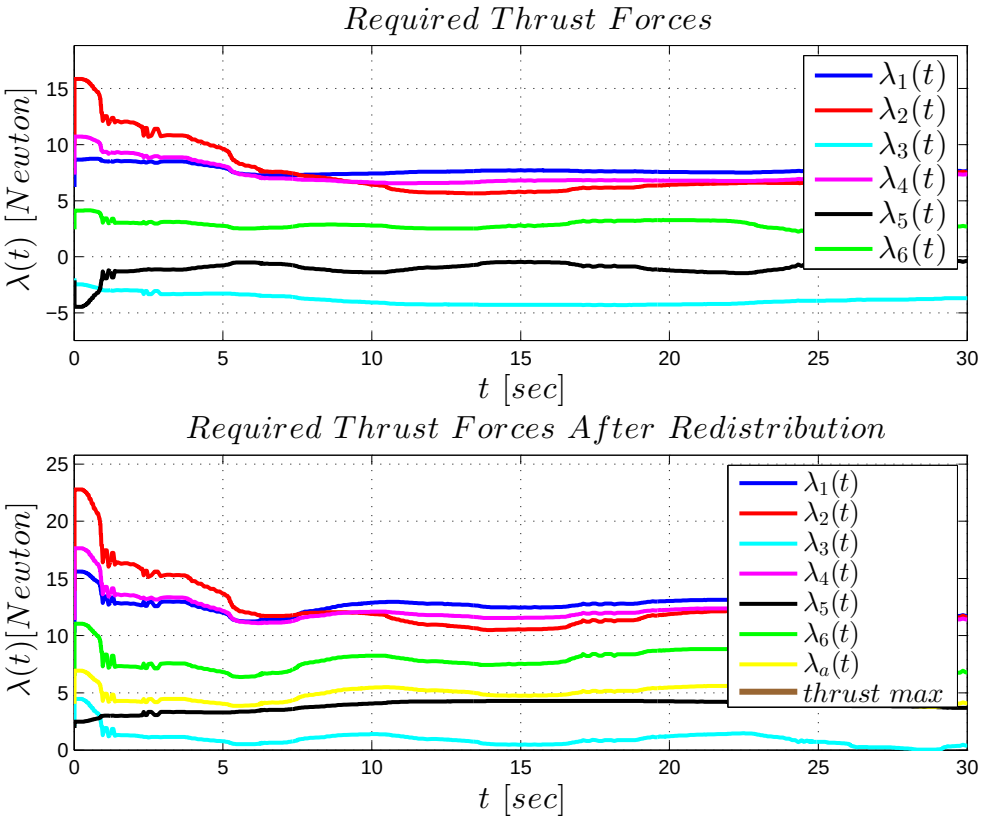

FIGURE 6.2: Required Thrust Forces Using Redistribution Algorithm in Scenario 1

Parameter	Description	Value
$\xi_e(0)$	Initial End-Effector Position/Orientation	$[-0.23\ 0.015\ 0.23\ 0\ 0\ 0]^\tau$
$p(0)$	Initial Body-Frame Position	$[0\ 0\ 0]^\tau$
$\nu(0)$	Initial Body-Fixed Velocities	$[0\ 0\ 0\ 0\ 0\ 0]^\tau$
$\hat{\theta}(0)$	Initial Parameter Estimation Conditions	$0.7\ \mathbf{diag}\{1,1,1,1,1,1\}$
$\hat{\Delta}(0)$	Initial Parameter Estimation Conditions	$[0,0,0,0,0,0]^\tau$
K_1	Gain of kinematic Controller	$0.3\ \mathbf{diag}\{1,1,1,1,1,1\}$
K_2	Gain of Dynamic Controller	$6\ \mathbf{diag}\{1,1,1,1,1,1\}$
$\theta^\star_\lambda$	Unknown Actuator Parameters	$0.8\ \mathbf{diag}\{1,1,1,1,1,1\}$
Γ_θ	Adaptation Gain Matrix	$0.2\ \mathbf{diag}\{1,1,1,1,1,1\}$
Γ_Δ	Adaptation Gain Matrix	$8\ \mathbf{diag}\{1,1,1,1,1,1\}$
σ	σ-Modificatioon Gain	1.5
$d(t)$	Disturbance	$[1.2\ 0.1\sin(t)\ 0.2\sin(t)\ 0.5\ 0.7\ 2\cos(t)]^\tau$
δ	Projection Parameter	0.05

TABLE 6.2: Simulation Parameters for Scenario 2

Scenario 3: In this scenario the end-effector of the proposed aerial manipulator is forced to track the trajectory $p_{\mathrm{e,des}}(t) = [\sin(t)\ \cos(t)\ 3\sin(t)]^\tau$ with regulated orientation $\Theta(t) = [0\ 0\ 0]^\tau$ with reference to Earth-Fixed frame and 15% controller effectiveness reduction. The parameters for this simulation are depicted in Table 6.3 and the corresponding simulation results in Figures 6.5,6.6.

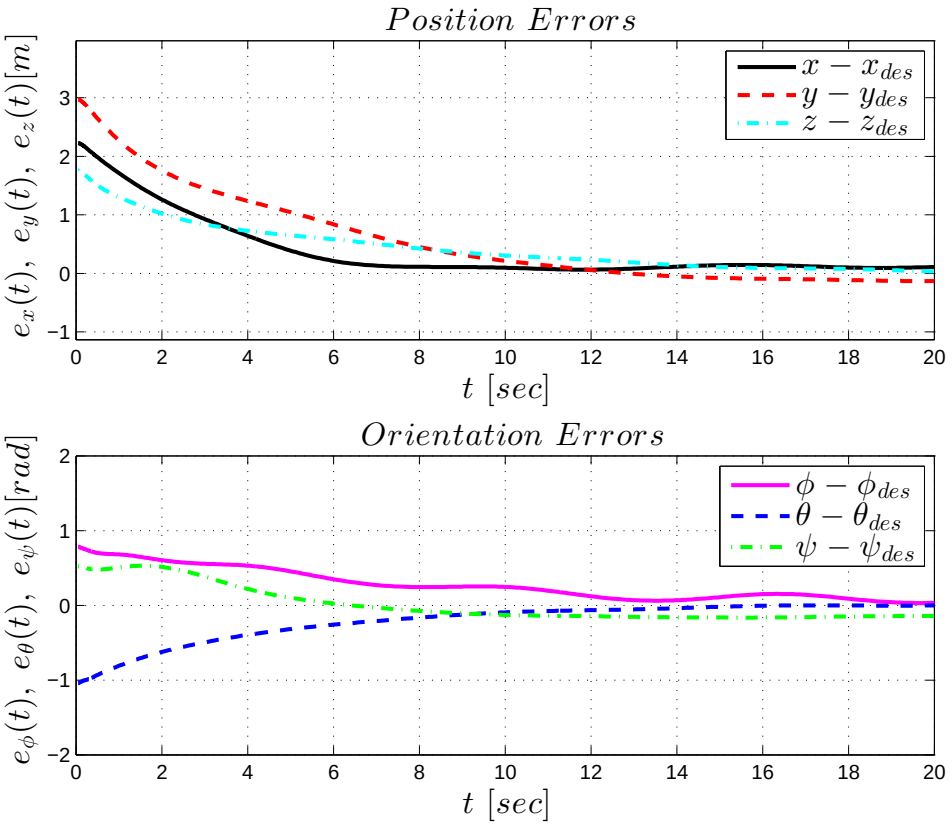

FIGURE 6.3: Position and Orientation Errors in Scenario 2

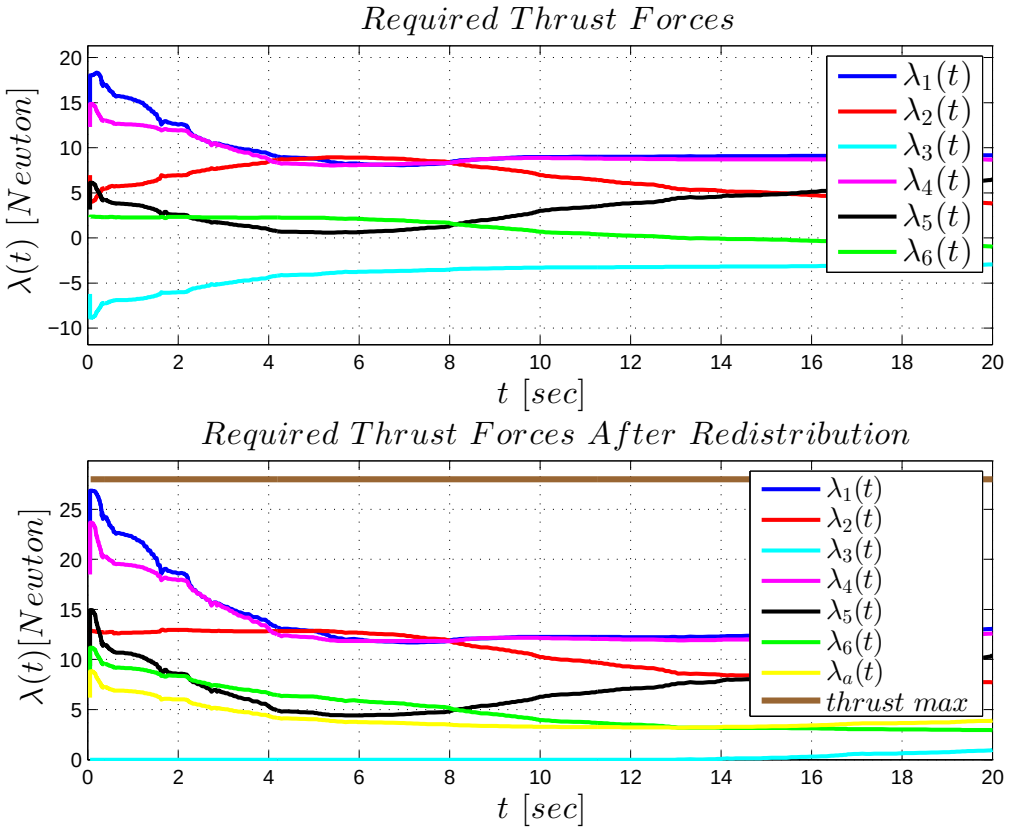

FIGURE 6.4: Required Thrust Forces Using Redistribution Algorithm in Scenario 2

Parameter	Description	Value
$\xi_e(0)$	Initial End-Effector Position/Orientation	$[-0.23\ 0.015\ 0.23\ 0\ 0\ 0]^\tau$
$p(0)$	Initial Body-Frame Position	$[0\ 0\ 0]^\tau$
$\nu(0)$	Initial Body-Fixed Velocities	$[0\ 0\ 0\ 0\ 0\ 0]^\tau$
$\hat{\theta}(0)$	Initial Parameter Estimation Conditions	$0.7\ \mathbf{diag}\{1,1,1,1,1,1\}$
$\hat{\Delta}(0)$	Initial Parameter Estimation Conditions	$[0,0,0,0,0,0]^\tau$
K_1	Gain of kinematic Controller	$\mathbf{diag}\{1,1,1,0.1,0.1,0.1\}$
K_2	Gain of Dynamic Controller	$10\ \mathbf{diag}\{1,1,1,1,1,1\}$
$\theta^\star_\lambda$	Unknown Actuator Parameters	$0.85\ \mathbf{diag}\{1,1,1,1,1,1\}$
Γ_θ	Adaptation Gain Matrix	$0.2\ \mathbf{diag}\{1,1,1,1,1,1\}$
Γ_Δ	Adaptation Gain Matrix	15
σ	σ-Modificatioon Gain	2.5
$d(t)$	Disturbance	$[\sin(t)\ 0.2\ 0.5\ \ \cos(t)\ 0.5\ 0.5]^\tau$
δ	Projection Parameter	0.05

TABLE 6.3: Simulation Parameters for Scenario 3

Scenario 4: In this scenario the end-effector of the proposed aerial manipulator is forced to track the trajectory $p_{\text{e,des}} = [\cos(0.5t)\ \sin(0.5t)\ 1.5 + 0.5t]^\tau$ with regulated desired orientation $\Theta(t) = [0\ 0\ 0]^\tau$ with reference to Earth-Fixed frame and 10 % controller effectiveness reduction. The parameters for this simulation are depicted in Table 6.4 and the corresponding simulation results in Figures 6.7,6.8.

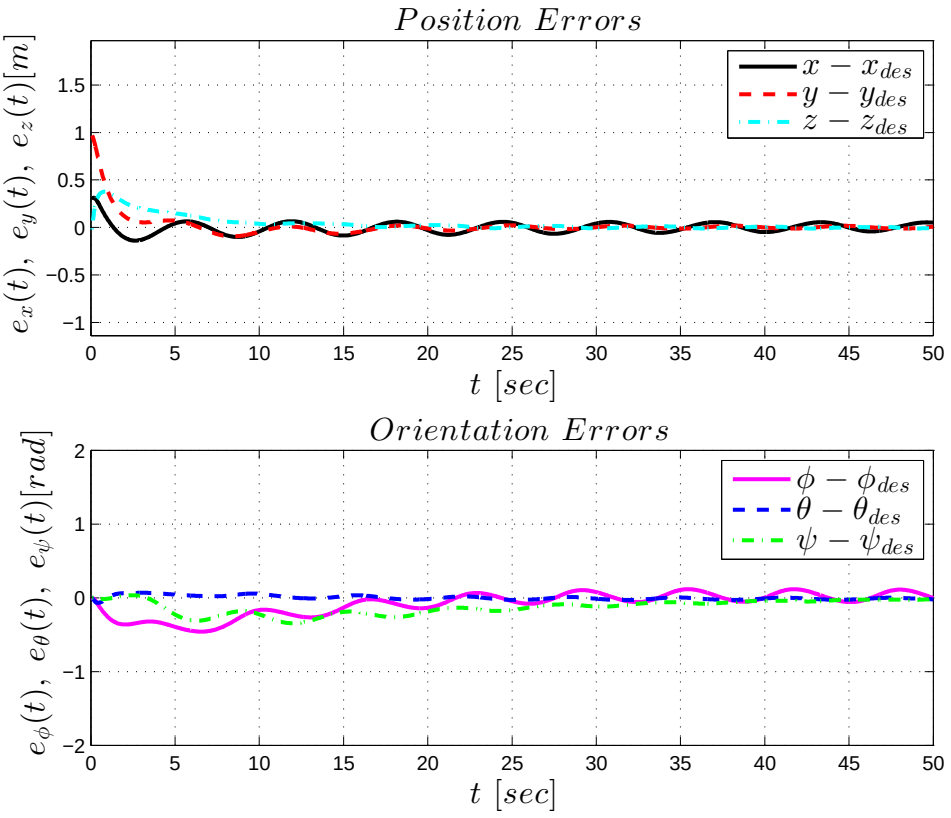

FIGURE 6.5: Position and Orientation Errors in Scenario 3

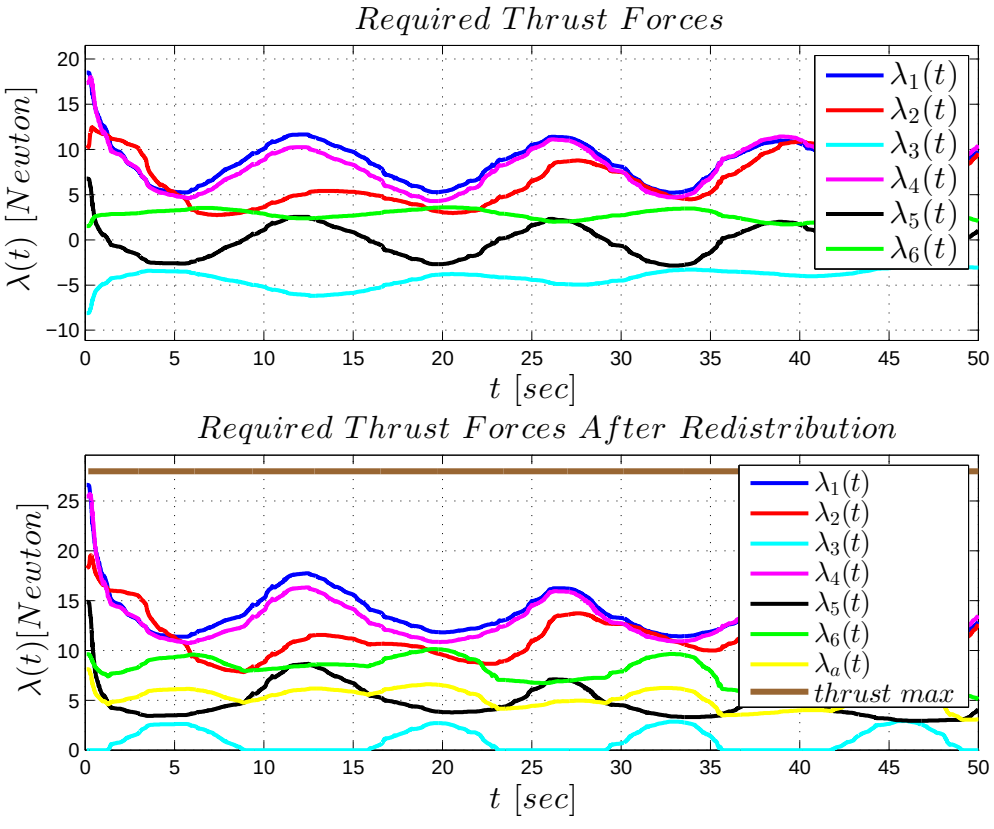

FIGURE 6.6: Required Thrust Forces Using Redistribution Algorithm in Scenario 3

Parameter	Description	Value
$\xi_e(0)$	Initial End-Effector Position/Orientation	$[-0.23\ 0.015\ 0.23\ 0\ 0\ 0]^\tau$
$p(0)$	Initial Body-Frame Position	$[0\ 0\ 0]^\tau$
$\nu(0)$	Initial Body-Fixed Velocities	$[0\ 0\ 0\ 0\ 0\ 0]^\tau$
$\hat{\theta}(0)$	Initial Parameter Estimation Conditions	$0.7\ \mathbf{diag}\{1,1,1,1,1,1\}$
$\hat{\Delta}(0)$	Initial Parameter Estimation Conditions	$[0,0,0,0,0,0]^\tau$
K_1	Gain of kinematic Controller	$\mathbf{diag}\{0.5,0.5,0.5,0.3,0.3,0.3\}$
K_2	Gain of Dynamic Controller	$8\ \mathbf{diag}\{1,1,1,1,1,1\}$
$\theta_\lambda^\star$	Unknown Actuator Parameters	$0.90\ \mathbf{diag}\{1,1,1,1,1,1\}$
Γ_θ	Adaptation Gain Matrix	$0.5\ \mathbf{diag}\{1,1,1,1,1,1\}$
Γ_Δ	Adaptation Gain Matrix	5
σ	σ-Modificatioon Gain	0.5
$d(t)$	Disturbance	$[0.5\ \cos(t)\ 0.5\ 0.5\ \sin(t)\ 0.5]^\tau$
δ	Projection Parameter	0.05

TABLE 6.4: Simulation Parameters for Scenario 4

Scenario 5: In this scenario the end-effector of the proposed aerial manipulator is forced to track the trajectory $p_{\text{e,des}} = [\cos(0.5t)\ \sin(0.5t)\ 1.5 + 0.5t]^\tau$ with regulated desired orientation $\Theta(t) = \left[\frac{\pi}{3}\ \frac{\pi}{6}\ -\frac{\pi}{4}\right]^\tau$ with reference to Earth-Fixed frame and 10 % controller effectiveness reduction. The parameters for this simulation are depicted in Table 6.5 and the corresponding simulation results in Figures 6.9,6.10.

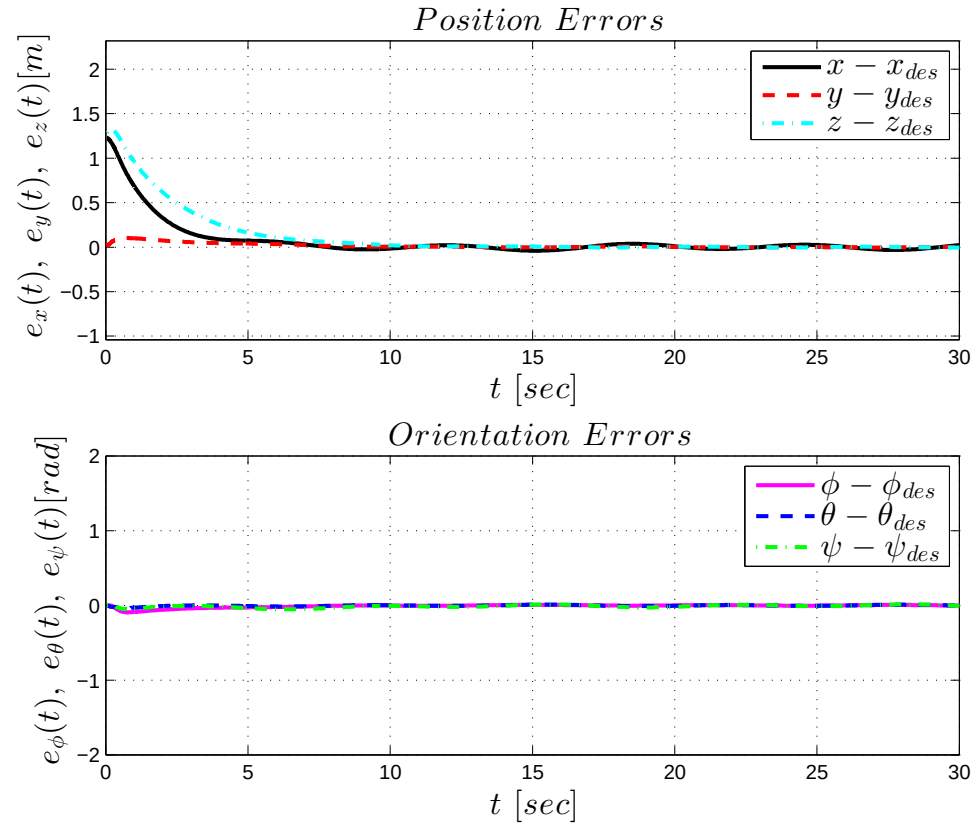

FIGURE 6.7: Position and Orientation Errors in Scenario 4

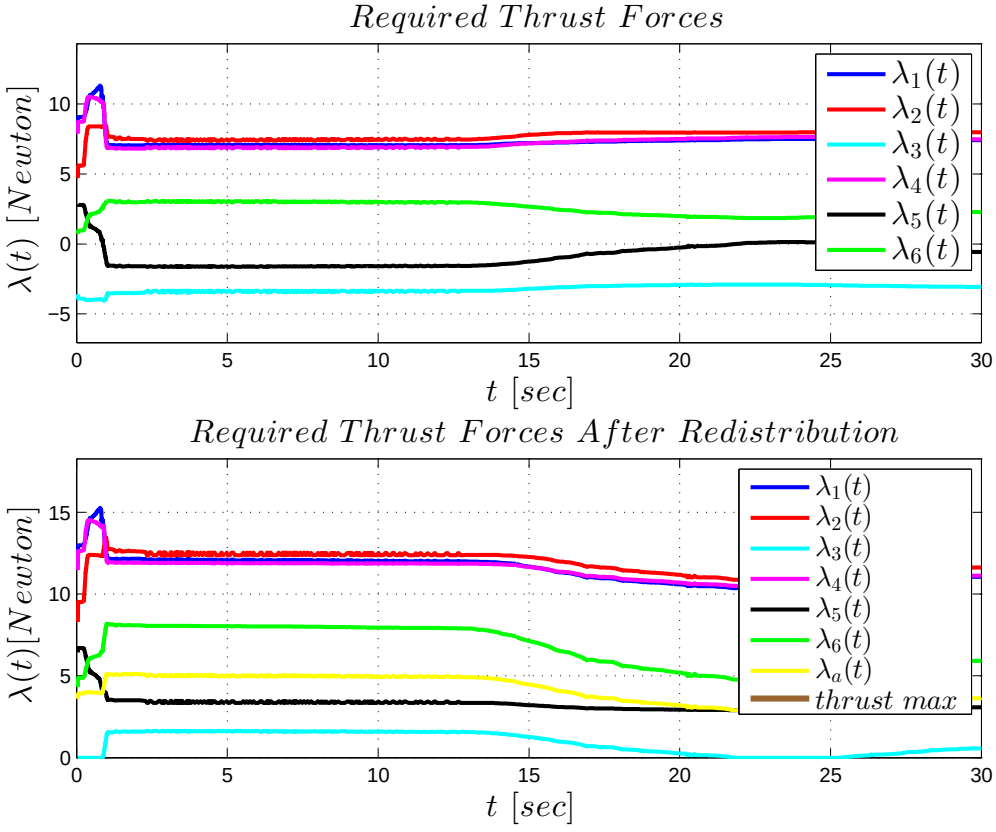

FIGURE 6.8: Required Thrust Forces Using Redistribution Algorithm in Scenario 4

Parameter	Description	Value
$\xi_e(0)$	Initial End-Effector Position/Orientation	$[-0.23\ 0.015\ 0.23\ 0\ 0\ 0]^\tau$
$p(0)$	Initial Body-Frame Position	$[0\ 0\ 0]^\tau$
$\nu(0)$	Initial Body-Fixed Velocities	$[0\ 0\ 0\ 0\ 0\ 0]^\tau$
$\hat{\theta}(0)$	Initial Parameter Estimation Conditions	$0.7\ \mathbf{diag}\{1,1,1,1,1,1\}$
$\hat{\Delta}(0)$	Initial Parameter Estimation Conditions	$[0,0,0,0,0,0]^\tau$
K_1	Gain of kinematic Controller	$\mathbf{diag}\{0.8,0.8,0.8,0.3,0.3,0.3\}$
K_2	Gain of Dynamic Controller	$5\ \mathbf{diag}\{1,1,1,1,1,1\}$
$\theta^\star_\lambda$	Unknown Actuator Parameters	$0.90\ \mathbf{diag}\{1,1,1,1,1,1\}$
Γ_θ	Adaptation Gain Matrix	$0.5\ \mathbf{diag}\{1,1,1,1,1,1\}$
Γ_Δ	Adaptation Gain Matrix	13
σ	σ-Modificatioon Gain	1.5
$d(t)$	Disturbance	$[1.2\ 0.8\ \cos(t)\ 0.8\ 0.9\ \cos(t)]^\tau$
δ	Projection Parameter	0.05

Table 6.5: Simulation Parameters for Scenario 5

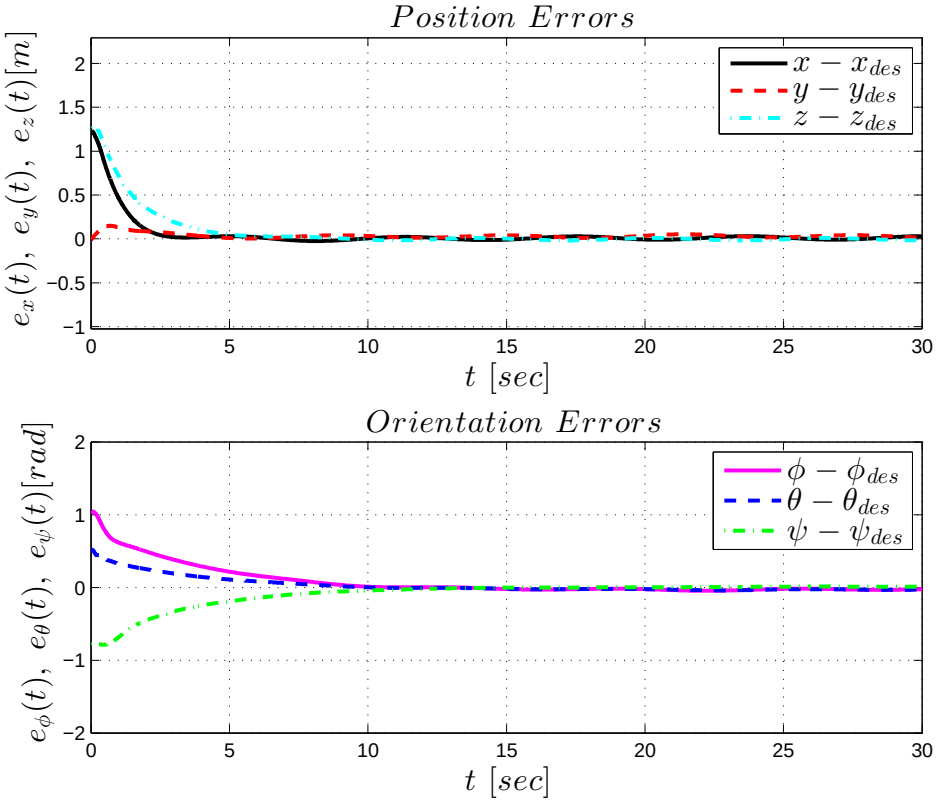

FIGURE 6.9: Position and Orientation Errors in Scenario 5

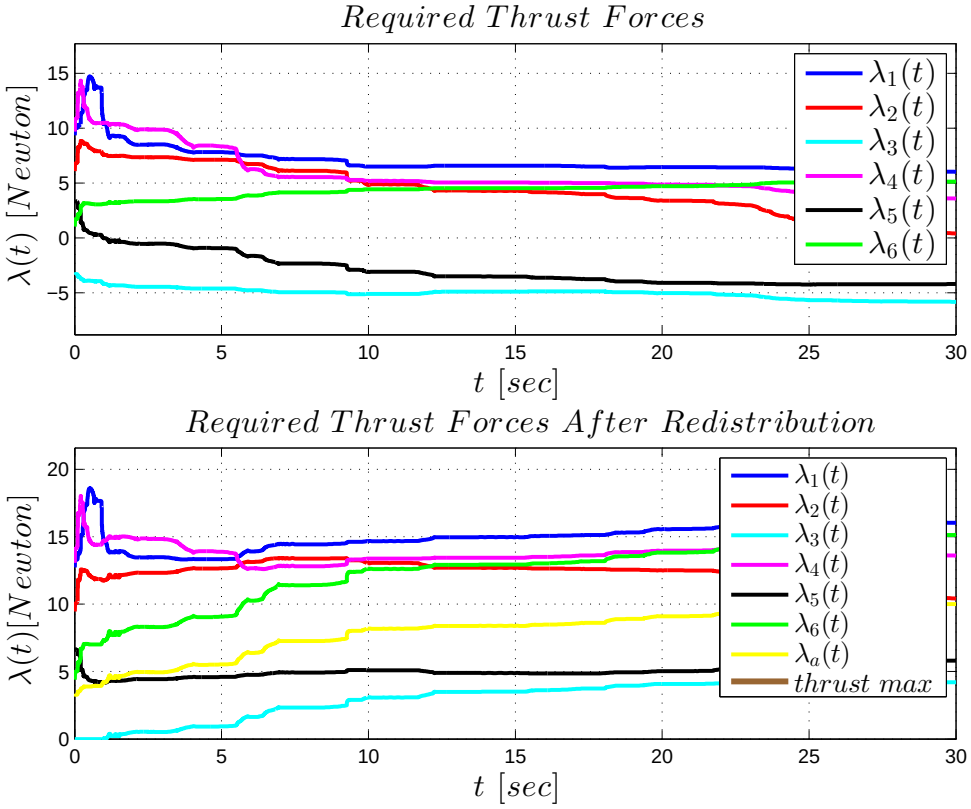

FIGURE 6.10: Required Thrust Forces Using Redistribution Algorithm in Scenario 5

Chapter 7

Conclusion and Future Directions

Aerial robots physically interacting with the environment could be very useful for many applications. In this thesis, we proposed a completely novel aerial manipulator that interacts with the environment via an end-effector by applying desired forces and torques in six DoF task space. We have presented extensively all necessary issues relevant to the kinematic differential equations, geometry transformations, static and dynamic equations which constitute a well-defined mechanism for the free motion of the proposed system in space.

It has proven that the system, with the proposed geometry, which is the result of technical optimization problems, is exact controllable and linearizable. A robust adaptive backstepping controller is designed in order to control the exact position and orientation of the end-effector in 3D space. Simulations from Chapter 6 illustrated that the system performs desired manipulation tasks efficiently irrespectively of the presence of unmodeled dynamics, modelling errors, actuation failures, external and environmental disturbances. Figures from Chapter 6 depicted that the controller provides fast adaptation of the unknown parameters, accurate disturbance rejection of unknown disturbances and fair transient performance in the steady state. Furthermore, the required thrust force is within actuators bounds, which underlie an extremely significant result in the field of aerial robotics. All these conditions are sufficient to lead us to the final construction of the system.

With regards to the future directions, first an extensively bending stress study for every bracket of the system should be performed, in order to choose the exact material that will compose the system. This is vital issue in order to avoid possible oscillations among the brackets during the flight tests. Future work mainly involves

the construction of the proposed aerial robot in the Control Systems Lab NTUA and the conduction of experimental trials for the proposed framework with the actual system. The experiments should be done in order to verify the theoretical results of this thesis. The integrated system needs to be equipped with force/torque sensors which will have the ability to measure the required actuation forces and torques from the end-effector. This will enable us to perform more advanced manipulation tasks such as carrying loads, interaction with the environment, industrial inspections and cooperation with other aerial robots since the end-effector will be able to apply accurate desired force/torque in an object. Furthermore, concerning the system identification, a nonlinear system approximation with Neural Networks will be ideal, providing more effectiveness in the controller robustness design. Ultimately, an embedded controller software should be programmed in C++, for the implementation of the high-level controller that was designed in this thesis in order to control the aerial robot in real-time applications.

Bibliography

[1] G. Gavridis. *"Control Oriented Aerodynamic Design Optimization For An Aerial Manipulator"*. Diploma Thesis, National Technical University of Athens (NTUA), 2014.

[2] L. Gentili, R. Naldi, and L. Marconi. "Modeling and Control of VTOL UAVs Interacting with the Environment". *47th IEEE Conference on Decision and Control (CDC)*, pages 1231–1236, 2008.

[3] A. Torre, D. Mengoli, R. Naldi, F. Forte, A. Macchelli, and L. Marconi. "A Prototype of Aerial Manipulator". *IEEE/RSJ International Conference on Intelligent Robots and Systems (IROS)*, pages 2653–2654, 2012.

[4] F. Forte, R. Naldi, A. Macchelli, and L. Marconi. "Impedance Control of an Aerial Manipulator". *American Control Conference (ACC)*, pages 3839–3844, 2012.

[5] L. Marconi, R. Naldi, and L. Gentili. "Modelling and Control of a Flying Robot Interacting with the Environment". *Automatica*, 47(12):2571–2583, 2011.

[6] A. Keemink, M. Fumagalli, S. Stramigioli, and R. Carloni. "Mechanical Design of a Manipulation System for Unmanned Aerial Vehicles. *IEEE International Conference on Robotics and Automation (ICRA)*, pages 3147–3152, 2012.

[7] A. Albers, S. Trautmann, T. Howard, T. Nguyen, M. Frietsch, and C. Sauter. "Semi-Autonomous Flying Robot for Physical Interaction with Environment". *IEEE Conference on Robotics Automation and Mechatronics (RAM)*, pages 441–446, 2010.

[8] P. Pounds, D. Bersak, and A. Dollar. "The Yale Aerial Manipulator: Grasping in Flight". *IEEE International Conference on Robotics and Automation (ICRA)*, pages 2974–2975, 2011.

[9] P. Pounds, D. Bersak, and A. Dollar. "Grasping from the Air: Hovering Capture and Load Stability". *IEEE International Conference on Robotics and Automation (ICRA)*, pages 2491–2498, 2011.

[10] P. Pounds and A. Dollar. "Aerial Grasping from a Helicopter UAV Platform". *Experimental Robotics*, 79:269–283, 2014.

[11] P. Pounds, D. Bersak, and A. Dollar. "Stability of Small-Scale UAV Helicopters and Quadrotors with added Payload Mass Under PID Control". *Autonomous Robots*, 33(1-2):129–142, 2012.

[12] D. Mellinger, Q. Lindsey, M. Shomin, and V. Kumar. "Design, Modeling, Estimation and Control for Aerial Grasping and Manipulation". *IEEE/RSJ International Conference on Intelligent Robots and Systems (IROS)*, pages 2668–2673, 2011.

[13] V. Ghadiok, J. Goldin, and R. Wei. "Autonomous Indoor Aerial Gripping Using a Quadrotor". *IEEE/RSJ International Conference on Robots and Systems (IROS)*, pages 4645–4651, 2011.

[14] V. Ghadiok. *"Autonomous Aerial Manipulation Using a Quadrotor"*. Phd Thesis, Utah State University, 2011.

[15] N. Michael, J. Fink, and V. Kumar. "Cooperative Manipulation and Transportation with Aerial Robots". *Autonomous Robots*, 30(1):73–86, 2011.

[16] D. Mellinger, M. Shomin, N. Michael Nathan, and V. Kumar. "Cooperative Grasping and Transport Using Multiple Quadrotors". *Distributed Autonomous Robotic Systems*, 83:545–558, 2013.

[17] Q. Lindsey, D. Mellinger, and V. Kumar. "Construction with Quadrotor Teams". *Autonomous Robots*, 33(3):323–336, 2012.

[18] R. Ritz, W. Muller, M. Hehn, and R. D'Andrea. "Cooperative Quadrocopter Ball Throwing and Catching". *IEEE/RSJ International Conference onIntelligent Robots and Systems (IROS),*, pages 4972–4978, 2012.

[19] F. Huber, K. Kondak, K. Krieger, D. Sommer, M. Schwarzbach, M. Laiacker, I. Kossyk, S. Parusel, S. Haddadin, and A. Albu-Schaffer. "First Analysis and Experiments in Aerial Manipulation Using Fully Actuated Redundant Robot Arm". *IEEE/RSJ International Conference on Intelligent Robots and Systems (IROS)*, pages 3452–3457, 2013.

[20] K. Kondak, A. Krieger, M. Schwarzbach, M.Laiacker, I. Maza, A. Rodriguez-Castano, and A. Ollero. "Closed-Loop Behavior of an Autonomous Helicopter Equipped with a Robotic Arm for Aerial Manipulation Tasks". *International Journal of Advanced Robotics Systems*, 10:145, 2013.

[21] G. Jiang and R. Voyles. Hexrotor UAV Platform Enabling Dextrous Interaction with Structures-Flight Test. *2013 IEEE International Symposium on Safety, Security, and Rescue Robotics (SSRR)*, pages 1–6, 2013.

[22] R. Voyles and G. Jiang. "Hexrotor UAV Platform Enabling Dextrous Interaction with Structures - Preliminary Work". *IEEE International Symposium on Safety, Security, and Rescue Robotics (SSRR)*, pages 1–7, 2012.

[23] G. Jiang and R. Voyles. "Hexrotor UAV Platform Enabling Dextrous Aerial Mobile Manipulation". *International Micro Air Vehicle Conference and Flight Completion (IMAV2013)*, 2013.

[24] G. Jinag. *"Dextrous Hexrotor UAV Platform"*. Master Thesis, University of Denver, 2013.

[25] M. Kobilarov. "Nonlinear Trajectory Control of Multi-Body Aerial Manipulators". *Journal of Intelligent and Robotic Systems*, 73(1-4):679–692, 2014.

[26] S. Kim, S Choi, and H. Kim. "Aerial Manipulation Using a Quadrotor with a two DOF Robotic Arm". *IEEE/RSJ International Conference on Intelligent Robots and Systems (IROS)*, pages 4990–4995, 2013.

[27] M. Orsag, C. Korpela, and P. Oh. "Modeling and Control of MM-UAV: Mobile Manipulating Unmanned Aerial Vehicle". *Journal of Intelligent and Robotic Systems*, 69(1-4):227–240, 2013.

[28] V. Lippiello and F. Ruggiero. "Cartesian Impedance Control of a UAV with a Robotic Arm". *IFAC Symposium on Robot Control*, 2012.

[29] V. Lippiello and F. Ruggiero. "Exploiting Redundancy in Cartesian Impedance Control of UAVs Equipped with a Robotic Arm". *IEEE/RSJ International Conference on Intelligent Robots and Systems (IROS)*, pages 3768–3773, 2012.

[30] G. Arleo, F. Caccavale, G. Muscio, and F. Pierri. "Control of Quadrotor Aerial Vehicles Equipped with a Robotic Arm". *21st Mediterranean Conference on Control Automation (MED)*, pages 1174–1180, 2013.

[31] A. Khalifa, M. Fanni, A. Ramadan, and A. Abo-Ismail. "Modeling and Control of a New Quadrotor Manipulation System". *First International Conference on Innovative Engineering Systems (ICIES)*, pages 109–114, 2012.

[32] A. J. Cano, J. Martin, G. Heredia, A. Ollero, and R. Cano. "Control of an Aerial Robot with Multi-Link Arm for Assembly Tasks". *IEEE International Conference on Robotics and Automation (ICRA)*, pages 4916–4921, 2013.

[33] G. Padfield. *"Helicopter Flight Dynamics, The Theory and Application of Flying Qualities and Simulation Modelling"*. AIAA Education Series. American Institute of Aeronautics and Astronautics, 1996.

[34] L. N. Trefethen and D. Bau. *"Numerical Linear Algebra"*. SIAM, 1997.

[35] P. Gill, W. Murray, and M. Wright. *"Numerical Linear Algebra and Optimization"*. Addison-Wesley Publishing Company, 1991.

[36] K. Murty. *"Linear Complementarity, Linear and Nonlinear Programming"*. Sigma Series in Applied Mathematics. Berlin: Heldermann Verlag, 1988.

[37] M. Stein. "Large Sample Properties of Simulations Using Latin Hypercube Sampling". *Technometrics*, 29(2):143–151, 1987.

[38] M. McKay, R. Beckman, and W. Conover. "A Comparison of Three Methods for Selecting Values of Input Variables in the Analysis of Output from a Computer Code". *Technometrics*, 42(1):55–61, 2000.

[39] C. Audet and J. Dennis. "Analysis of Generalized Pattern Searches". *SIAM Journal on Optimization*, 13(3):889–903, 2003.

[40] C. Audet and J. Dennis. "A Pattern Search Filter Method for Nonlinear Programming without Derivatives". *SIAM Journal on Optimization*, 14(4):980–1010, 2004.

[41] V. Martinez. *"Modelling of the Flight Dynamics of a Quadrotor Helicopter"*. Master Thesis, Cranfield University, Departement of Aerospace Sciences, 2007.

[42] R. Prouty. *"Helicopter Performance, Stability and Control"*. R.E. Krieger Publishing Company, 1995.

[43] G. Antonelli. *"Underwater Robots"*. Springer Tracts in Advanced Robotics. Springer International Publishing, 2013.

[44] T. Fossen. *"Guidance and Control of Ocean Vehicles"*. John Wiley and Sons, 1994.

[45] D. Bernstein. *"Geometry, Kinematics, Statics and Dynamics"*. University of Michigan, 2013.

[46] B.Siciliano, L. Sciavicco, and L. Villani. *"Robotics: Modelling, Planning and Control"*. Advanced Textbooks in Control and Signal Processing. Springer, 2009.

[47] T. Madani and A. Benallegue. "Backstepping Control for a Quadrotor Helicopter". *IEEE/RSJ International Conference on Intelligent Robots and Systems (IROS)*, pages 3255–3260, 2006.

[48] M. Huang, B. Xian, C. Diao, K. Yang, and Y. Feng. "Adaptive Tracking Control of Underactuated Quadrotor Unmanned Aerial Vehicles via Backstepping". *American Control Conference (ACC)*, pages 2076–2081, 2010.

[49] B. Siciliano and L. Villani. *"Robot Force Control"*. Kluwer International Series in Engineering and Computer Science: Robotics, Vision, Manipulation and Sensors. Springer, 1999.

[50] A. Bloch, P. Crouch, J. Baillieul, and J. Marsden. *"Nonholonomic Mechanics and Control"*. Interdisciplinary Applied Mathematics. Springer, 2003.

[51] A. Isidori. *"Nonlinear Control Systems"*. Communications and Control Engineering. Springer, 1995.

[52] H. Nijmeijer and A. V. D. Schaft. *"Nonlinear Dynamical Control Systems"*. U.S. Government Printing Office, Springer, 1990.

[53] H. Khalil. *"Nonlinear Systems"*. Prentice Hall, 2002.

[54] J. Slotine and W. Li. *"Applied Nonlinear Control"*. Prentice Hall, 1991.

[55] T. John Koo, Y. Ma, and S. Sastry. "Nonlinear Control of a Helicopter Based Unmanned Aerial Vehicle Model". 2001.

[56] M. Krstić, I. Kanellakopoulos, and P. Kokotović. *"Nonlinear and Adaptive Control Design"*. Adaptive and Learning systems for Signal Processing, Communications and Control. Wiley, 1995.

[57] R. Olfati-Saber. *"Nonlinear Control of Underactuated Mechanical Systems with Application to Robotics and Aerospace Vehicles"*. Phd Thesis, Massachusetts Institute of Technology, 2000.

[58] Ahmet Cezayirli. *"Adaptive Control of Nonlinear Systems Using Multiple Identification Models"*. Phd Thesis, Bogazici University, 2007.

[59] E. Lavretsky and K. Wise. *"Robust and Adaptive Control: with Aerospace Applications"*. Advanced Textbooks in Control and Signal Processing. Springer, 2012.

[60] P. Ioannou and J. Sun. *"Robust Adaptive Control"*. Control Theory. PTR Prentice-Hall, 1996.

[61] H. Khalil. "Adaptive Output Feedback Control of Nonlinear Systems Represented by Input-Output Models". *IEEE Transactions on Automatic Control*, 41 (2):177–188, 1996.

[62] W. Dixon, A. Behal, D. Dawson, and S. Nagarkatti. *"Nonlinear Control of Engineering Systems"*. Birkhauser Boston, 2002.

[63] P. Corke. *"Robotics, Vision and Control: Fundamental Algorithms in Matlab"*. Springer, 2011.